

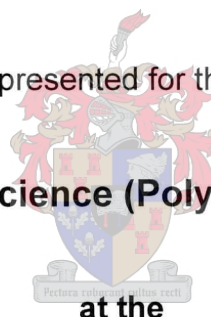
# THE EFFECT OF IODO ALKYL CHAIN TRANSFER AGENTS ON THE SEEDED EMULSION HOMO- AND CO-POLIMERISATION OF STYRENE AND BUTYL ACRYLATE

by

**CORNELIS PETRUS BEYERS**

Thesis presented for the degree

**Master of Science (Polymer Science)**



at the

**University of Stellenbosch**

Study Leaders:

Prof. RD Sanderson  
University of Stellenbosch

Mr. D de Wet-Roos  
University of Stellenbosch

External Examiner:

Prof. B Klumperman  
Technical University of  
Eindhoven

**MARCH 1999**

## DECLARATION

I, the undersigned, hereby declare that the work contained in this thesis is my own original work and that I have not previously in its entirety or in part submitted it at any university for a degree.

CP BEYERS

10 February 1999

## SYNOPSIS

A free-radical polymerisation process, which has characteristics of a living polymerisation system, as it is capable of producing polymers of pre-determined molecular masses with a narrow molecular mass distribution, is discussed. It is also possible to make block-copolymers by adding adding different monomers. The basic objective was to describe, discuss and explain the results of the effects of alkyl iodides as chain transfer agents on the seeded emulsion homo- and co-polymerisation of styrene and butyl acrylate. Iodoacetonitrile and 1-phenylethyl iodide were used as alkyl iodides, acting as degenerative chain transfer agents.

First, the effects of these alkyl iodides as chain transfer agents on the molecular mass, molecular mass distribution, glass transition temperature, conversion and particle size for the seeded emulsion polymerisation of styrene were studied. Second, the effects of alkyl iodides as chain transfer agents on the kinetics of radical emulsion polymerisation, especially the average amount of radicals per latex particle, were investigated. Third, the possibility of producing block-copolymers by emulsion polymerisation, using alkyl iodides as chain transfer agents, was investigated.

To the best of the author's knowledge, results of work carried out in this study offer the first proof that the "living"/controlled radical polymerisation of styrene, with alkyl iodides as chain transfer agents, can be successfully carried out in emulsion. Addition of different alkyl iodides as chain transfer agents, in different concentrations, led to marked changes in the molecular mass, molecular mass distribution, glass transition temperature, conversion and particle size for the seeded emulsion polymerisation of styrene. The molecular masses of the polystyrene that was produced ranged from 156 to 663 577 while the average molecular mass distribution was below 2. Addition of these alkyl iodides to a seeded styrene polymerisation under zero-one conditions led to an average number of free radicals per latex particle that was greater than 1. A styrene seed latex with functional iodine end-groups was created and was successfully co-polymerised with butyl acrylate to produce a perfect styrene-butyl acrylate block-copolymer.

This work has industrial importance as it allows the molecular mass, molecular mass distribution and particle size of polymers to be controlled. These factors are directly related to their micro- and macrostructure of polymers.

## OPSOMMING

Die vrye-radikaal polimerisasie proses wat die eienskappe van 'n lewendige polimerisasie sisteem toon, omdat dit moontlik is om 'n polimeer met voorafbepaalde molekulêre massas en 'n baie klein molekulêre massa verspreiding te berei, is bespreek. Dit is ook moontlik om, deur die byvoeging van 'n tweede monomeer, 'n blok kô-polimere te maak. Die doel was om die effekte wat alkieljodiede as kettingoordragagente op die "seed" homo- en kô-polimerisasie van stireen en butiel akrielaat gehad het te beskryf en te verklaar. Jodoasetonitriël en 1-fenieletieljodied is gebruik as degeneratiewe kettingoordragagente.

Eerstens is die uitwerking van hierdie alkieljodiede as kettingoordragagente op die molekulêre massa, molekulêre massa verspreiding, glas oorgang temperatuur, opbrengs en partikelgrote van die "seed" emulsie polimerisasie van stireen bestudeer. Tweedens is na die uitwerking van alkieljodiede op die kinetika van 'n emulsie radikaal polimerisasie gekyk met spesifieke klem op die gemiddelde aantal radikale per emulsie partikel. Derdens is die moontlikheid om blok kô-polimere te berei ondersoek.

Na die beste van die outeur se wete is die resultate van hierdie studie die eerste bewys dat die "lewendige"/gekontroleerde radikaal polimerisasie van stireen met alkieljodiede as kettingoordragagente suksesvol in emulsie polimerisasie uitgevoer kan word. Die byvoeging van verskillende alkieljodiede, in verskillende konsentrasies, het aanleiding gegee tot opmerklike veranderinge in die molekulêre massa, molekulêre massa verspreiding, glas oorgang temperatuur, opbrengs en partikelgrote van die "seed" emulsie polimerisasie van stireen. Die molekulêre massas van die bereide polistireen het gewissel tussen 156 en 663 577 en die gemiddelde molekulêre massa verspreiding was onder 2. Byvoeging van die alkieljodiede by die "seed" polimerisasie van stireen onder zero-een toestande het 'n gemiddelde aantal radikale per emulsie partikel van bo 1 gelewer. 'n Funktionele "seed" emulsie met jodium eindgroepe was geproduseer na 'n suksesvolle kô-polimerisasie met butiel akrielaat en 'n perfekte stireen-butiel akrilaat kô-polimeer is verkry.

Hierdie werk het industriële belang aangesien dit die beheer van molekulêre massa, molekulêre massa verspreiding en partikelgrote moontlik maak wat 'n direkte effek het op die mikro- en makro strukture van die polimeer.

## Acknowledgements

I wish to express my sincere gratitude to:

**Prof. RD Sanderson**, Director of the Institute for Polymer Science, University of Stellenbosch, for his advise assistance and encouragement.

**Mr. D de–Wet Roos**, Senior Researcher at PLASCON Ltd., who guided and helped me. It is with his willingness to help and his patients that I was able to complete this dissertation so effectively and such a short time.

**Dr. Nico Laubscher**, Statician, who helped me with the statistical analysis of the disertation.

**Dr. Margie Hurndall**, who took care of the technical aspects of the disertation.

**My wife, Henèlia**, for her encouragement, love, time and patience. Her abillity to combine my vision into hers motivated me even further.

**My parents**, for their love, encouragement and their trust in my abilities over the years.

***SOLI DEO GLORIA***

(all glory belongs to God)

## LIST OF FIGURES

---

### CHAPTER 2

Figure 2.1:	An illustration of the major free-radical reactions taking place in and around a latex particle	9
Figure 2.2:	Dissociation of an alkoxyamine to produce the chain transfer agent TEMPO	13
Figure 2.3:	The chain transfer reaction for RAFT	16

---

### CHAPTER 3

Figure 3.1	Resonance stabilisation of the radical after chain transfer to IAN	28
Figure 3.2	Resonance stabilisation of the radical after chain transfer to PEI	28
Figure 3.3	$\ln(M_n)$ for the 16 runs of the fractional factorial design	40
Figure 3.4	Response surface plot of the concentration of CTA and type of CTA for the response $\ln(M_n)$	42
Figure 3.5	$M_w/M_n$ for the 16 runs in the fractional factorial design	43
Figure 3.6	Response surface plot of the concentration of CTA and type of initiator for the response $M_w/M_n$	44
Figure 3.7	Response surface plot of the concentration of CTA and type of CTA for the response $M_w/M_n$	45
Figure 3.8	Particle sizes of latex particles for the 16 runs of the fractional factorial design	47
Figure 3.9	Response surface plot of the concentration of monomer and type of initiator for the response particle size	48
Figure 3.10	Fractional conversion of monomer to polymer of the 16 runs in the fractional factorial design	49
Figure 3.11	Response surface plot of the concentration of monomer and type of initiator on the response fractional conversion of monomer to polymer	50
Figure 3.12:	Possible mechanism for the formation of $I_2$ from a polymer or CTA with an iodine chain-end	51
Figure 3.13:	Possible mechanism for the formation of HI from a polymer or CTA with an iodine chain-end	51

Figure 3.14: $T_g$ of the polymers for the 16 runs of the fractional factorial design	52
Figure 3.15: Response surface plot of the concentration of initiator and concentration of CTA for the response $T_g$	54

---

**CHAPTER 4**

Figure 4.1: All the possible reactions that can take place in an emulsion polymerisation	62
Figure 4.2: The average number of free radicals per latex particle for Runs 1 – 4 over the reaction time	77
Figure 4.3: Average number of free radicals over time for the seeded emulsion polymerisation of styrene in the presence of IAN	78
Figure 4.4: Average number of free radicals against conversion for the seeded emulsion polymerisation of styrene in the presence of IAN	78
Figure 4.5: Graph of $\ln P(M)$ against molecular mass for the chain transfer from styrene to IAN	81
Figure 4.6: Graph of $\ln P(M)$ against molecular mass for the chain transfer from styrene to PEI	81
Figure 4.7: Plot of the gradient of $\ln P(M)$ against $M$ vs. $[IAN]/[M]$	82
Figure 4.8: Plot of the gradient of $\ln P(M)$ against $M$ vs. $[PEI]/[M]$	82

---

**CHAPTER 5**

Figure 5.1: Separation modes in the liquid chromatography of polymers	89
Figure 5.2: Pareto chart of the main effects of $M_n$ in the co-polymerisation of styrene and BA	98
Figure 5.3: Pareto chart of the main effects of $M_w/M_n$ in the co-polymerisation of styrene and BA.	98
Figure 5.4: G-HPLC analysis of Runs 1 – 8 and the reference using ELSD	99

**APPENDIX A**


---

Figure A.1:	Two-dimensional representation of the experimental space and main effects of a $2^3$ factorial design	Aii
Figure A.2:	Two-dimensional representation of a normally distributed data set	Aiv
Figure A.3:	Geometric representation of a normally distributed data set showing the critical $\bar{X}$ value above which $H_0$ is rejected in the t-statistic test	Avi
Figure A.4:	Geometric representation of a $2^3$ -factorial design with the contrasting sides representing the main effects of factor A	Ax

**APPENDIX B**


---

Figure B.1:	Response surface of $\ln(M_n)$ for the variables initiator concentration and CTA concentration	Bi
Figure B.2:	Response surface of $\ln(M_n)$ for the variables monomer concentration and the type of initiator	Bii
Figure B.3:	Response surface of $\ln(M_n)$ for the variables monomer concentration and initiator concentration	Bii
Figure B.4:	Response surface of $\ln(M_n)$ for the variables monomer concentration and type of CTA	Biii
Figure B.5:	Response surface of $\ln(M_n)$ for the variables monomer concentration and CTA concentration	Bii
Figure B.6:	Response surface of $\ln(M_n)$ for the variables Type of initiator and initiator concentration	Biv
Figure B.7:	Response surface of $\ln(M_n)$ for the variables type of initiator and type of CTA	Biv
Figure B.8:	Response surface of $\ln(M_n)$ for the variables type of initiator and CTA concentration	Bv
Figure B.9:	Response surface of $\ln(M_n)$ for the variables type of initiator and type of CTA	Bv
Figure B.10:	Response surface of $M_w/M_n$ for the variables monomer concentration and type of initiator	Bvi

Figure B.11: Response surface of $M_w/M_n$ for the variables monomer concentration and initiator concentration	Bvi
Figure B.12: Response surface of $M_w/M_n$ for the variables monomer concentration and type of CTA	Bvii
Figure B.13: Response surface of $M_w/M_n$ for the variables monomer concentration and CTA concentration	Bvii
Figure B.14: Response surface of $M_w/M_n$ for the variables initiator concentration and type of CTA	Bviii
Figure B.15: Response surface of $M_w/M_n$ for the variables initiator concentration and CTA concentration	Bviii
Figure B.16: Response surface of $M_w/M_n$ for the variables type of initiator and initiator concentration	Bix
Figure B.17: Response surface of $M_w/M_n$ for the variables type of initiator and type of CTA	Bix
Figure B.18: Response surface of particle size for the variables initiator monomer concentration and type of CTA	Bx
Figure B.19: Response surface of particle size for the variables Initiator monomer concentration and CTA concentration	Bx
Figure B.20: Response surface of particle size for the variables initiator concentration and type of CTA	Bxi
Figure B.21: Response surface of particle size for the variables initiator concentration and CTA concentration	Bxi
Figure B.22: Response surface of particle for the variables CTA concentration and type of CTA	Bxii
Figure B.23: Response surface of particle for the variables monomer concentration and initiator concentration	Bxii
Figure B.24: Response surface of particle for the variables type of initiator and type of CTA	Bxiii
Figure B.25: Response surface of particle for the variables CTA concentration and type of initiator	Bxiii
Figure B.27: Response surface of conversion for the variables monomer concentration and type of initiator	Bxiv
Figure B.28: Response surface of conversion for the variables monomer concentration and initiator concentration	Bxiv

Figure B.29: Response surface of conversion for the variables monomer concentration and type of CTA	Bxv
Figure B.30: Response surface of conversion for the variables monomer concentration and CTA concentration	Bxv
Figure B.31: Response surface of conversion for the variables initiator concentration and type of initiator	Bxvi
Figure B.32: Response surface of conversion for the variables initiator concentration and type of CTA	Bxvi
Figure B.33: Response surface of conversion for the variables type of initiator and CTA concentration	Bxvii
Figure B.34: Response surface of conversion for the variables initiator concentration and CTA concentration	Bxvii
Figure B.35: Response surface of conversion for the variables type of CTA and CTA concentration	Bxviii
Figure B.36: Response surface of $T_g$ for the variables type of CTA and CTA concentration	Bxviii
Figure B.37: Response surface of $T_g$ for the variables type of CTA and initiator concentration	Bxix
Figure B.38: Response surface of $T_g$ for the variables type of CTA and CTA concentration	Bxix
Figure B.39: Response surface of $T_g$ for the variables type of initiator and initiator concentration	Bxx
Figure B.40: Response surface of $T_g$ for the variables monomer concentration and CTA concentration	Bxx
Figure B.41: Response surface of $T_g$ for the variables monomer concentration and type of CTA	Bxxi
Figure B.42: Response surface of $T_g$ for the variables monomer concentration and initiator concentration	Bxxi
Figure B.43: Response surface of $T_g$ for the variables monomer concentration and type of initiator	Bxxii
Figure B.44: Response surface of $T_g$ for the variables type of initiator and CTA	Bxxii
Figure B.45: Response surface of $T_g$ for the variables CTA concentration and type of CTA	Bxxiii

**APPENDIX C**

Figure C.1:	Normal probability plot of the effects of the variables on the response $\ln(M_n)$	Ci
Figure C.2:	Normal probability plot of the effects of the variables on the response $M_w/M_n$	Cii
Figure C.3:	Normal probability plot of the effects of the variables on the response particle size	Cii
Figure C.4:	Normal probability plot of the effects of the variables on the response conversion of monomer to polymer	Ciii
Figure C.5:	Normal probability plot of the effects of the variables on the response	Ciii

**APPENDIX D**

Figure D.1:	Pareto chart of the effects of the variables on the response $\ln(M_n)$	Di
Figure D.2:	Pareto chart of the effects of the variables on the response $M_w/M_n$	Di
Figure D.3:	Pareto chart of the effects of the variables on the response particle size	Dii
Figure D.4:	Pareto chart of the effects of the variables on the response conversion of monomer to polymer	Dii
Figure D.5:	Pareto chart of the effects of the variables on the response $T_g$	Diii

**APPENDIX F**

Figure F.1:	Normal probability plot of the residuals of $\ln(M_n)$	Fii
Figure F.2:	Normal probability plot of the residuals of $M_w/M_n$	Fii
Figure F.3:	Normal probability plot of the residuals of conversion	Fiii
Figure F.4:	Normal probability plot of the residuals of conversion	Fiii

**APPENDIX G**

Figure G.1:	The relation between the fractional conversion of monomer to polymer and the fractional increase in the particle size of the latex particles	Gi
-------------	--	----

## LIST OF TABLES

### CHAPTER 3

Table 3.1:	Variables investigated in the fractional factorial design to determine the main effects on the different responses with their respective high and low values	29
Table 3.2:	The factor levels for a 16 run fractional factorial design	29
Table 3.3:	Confounding interactions for a 16 run fractional factorial design	29
Table 3.4:	Molecular mass of the PS standards used to calibrate the GPC columns	35
Table 3.5:	Variables investigated in the 2 <sup>2</sup> -factorial design to determine the distribution for the CTAs between the water and oil phase	36
Table 3.6:	The factor levels for 2 <sup>2</sup> -factorial design to determine the distribution for the CTAs between the water and oil phase	36
Table 3.7:	Responses measured for the 16 run fractional factorial design.	39
Table 3.8:	ANOVA table of the main effects on the response Ln(M <sub>n</sub> )	41
Table 3.9:	ANOVA table of the main effects on the response M <sub>w</sub> /M <sub>n</sub>	43
Table 3.10:	ANOVA table of the main effects on the response particle size	47
Table 3.11:	ANOVA table of the main effects on the response fractional conversion of monomer to polymer	49
Table 3.12:	ANOVA table of the main effects on the response T <sub>g</sub> of the polymers	53
Table 3.13:	Results of the two 2 <sup>2</sup> -factorial designs to determine the distribution for IAN and PEI between the water and oil phase.	55
Table 3.14:	A summary of the stepwise regression of the 2 <sup>2</sup> -factorial design for the distribution of IAN between the water and oil phase.	55

### CHAPTER 4

Table 4.1:	Water solubility of chemical species resembling the propagating radical after transfer of the radical to the hydrophilic CTA	67
Table 4.2:	Different IAN concentrations used to determine the average number of free radicals per particle in a seeded emulsion polymerisation of styrene	73
Table 4.3:	The constants used to calculate the initiator concentration necessary to reach a 10% conversion of styrene monomer to polymer in the presence of chain transfer agents	74

Table 4.4:	Concentrations of the CTAs used for the different runs to obtain $k_{tr,CTA}$ for IAN and PEI	74
Table 4.5:	Table of the gradients of the plots of $\ln P(M)$ vs. $M$ for IAN and PEI at different concentrations of the CTA in the bulk polymerisation of styrene	80
Table 4.6:	$k_{tr,CTA}$ values for IAN and PEI in the solution polymerisation of styrene	83

---

## CHAPTER 5

Table 5.1:	Variables investigated in the factorial design with their respective high and low levels	91
Table 5.2:	The factor levels for the different co-polymerisation runs in the co-polymerisation of styrene and BA	92
Table 5.3:	The gradient used for the different solvents to separate the copolymer from the homopolymer	95
Table 5.4:	Table of the standards used to calibrate the column	96
Table 5.5:	Results of the GPC analysis on the styrene-butyl acrylate copolymers prepared	96

---

## APPENDIX A

Table A.1:	The factor levels as well as the treatments for a $2^3$ -factorial design	Aix
Table A.2:	ANOVA of the main factor effects of a $2^3$ -factorial design	Axi
Table A.3:	ANOVA for a linear regression model	Axii

---

## APPENDIX E

Table E.1:	Summary of the stepwise regression of the response $\ln(M_n)$ .	Ei
Table E.2:	Summary of the stepwise regression of the response MWD	Eii
Table E.3:	Summary of the stepwise regression of the response particle size	Eiii
Table E.4:	Summary of the stepwise regression of the response conversion	Eiv
Table E.5:	Summary of the stepwise regression of the response $T_g$	Ev

---

## APPENDIX F

Table F.1	Equations used to fit the data points for $\bar{n}$ versus time.	Fi
-----------	--	----

## LIST OF ABBREVIATIONS

ACN	acetonitrile
AIBN	azobis(isobutyronitrile)
ATRP	atom transfer radical polymerisation
BA	butyl acrylate
COV	coefficient of variation
CTA	chain transfer agent
df	degrees of freedom
DDI	distilled de-ionised water
DMF	N,N-dimethylformamide
DP	degree of polymerisation
$\overline{DP}$	average degree of polymerisation
DSC	differential scanning calorimetry
ELSD	evaporative light scattering detector
FID	flame ionisation detector
GC	gas chromatograph
G-HPLC	gradient high performance liquid chromatograph
GPC	gel permeation chromatography
IAN	iodoacetonitrile
IR	infrared
KPS	potassium persulphate
MMD	molecular mass distribution
MTEMPO	4-methoxy-2,2,6,6-tetramethylpiperidine-1oxyl
$M_n$	number average molecular mass of a polymer
$M_w$	mass average molecular mass of a polymer
$M_w/M_n$	polydispersity
NMR	nuclear magnetic resonance
PBA	poly(butyl acrylate)
PCS	photon correlation spectroscopy
PDI	polydispersity index

PEI	1-phenylethyl iodide
PS	polystyrene
RAFT	reversible addition-fragmentation chain transfer
SEC	size exclusion chromatography
SS	sum of squares
TBHP	tertiary butylhydroperoxide
TEMPO	2,2,6,6-tetramethylpiperidine-1-oxyl
T <sub>g</sub>	glass transition temperature
THF	tetrahydrofuran
VOC	volatile organic solvents
WISP	Waters intelligent sample processor

## LIST OF SYMBOLS

$a$	total surface area of the particles
$A_{st}$	area of the sample peak
$A_i$	area of the internal standard peak
$C_m$	concentration of a solute in the mobile phase
$C_s$	concentration of a solute in the stationary phase
$C_{aq}$	equilibrium solubility of the monomer in the aqueous phase
$C_p$	monomer concentration within the latex particles
$C_M$	equilibrium solubility of the monomer in the particle
$C_{CTA,p}$	CTA concentration in the latex particle
$C_{CTA,aq}$	CTA concentration in the aqueous phase
$C_{m,aq}$	monomer concentration in the aqueous phase
$C_{m,p}$	monomer concentration in the latex particle
$d(H)$	hydrodynamic diameter
$d_M$	density of monomer
$d_p$	density of polymer
$D$	diffusion coefficient
$D_{m,aq}$	diffusion coefficient of a monomeric free radical in the aqueous phase
$D_{CTA,aq}$	diffusion coefficient of a CTA free radical in the aqueous phase
$E(y)$	expected value of $y$
$f$	efficiency factor of the initiator
$F$	value obtained for the F-test at a certain confidence level
$H_0$	null-hypothesis
$H_1$	alternative hypothesis
$I_2$	initiator
$I^*$	initiating radical
$IM_1^*$	first propagating radical
$IM_{i+1}^*$	propagating radical consisting of $i+1$ monomer units
$k$	boltzmann's constant
$k_{act}$	rate constant for the activation of a CTA in a degenerative transfer reaction
$k_{deact}$	rate constant for the de-activation of a CTA in a degenerative transfer reaction

$k_d$	first-order rate coefficient for the dissociation of the initiator
$k_{dm}$	first-order rate coefficient for the desorption of the monomeric free radical from the particle into the aqueous phase
$k_{ex}$	exit rate coefficient for a radical from the latex particle
$k_{ex,CTA}$	Exit rate coefficient for a CTA radical from the latex particle
$k_{ex,m}$	exit rate coefficient for a monomeric radical from the latex particle
$k_p$	generic rate coefficient for propagation
$k_{p,aq}$	rate coefficient for propagation in the aqueous phase
$k_t$	second-order rate coefficient for termination within latex particles
$k_{t,aq}$	second-order rate coefficient for termination within the aqueous phase
$k_{tr,CTA}$	second-order rate coefficient for transfer to a CTA
$k_{tr,m}$	second-order rate coefficient for transfer to monomer
$k_{p1}$	rate coefficient for the first monomer to attach itself to the radical.
L	least squares function
$m_M$	mass of monomer per total volume(discrete plus continuous) in the reaction vessel
$m_M^0$	initial mass of the monomer per total volume (discrete plus continuous) in the reaction vessel
M	monomer
$M_0$	molecular mass of the monomer
$M_{aq}$	monomer in the aqueous phase
$M_n$	number average molecular mass
$M_t^n$	transitional metal
$M_t^{n+1}$	oxidised transitional metal
$M_w$	weight average molecular mass
n	number of data points in a sample set
$\bar{n}$	average number of free radicals per particle
$n_m^0$	initial number of moles of monomer present in latex particles per unit volume of aqueous phase
N	total number of observations in a population mean
N	total number of particles in the reaction vessel
$N_A$	Avogadro constant
$N_C$	latex particle density
$N_n$	number of latex particles containing n free radicals

$P_{\text{ex,CTA}}$	probability of exit from a latex particle by for a CTA free radical
$P_{\text{ex,m}}$	probability of exit from a latex particle by for a monomeric free radical
$P(M)$	number molecular mass distribution
$r_s$	radius of the swollen latex particle
$r_u$	radius of the unswollen latex particle
$R^*$	active radical specie that is formed after transfer of the iodine atom took place
$R^2$	coefficient of multiple determination
$R-X$	alkyl halide
$s$	sample standard deviation
$s^2$	sample variance
$SS$	sum of squares
$SS_A$	sum of squares of factor A
$SS_{AB}$	sum of squares of the interaction between factor A and factor B
$SS_B$	sum of squares of factor B
$SS_C$	sum of squares of the columns
$SS_E$	sum of squares of the total variation
$SS_R$	sum of squares of the rows
$SS_T$	total sum of squares
$T$	absolute temperature
$T^*$	any radical unit
$V_{Sm}$	partial molar volume of the monomer
$V_{Sp}$	partial molar volume of the polymer
$V(y)$	variance of $y$
$X$	fractional conversion
$\bar{X}$	critical value for the rejection of $H_0$
$y_i$	any sample set with $i = 1, 2, 3, \dots, n$
$y_{ij}$	response of the $j^{\text{th}}$ batch in the $i^{\text{th}}$ run
$z$	critical degree of polymerisation for entry into a latex particle

$\beta_i$	$i^{\text{th}}$ regression coefficient
$\beta_j$	effect of the $j^{\text{th}}$ level of the factor B
$\varepsilon$	random error term
$\gamma_k$	effect of the $k^{\text{th}}$ level of the factor C
$\eta$	viscosity
$\mu$	population mean value
$\nu$	volume of the swollen particles
$\rho$	pseudo–first–order rate coefficient for entry of free radicals into a latex particle
$\rho_m$	pseudo–first–order rate coefficient for entry of monomeric free radicals (z–mers) into a latex particle
$\rho_{\text{CTA0}}$	pseudo–first–order rate coefficient for entry of CTA free radicals (z–mers) into a latex particle
$\sigma$	standard deviation of the population.
$\sigma^2$	population variance
$\tau_i$	effect of the $i^{\text{th}}$ level of the factor A <sub>0</sub>

# INDEX

LIST OF FIGURES	i
LIST OF TABLES	vi
LIST OF ABBREVIATIONS	viii
LIST OF SYMBOLS	x

---

## CHAPTER 1

### INTRODUCTION

1.1	Background to the thesis	1
1.2	Importance of “living”/controlled radical polymerisation	1
1.3	“Living”/controlled emulsion polymerisation	2
1.4	Objectives	3
1.5	Outline of the thesis	5
1.6	Bibliography	6

---

## CHAPTER 2

### HISTORICAL BACKGROUND

2.1	Emulsion polymerisation	8
2.2	“Living”/controlled radical polymerisation	10
2.3	Chain transfer agents used in “living”/controlled radical polymerisation	12
2.3.1	Nitroxides as chain transfer agents	12
2.3.2	Macromolecular organometallic reagents as chain transfer agent	14
2.3.3	Atom transfer radical polymerisation as chain transfer reaction	14
2.3.4	Degenerative transfer as chain transfer reaction	15
2.3.5	Iniferters as chain transfer agents	15
2.3.6	Reversible addition–fragmentation chain transfer as chain transfer reaction	16
2.4	Bibliography	17

---

**THE EFFECTS OF ALKYL IODIDE CHAIN TRANSFER AGENTS ON THE PROPERTIES OF A SEEDED EMULSION POLYMERISATION OF STYRENE**

3.1	Introduction	21
3.2	Objectives	22
3.3	Theory	22
3.3.1	Chain transfer in radical polymerisation reactions	22
3.3.2	Chain transfer agents used in “living”/controlled radical polymerisation	23
3.3.3	Control of molecular masses with chain transfer agents	25
3.3.4	Control of molecular mass distributions with chain transfer agents	25
3.3.5	Chain transfer by means of degenerative transfer reactions	26
3.3.6	Iodoacetonitrile and 1–phenylethyl iodide as degenerative chain transfer agents	27
3.4	Experimental	28
3.4.1	Planning	28
3.4.2	Synthesis of 1-phenylethyl iodide	30
3.4.3	Particle size analysis of the latex particles	31
3.4.4	Preparation of the seed latex	32
3.4.5	Latex purification procedure	33
3.4.6	The seeded emulsion polymerisation of styrene in the presence of degenerative reacting chain transfer agents	33
3.4.7	Molecular mass and molecular mass distribution determinations	35
3.4.8	Glass transition temperature determinations	36
3.4.9	Determining the distribution of 1–phenylethyl iodide and iodoacetonitrile between the water and oil phase	36
3.4.10	The internal standard method of quantitative gas chromatogram evaluation via peak area	37
3.5	Results and discussion	38
3.5.1	Effects on the response molecular mass of the polymer	40
3.5.2	Effects on the response molecular mass distributions of the polymer	42
3.5.3	Effects on the response particle size of the latex particles	46
3.5.4	Effects on the response fractional conversion of monomer to polymer	48
3.5.5	Effects on the response glass transition temperature	52

3.5.6	The distribution of 1–phenylethyl iodide and iodoacetonitrile between the water and oil phase	54
3.6	Conclusions	56
3.7	Recommendations for future studies	56
3.8	Bibliography	57

---

## CHAPTER 4

### KINETICS OF THE SEEDED EMULSION POLYMERISATION OF STYRENE IN THE PRESENCE OF AN ALKYL IODIDE CHAIN TRANSFER AGENT

4.1	Introduction	60
4.2	Objectives	60
4.3	Theory	61
4.3.1	Emulsion polymerisation	61
4.3.2	The kinetics of emulsion polymerisation	64
4.3.3	Determining the rate coefficient of transfer to the chain transfer agent ( $k_{tr,CTA}$ )	69
4.3.4	Determining the initiator concentration to obtain a 10% conversion of monomer to polymer	71
4.4	Experimental	72
4.4.1	Determining the average number of free radicals per particle	72
4.4.2	Determining the initiator concentration necessary to obtain a 10% conversion to calculate the rate transfer constants for a chain transfer agent	73
4.4.3	Determining the rate transfer constants for iodoacetonitrile and 1–phenylethyl iodide	74
4.5	Results	75
4.5.1	Determining the average number of free radicals per particle	75
4.5.2	Transfer constants for chain transfer to iodoacetonitrile and 1–phenylethyl iodide	80
4.6	Conclusions	83
4.7	Recommendations for future study	84
4.8	Bibliography	84

**CHAPTER 5****CO-POLYMERISATION OF A FUNCTIONAL STYRENE SEED WITH BUTYL  
ACRYLATE**

5.1	Introduction	87
5.2	Objectives	87
5.3	Theory	88
5.3.1	The synthesis of block copolymers	88
5.3.2	Gradient high performance liquid chromatography (G-HPLC)	89
5.4	Experimental	91
5.4.1	Planning	91
5.4.2	Preparation of the functional styrene seed	92
5.4.3	Co-polymerisation of styrene and butyl acrylate	94
5.4.4	Gradient high performance liquid chromatography analysis	94
5.5	Results and discussion	97
5.5.1	Gel permeation chromatography analysis	97
5.5.2	Gradient high performance liquid chromatography analysis	97
5.6	Conclusions	100
5.7	Recommended future studies	100
5.8	Bibliography	101

**CHAPTER 6****CONCLUSIONS**

6.	Conclusions	102
----	-------------	-----

**APPENDIX A****EXPERIMENTS BASED ON AN EXPERIMENTAL DESIGN**

A.1	Introduction	A.i
A.2	Basic statistics	A.iii
A.2.1	Definitions	A.iv
A.2.2	Analysis of results	A.vi
A.2.3	Analysis of variance (ANOVA)	A.vii
A.3	2-level factorial designs	A.x
A.3.1	Main effects	A.xii

A.3.2	Statistical analysis	A.xiii
A.3.3	Regression model	A.xv
A.3.4	Response surfaces	A.xvi
A.4	Statistical package	A.xvii
A.5	Bibliography	A.xvii

---

**APPENDIX B**

**THE RESPONSE SURFACE PLOTS FOR THE RESPONSES OF THE  $2^{5-1}$ -  
FRACTIONAL FACTORIAL DESIGN**

Response surface plots	B.i
------------------------	-----

---

**APPENDIX C**

**NORMAL PROBABILITY PLOTS OF THE EFFECTS OF THE  $2^{5-1}$ -FRACTIONAL  
FACTORIAL DESIGN**

Normal probability plots of the effects	C.i
---	-----

---

**APPENDIX D**

**PARETTO CHARTS OF THE EFFECTS OF THE  $2^{5-1}$ -FRACTIONAL FACTORIAL  
DESIGN**

Pareto charts	D.i
---------------	-----

---

**APPENDIX E**

**STEPWISE REGRESSION OF THE  $2^{5-1}$ -FRACTIONAL FACTORIAL DESIGN**

Stepwise regression of the $2^{5-1}$ -factorial design	E.i
--	-----

---

**APPENDIX F**

**PLOT OF THE AVERAGE NUMBER OF FREE RADICALS PER LATEX PARTICLE**

Plot of the average number of free radicals per latex particle for the  $\bar{n}$  vs. time plots      Fi

---

**APPENDIX G**

**RELATION BETWEEN THE CONVERSION OF MONOMER TO POLYMER AND THE  
PARTICLE SIZE**

Fractional conversion *versus* particle size      Gi

# CHAPTER 1

## INTRODUCTION

### 1.1 BACKGROUND TO THE THESIS

The thesis describes a free-radical polymerisation process which has characteristics of a living polymerisation system as it is capable of producing polymers of pre-determined molecular masses with a narrow molecular mass distribution (MMD) and, further, by successively adding different monomers, it can be used to make block-copolymers. The process can also be used to produce polymers of more complex structure such as star polymers, core-shell polymers and gradient polymers. A polymer is defined as a substance of molecules characterised by the multiple repetition of one or more molecule units while polymerisation is the process of converting these monomer units into a polymer.<sup>1</sup> Co-polymerisation is defined as a polymerisation in which two or more structurally distinct monomers are incorporated into the same polymer chain.<sup>2</sup> A "living" system is one in which an active propagating polymer chain is end-capped to produce a dormant polymer chain. The dormant chain can be reactivated in a subsequent step, allowing further polymerisation of the polymer chain.<sup>3</sup>

### 1.2 IMPORTANCE OF "LIVING"/CONTROLLED RADICAL POLYMERISATION

The control of the micro- and macrostructure of polymers is of industrial importance. The macro properties of industrial products are directly related to their molecular mass, MMD and particle size, etc.<sup>4</sup>

Polymeric formulations are constantly being revised to obtain the best industrial polymers in a very competitive market. Traditional polymers, and even polymer blends, do not always provide the optimum properties that a manufacturer seeks, for example the correct glass transition temperature ( $T_g$ ) and tensile strength. In the paint industry, at present,

paint–bases consisting of a copolymer structure are considered to be the best structure to obtain these properties.

Emulsion polymerisation is an industrially important process used, for example, to make binders, adhesives and a host of other commodity and hi-tech materials. The fundamentals in this field involve both free-radical polymerisation and colloid science, and the mechanisms of emulsion polymerisation are both complex and difficult to deduce experimentally. Methods to control emulsion polymerisation are widely sought.

One reason why it is especially paint–formulations that are constantly revised is to achieve a reduction in the concentration of organic solvents in polymers, to prevent volatile organic solvents (VOC) being emitted into the atmosphere. Making use of water–based paint systems is one possible answer to the problem. It is for this reason that the polymerisation to create polymers for paint formulations are done in emulsion where water is the medium of polymerisation. Problems are encountered in creating more tailored structures as radical polymerisation has a high rate of propagation, making it very difficult to control the structures of the polymers that are formed.

### **1.3 “LIVING”/CONTROLLED EMULSION POLYMERISATION**

Unlike other vinyl–polymerisation methods, radical polymerisation can be used with numerous monomers because it tolerates a wide variety of functional groups. It is much less sensitive than anionic or cationic processes for it can be used in different reaction media and reactions proceed at convenient temperatures. This makes it suitable to polymerise in water, especially in emulsion polymerisation.

As was mentioned in section 1.2, the control of the molecular mass and MMD of polymers leads to control over the macro properties of the product. Although the understanding and development of theoretical descriptions of an emulsion polymerisation is complex, because of the heterogeneity of the system, mechanistic models have been developed in order to obtain some control of the MMD, molecular mass and other important variables.

A new method referred to as “living”/controlled radical polymerisation has been widely published. “Living”/controlled radical polymerisation refers to a specific type of polymerisation in which the active centre remains dormant after complete polymerisation, preventing irreversible, bi-molecular termination from taking place. This then allows new monomer to be added to the existing chains after re-initiation. To achieve this, a chain transfer agent (CTA) that is able to activate and de-activate propagating radicals, reversibly, is required.<sup>5</sup> “Living”/controlled radical polymerisation has proved to be a very effective way of controlling the molecular mass and especially the MMD of polymers. A further advantage is its ability to control the morphology of the polymers and produce “perfect” block-copolymers<sup>6</sup>, gradient copolymers<sup>7</sup> and end functional polymers<sup>8</sup>.

Polymers produced via “living”/controlled radical polymerisation have the following advantages:<sup>6</sup>

- The fine structure of the polymer can be controlled.
- The molecular mass of the polymer can be controlled.
- The morphology of the particle can be controlled.
- Functional seed latex can be produced leading to macromonomers (macromers) with either iodine end-groups or double bonds.
- Iodine end-groups can be reacted with various reagents to produce other specific end-groups.

#### 1.4 OBJECTIVES

To date, most of the experimental work which has been done on “living”/controlled radical polymerisation was done in bulk and solution.<sup>9-13</sup> Results of only a few investigations into “living”/controlled radical polymerisation in emulsion have been described in the literature.<sup>14-16</sup>

Alkyl iodides proved to be effective CTAs in bulk and solution polymerisation because they need low activation energy for transfer of the iodine atom to take place. No mention of

work being done on the use of alkyl iodides to obtain a “living” radical polymerisation in emulsion has been found. The basic aim of this thesis is therefore to describe the results of the effects of alkyl iodides as CTAs on the seeded emulsion homo- and co-polymerisation of styrene and butyl acrylate.<sup>8,11,17</sup> Styrene and butyl acrylate were used because the constants describing an emulsion polymerisation of these monomers are well known. There were three main objectives of this work.

First, the effects of selected variables on certain responses were to be investigated in the seeded emulsion polymerisation of styrene. The variables included the use of: two different alkyl iodides as CTAs, different concentrations of the CTAs, different monomer concentrations, different types of initiators and different initiator concentrations. The alkyl iodides that were to be used were iodoacetonitrile (IAN) and 1-phenylethyl iodide (PEI) because of their effective ability to produce “living”/controlled radical polymerisation reactions.<sup>16</sup> The responses to be investigated included the following physical properties of the synthesised polymers: the molecular mass, MMD,  $T_g$ , conversion of monomer to polymer and particle sizes of the latex particles. A  $2^{k-l}$ -fractional factorial design was to be used for the design and analysis of the experiments.

Second, the effect IAN, as CTA, has on the kinetics of a seeded styrene emulsion polymerisation was to be investigated. Attention was to be focused on the conversion of monomer to polymer to calculate the change in the average number of radicals per latex particle ( $\bar{n}$ ) and calculating the second-order rate coefficient of transfer from the propagating radical to the CTA ( $k_{tr,CTA}$ ). A gas chromatograph (GC) was to be used to determine the conversion of monomer to polymer while a gel permeation chromatograph (GPC) was to be used to determine  $k_{tr,CTA}$ .

Third, the possibility of producing block-copolymers in emulsion with alkyl iodides as CTAs was investigated. It was the aim to produce a functional styrene seed with a dormant chain-end and use the functional seed to co-polymerise in a second stage with butyl acrylate to produce styrene-butyl acrylate block-copolymers. Gradient high performance liquid chromatography (G-HPLC) was to be used to verify that a block copolymer was formed.

## 1.5 OUTLINE OF THE THESIS

- Chapter 1:  
An introduction of the investigation covered by the thesis is given.
- Chapter 2:  
An historical review of the background to radical polymerisation, emulsion polymerisation and “living”/controlled polymerisation is done.
- Chapter 3:  
The effects of alkyl iodides as CTAs on the molecular mass, MMD,  $T_g$ , conversion and particle size for the seeded emulsion polymerisation of styrene are investigated, using a fractional factorial design, and discussed.
- Chapter 4:  
The effects of alkyl iodides as CTAs on the kinetics of radical emulsion polymerisation, especially the average amount of radicals per latex particle are investigated and discussed.
- Chapter 5:  
The possibility of producing block–copolymers by emulsion polymerisation using alkyl iodides as CTAs are investigated.
- Chapter 6:  
The conclusions of the investigation related to the thesis are given.

All symbols and abbreviations used in the succeeding chapters are explained in the List of Symbols and the List of Abbreviations.

## 1.6 BIBLIOGRAPHY

1. Allen, G; Bevington, J.C. **Comprehensive Polymer Science: The synthesis, characterization, reactions & applications of polymers**, Pergamon Press, Oxford, pp 17 – 18, 1989.
2. Mark, H.F.; Bikales, N.M.; Overberger, C.G.; Menges, G.; Kroschwitz, J.I. **Polymer Encyclopedia**, Wiley & Sons, New York, Vol. 4, p192, 1985.
3. Matyjaszewski, K. *From “living” carbocationic to “living” radical polymerization*, **Journal of Macromolecular Science, Pure and Applied Chemistry**, A 31, 989, 1994.
4. Gowariker, V.R.; Viswanathan, N.V.; Sreedhar, J. **Polymer Science**, Wiley & Sons, New York, p. 136, 1986.
5. Matyjaszewski, K.: <http://www.chem.cmu.edu/Matyjaszewski.html>.
6. Gaynor, S.G.; Matyjaszewski, K. *Step-growth polymers as macroinitiators for “living” radical polymerization: Synthesis of ABA block copolymers*, **Macromolecules**, 30, 4241, 1997.
7. Greszta, D.; Matyjaszewski, K. *Gradient copolymers – a new class of materials*, **Polymer Preprints, American Chemical Society, Division Polymer Science**, 37, 569, 1996.
8. Nakagawa, Y.; Gaynor, S.G.; Matyjaszewski, K. *The synthesis of end functional polymers by “living” radical polymerization*, **Polymer Preparations, American Chemical Society, Division Polymer Chemistry**, 37, 577, 1996.
9. Doi, T.; Matsumoto, A.; Otsu, T. *Elucidation of mechanism for living radical polymerization of styrene with N,N-diethyldithiocarbamate derivatives as iniferters by the use of spin trapping technique*, **Journal of Polymer Science Part A: Polymer Chemistry**, 32, 2241, 1994.
10. Solomon, D.H.; Looney, M.G. *Structural control by living radical polymerization*, **Plastics Engineering**, New York, 40, 15, 1997.

11. Matyjaszewski, K.; Gaynor, S.; Wang, J-S. *Communications to the editor: Controlled radical polymerizations: The use of alkyl iodides in degenerative transfer*, **Macromolecules**, 28, 2093, 1995.
12. 11. Gaynor, S.; Wang, J-S.; Matyjaszewski, K. *Controlled radical polymerization by degenerative transfer: Effect of the structure of the transfer agent*, **Macromolecules**, 28, 8051, 1995.
13. Gaynor, S.; Wang, J-S.; Matyjaszewski, K. *Well defined polymers obtained through the use of controlled radical polymerization: The use of alkyl iodides as degenerative transfer reactions*, **Polymer Preprints, American Chemical Society, Division Polymer Chemistry**, 36, 467, 1995.
14. Bon, S.A.F.; Bosveld, M; Klumperman, B; German, A.L. *Controlled radical polymerization in emulsion*, **Macromolecules**, 30, 324, 1997.
15. Kukulj,D.; Davis, T.P.; Gilbert, R.G. *Catalytic chain transfer in miniemulsion polymerization*, **Macromolecules**, 30, 7661, 1997.
16. Kukulj,D.; Davis, T.P.; Suddaby, K.G.; Haddleton, D.M.;Gilbert, R.G. *Catalytic chain transfer for molecular weight control in the emulsion homo- and copolymerization of methyl methacrylate and butyl methacrylate*, **Journal of Polymer Science Part A: Polymer Chemistry**, 35, 859, 1997.
17. Gaynor, S.; Wang, J-S.; Matyjaszewski, K. *Controlled radical polymerization by degenerative transfer: Effect of the structure of the transfer agent*, **Macromolecules**, 28, 8051, 1995.

# CHAPTER 2

## HISTORICAL BACKGROUND

### 2.1 EMULSION POLYMERISATION

Emulsion polymerisation originated during the First World War. Since the first patent was published describing emulsion polymerisation, much work on the mechanisms and kinetics of emulsion polymerisation has been done.

Emulsion polymerisation is a method of free radical polymerisation, the mechanism of which is well documented by Moad<sup>1</sup>; carried out in a water medium. The product is an emulsion, also known as a latex. The main ingredients for an emulsion polymerisation are:

- Water as the reaction medium.
- A vinyl type monomer.
- Free radical initiators.
- Surfactants (surface-active agents), also called emulsifiers, that stabilise the latex particles in the water.
- Buffer to control the pH.
- Chain transfer agents to control the molecular mass of the polymers.

During an emulsion polymerisation, a reactor is charged with water and surfactant. Monomer is added and stirred to allow emulsification of the monomer. This is followed by the addition of the initiator to initiate the polymerisation.

Emulsion polymerisation has the following advantages over conventional radical polymerisation:<sup>2</sup>

- Heat of the reaction is easily dissipated.
- High rates of polymerisation are achieved.
- Products of high average molecular masses are achieved.
- The polymer is formed as a latex.
- Molecular mass can be controlled with CTAs.

- High conversions can be obtained.

Some of the disadvantages of emulsion polymerisation are:<sup>2</sup>

- The emulsion contains a large number of additives that may influence the quality of the final product.
- It may be necessary to separate the product from the water, thus leading to an extra processing step.
- Because of the heterogeneity of the system, the process is difficult to control.

The major reactions that take place in and around the latex particle in emulsion polymerisation are illustrated in Figure 2.1.<sup>3</sup> An explanation of the symbols used is given in the List of Symbols.

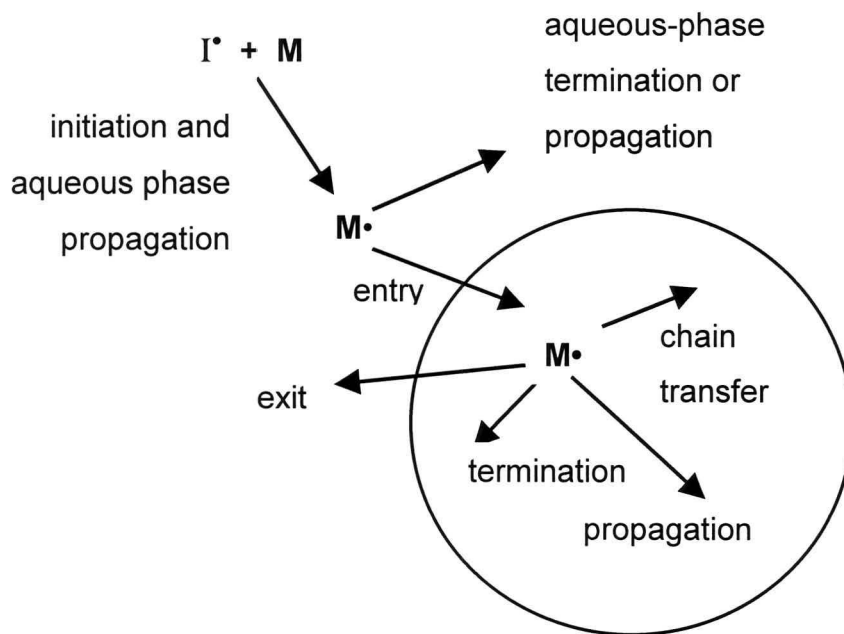


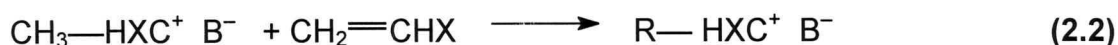
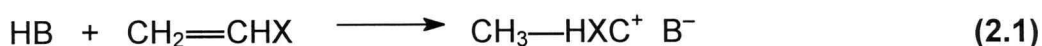
**Figure 2.1:**

**An illustration of the major free-radical reactions taking place in and around a latex particle.**

## 2.2 “LIVING”/CONTROLLED RADICAL POLYMERISATION

The first possibility of the living radical polymerisation of styrene in emulsion polymerisation was pointed out in 1957 using intermittent irradiation with ultra-violet light. The use of living radical polymerisation led to ultra high molecular mass polystyrene molecules with a polydispersity ( $M_w/M_n$ )<sup>4</sup> of 1.01 – 1.13, with  $M_w$  the mass average molecular mass of the polymers sensitive to the high molecular mass species and  $M_n$  the number average molecular mass of the polymers sensitive to the low molecular mass species. Besides “living”/controlled radical polymerisation, the only low  $M_w/M_n$  polymer molecules were produced by the use of ozonised polypropylene and some reducing agents as initiators.<sup>5</sup>

Living polymerisation is classically defined as a chain reaction during which no termination or transfer occurs, with the consequence that all polymer molecules in the system are capable of growth as long as there is monomer present. However, because of transfer and termination, this is not practically realised. A better definition of a living system is one in which the capacity of growth remains indefinite.<sup>6</sup> Living carbocationic polymerisation has been successfully used to produce polymer molecules with MMDs < 1.2. These low MMDs are obtained when the rate of transfer between the species in the reaction medium is greater than the rate of propagation. Usually a Lewis acid attacks a vinyl monomer as given in eq. 2.1 and eq. 2.2:

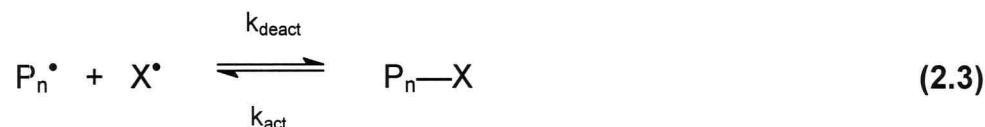


The propagating species is end-capped by the anion to prevent termination. This results in a living polymer chain.

Controlled radical polymerization is defined as a synthetic method for preparing polymers with predetermined molecular weights ( $DP = \Delta[M]/[I]_0$ ), low polydispersity and controlled functionality, leading to block co-polymers.<sup>6</sup>

According to Matyjaszewsky there are three requirements for controlled/"living" radical polymerisation.<sup>7</sup> The rate of propagation is proportional to the first power of the concentration of radicals present (see eq. 4.8), defining a first order reaction.<sup>8</sup> Further, the rate of termination is proportional to the second power of the concentration of radicals present (see eq. 4.8), defining a second order reaction.<sup>9</sup> Therefore, a small concentration of radicals need to be present in the system to ensure that the propagation rate is greater than the termination rate. To overcome this problem the chains must be relatively short. This can be achieved if the concentration of the growing chains is greater than the concentration of the free radicals initially produced at initiation. All the chains must possess the ability to grow during the entire reaction. The system would therefore consist of active radical centres that propagate as well as dormant species. During the reaction it must be possible for these dormant species to be activated and another radical to be deactivated. There should however be a dynamic equilibrium between the active radicals and the dormant species. Thirdly, initiation must occur very fast to provide a constant concentration of growing chains.

The reaction illustrating the activation and deactivation of a propagating polymer radical is given in eq. 2.3.



The characteristics of a "living"/controlled radical polymerisation are as follows:<sup>7</sup>

- All monomer is consumed.
- $M_n$  is a function of conversion.
- Constant amounts of active centres are present.
- Molecular mass can be controlled stoichiometrically.
- $MMD < 1.5$  at 100% conversions.
- Block co-polymers can be formed.

## 2.3 CHAIN TRANSFER AGENTS USED IN “LIVING”/CONTROLLED RADICAL POLYMERISATION

Two basic techniques exist for “living”/controlled radical polymerisations. The first is through reversible homolytic dissociation and the other through degenerative transfer. According to Matyjaszewski<sup>10</sup> there are four groups in which these techniques can be categorised. First, there are the non-catalytic systems with stable organic counter radicals such as nitroxides, dithiocarbamates, and bulky diaryl or triaryl alkyl radicals.<sup>11-16</sup> Second, there are non-catalysed systems with organometallic scavengers. It is cobalt which is normally used although the use of other compounds such as aluminium and chromium based systems have been reported.<sup>17-20</sup> Third, there is catalysed atom transfer radical polymerisation (ATRP) with alkylhalides as the dormant species. The transition metal compounds based on copper, iron, nickel; ruthenium etc. are used as reversible redox catalysts.<sup>21-34</sup> The fourth method is degenerative transfer, based on the bimolecular exchange reaction between alkyl iodides and conventional radical initiators.<sup>35-37</sup> Other techniques for trapping the radical to prevent bimolecular termination are described in the literature. One is the use of iniferters (*initiator, transfer agent and terminator*).<sup>37-41</sup> Currently the most exciting CTA mechanism being investigated is termed RAFT (Reversible addition-fragmentation chain transfer). Here the preferred class of CTA is the dithioesters.<sup>7</sup>

### 2.3.1 Nitroxides as chain transfer agents

A common example of nitroxides as chain transfer agents is the use of the alkoxyamine 1-*tert*-butoxy-2-phenyl-2-(1-oxy-2,2,6,6-tetramethylpiperidinyl)ethane to give TEMPO (2,2,6,6-tetramethylpiperidine-1oxyl). The reaction illustrating the dissociation of the alkoxyamine to produce TEMPO is given in Figure 2.1.<sup>13</sup>

Alkoxyamines are thermally labile. On thermolysis, the C–O bond on the alkoxyamine cleaves to form a nitroxide and an alkyl radical. The alkyl radical initiate polymerisation while the nitroxide can recombine with any radical, without initiating propagation.<sup>38</sup>

When TEMPO is used as the CTA, polydispersities of  $1.2 \leq M_w/M_n \leq 1.4$  are achieved. Polymerisation with TEMPO is restricted to styrene and styrene copolymers. It is, however, also possible to polymerise other monomers if nitroxides with larger steric or electrostatic repulsion are used. The temperature range for the reaction is 110–140°C and the reaction is well controlled with molecular masses < 50 000. The molecular masses can be predetermined by the ratio of reacted monomer to the initial concentration of TEMPO or its adducts.<sup>10</sup>

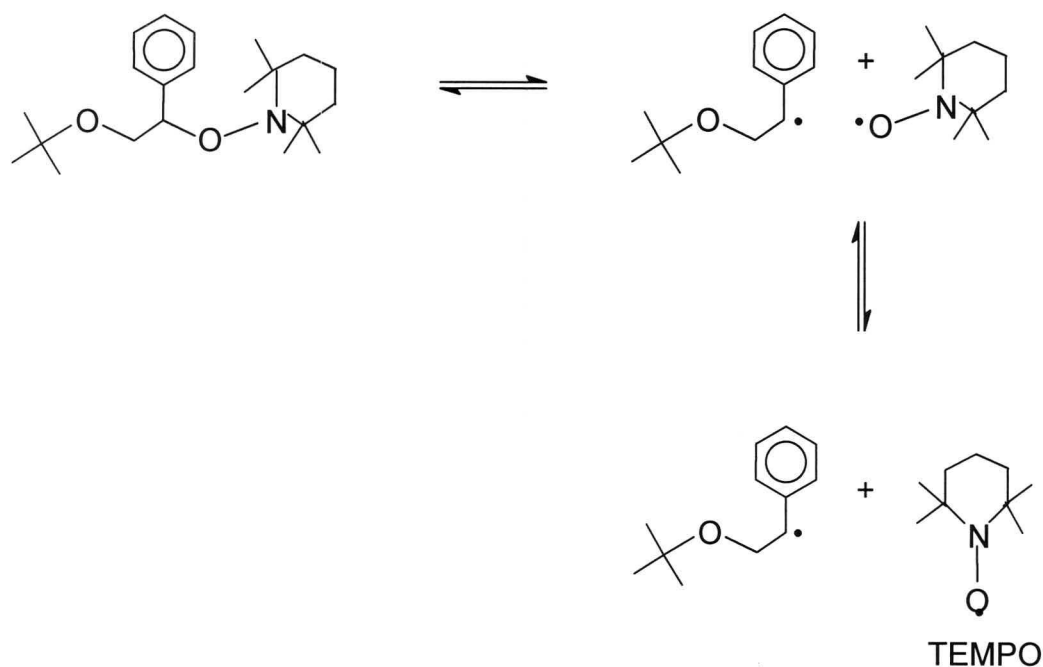


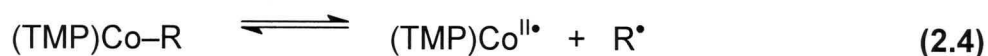
**Figure 2.2:**

**The dissociation of an alkoxyamine to produce the CTA TEMPO.**

In only one instance in the literature were “living”/controlled radical polymerisation used in emulsion polymerisation. In this specific case, Bon *et al* used TEMPO as CTA in a seeded system. They found that prolonged reaction times led to broadening of MMD. To their believe, this was probably due to the instability of the alkoxyamine bond. The system that was used functioned at elevated temperatures. Especially in emulsion polymerisation it is necessary to work at low temperatures.<sup>15</sup>

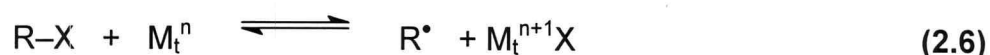
### 2.3.2 Macromolecular organometallics reagents as chain transfer agents

During radical polymerisation in the presence of macromolecular organometallics as chain transfer agents, the weak bond between a methyl group and cobalt atom is cleaved. Usually Co (II) porphyrin complexes are used.<sup>43</sup> Cobalt derivatives have a great affinity for hydrogen atoms, resulting in  $\beta$ -H abstraction during methacrylic polymerisation. The transfer of the  $\beta$ -H forms the basis of the catalytic chain transfer reaction. Other types of metals may also be used. An example of Co (II) porphyrin complexes as CTA is the polymerisation of acrylates by the organocobalt porphyrin complex, (tetramesitylporphyrinato)cobalt neopentyl (TMP)Co-CH<sub>2</sub>C(CH<sub>3</sub>)<sub>3</sub>.<sup>15</sup> The reaction is given in eq. 2.4 and eq. 2.5 where R = CH<sub>2</sub>C(CH<sub>3</sub>)<sub>3</sub>. Eq. 2.4 is the reversible activation and deactivation reaction of the CTA. The alkyl radical, R<sup>•</sup>, can be of any degree of polymerisation (DP).



### 2.3.3 Atom transfer radical polymerisation (ATRP) as chain transfer reaction

Using a simple alkyl halide as an initiator and a transition-metal species with suitable ligands as a catalyst, the ATRP of alkenes proceeds with a negligible amount of irreversible termination and other transfer reactions. Polymer molecules with predetermined molecular masses and a polydispersities < 1.2 are obtained. The mechanism for the reversible activation and deactivation of the CTA in ATRP is given in eq. 2.6.<sup>33</sup>



The alkyl radical, R<sup>•</sup>, can either polymerise similar to eq. 2.5 or be deactivated.

### 2.3.4 Degenerative transfer as chain transfer reaction

The low activation energy necessary to subtract the iodine atom from an alkyl iodide makes these chemical species effective CTAs. The alkyl iodide must have a radical stabilising substituent in order to efficiently transfer the iodide from the dormant to an active chain and *vice versa* for the radical. Because alkyl iodides do not generate radicals spontaneously, they participate exclusively in bimolecular exchange. The reaction is given in eq 2.7.<sup>36</sup>



Growing radicals react bi-molecularly with the CTA, to become a dormant species by transferring a group or atom. The new radical reacts with monomer to become a propagating polymer chain similar to eq. 2.5, making transfer of the iodine from another dormant chain possible. The transfer is thermodynamically neutral (degenerative). The total number of chains in the system is the sum of the chains generated by initiator and those formed by the transfer agent. Even if radicals terminate in the usual way, the maximum amount of irreversibly terminated chains cannot exceed the initiator concentration. When there is a large excess of the transfer agent present, relative to the initiator, the proportion of chains irreversibly terminated is very low and almost all chains will be end-capped with an iodide group that can be re-activated.

### 2.3.5 Iniferters as chain transfer agents

During thermolysis or photolysis, the initiator forms two radicals (see eq. 2.8). The one radical, unlike the other, is reactive towards the monomer and allows propagation, similar to the one given in eq. 2.5. The second radical is only capable of reversibly terminating the growing radical chain.





## 2.4 BIBLIOGRAPHY

1. Moad, G.; Solomon, D.H. **The Chemistry of Free Radical Polymerisation**. Elsevier Science Inc., Australia, 1995.
2. Gilbert, R.G. **Emulsion Polymerisation, a Mechanistic Approach**, Academic Press, London, p. 14 – 15, 1995.
3. Gilbert, R.G. **Emulsion Polymerisation, a Mechanistic Approach**, Academic Press, London, p. 69, 1995.
4. Billmeyer, F.W. **Textbook of Polymer Science**, 3<sup>rd</sup> ed., Wiley & Sons, New York, p. 18, 1984.
5. Otsu, T.; Yoshida, M.; Tazaki, T. *A model for living radical polymerization*, **Macromolecular Chemistry, Rapid Communications**, 3, 133, 1982.
6. Matyjaszewski, K. *From “living” carbocationic to “living” radical polymerization*, **Journal of Macromolecular Science, Pure and Applied Chemistry**, A 31, 989, 1994.
7. Le, T.P.T.; Moad, G.; Rizzardo, E.; Thang, S.H. **International Patent Application PCT/US97/12540; WO9801478** (Chemical Abstracts 128, 1998: 115390).
8. Laidler, K.J.; Meiser, J.H. **Physical Chemistry**, The Benjamin Cummings publishing company Inc., California, p. 350, 1982.
9. Laidler, K.J.; Meiser, J.H. **Physical Chemistry**, The Benjamin Cummings publishing company Inc., California, p. 351, 1982.
10. Matyjaszewski, K. <http://www.chem.cmu.edu/Matyjaszewski.html>.
11. Yoshida, E.; Okada, Y. *Living radical polymerization of styrene in the presence of 4-hydroxy-2,2,6,6-tetramethylpiperidine-1-oxyl and radical transformation of the resulting polymer by other radicals*, **Bulletin, Chemical Society of Japan.**, 70, 275, 1997.
12. Yoshida, E.; Tanimoto, S. *Living radical polymerization of styrene by a stable nitroxyl radical and macroazoinitiator*, **Macromolecules**, 30, 4018, 1997.
13. Hammouch, S.O.H.; Catala, J–M. *“Living radical” polymerization of styrene in the presence of a nitroxide compound*, **Macromolecular Rapid Communications**, 17, 683, 1996.
14. Moad, G.; Rizzardo, E. *Alkoxyamine–initiated living radical polymerization: Factors affecting alkoxyamine homolysis rates*, **Macromolecules**, 28, 8722, 1995.

15. Bon, S.A.F.; Bosveld, M.; Klumperman, B.; German, A.L. *Controlled radical polymerization in emulsion*, **Macromolecules**, 30, 324, 1997.
16. Yoshida, E.; Fujii, T. *Synthesis of well-defined polychlorostyrenes by living radical polymerization with 4-methoxy-2,2,6-tetramethylpiperidine-1-oxyl*, **Journal of Polymer Science, Part A: Polymer Chemistry**, 35, 2371, 1997.
17. Wei, M.; Wayland, B.B. *Quasi-living radical polymerization of acrylates by an organocobalt porphyrin complex at room temperature*, **Polymer Preprints, American Chemical Society, Division Polymer Chemistry**, 38, 681, 1997.
18. Davis, T.P.; Kukulj, D.; Haddleton, D.M.; Maloney, D.R. *Cobalt-mediated free-radical polymerization of acrylic polymers*, **Trends in Polymer Science**, 3, 365, 1995.
19. Wayland, B.B.; Poszmik, G.; Mukerjee, S.L.; Florian, S. *Living radical polymerization of acrylates by organocobalt porphyrin complexes*, **Journal of the American Chemical Society**, 116, 7943, 1994.
20. Mardare, D.; Gaynor, S.; Matyjaszewski, K. *Radical polymerization of vinyl acetate and methyl methacrylate using organochromium initiators complexed with macrocyclic polyamines*, **Polymer Preprints**, 35, 700, 1994.
21. Uegaki, H.; Kotani, Y.; Kamigaito, M.; Sawamoto, M. *Nickel-mediated living radical polymerization of methyl methacrylate*, **Macromolecules**, 30, 2249, 1997.
22. Percec, V.; Barboiu, B. *"Living" radical polymerization of styrene initiated by arenesulfonyl chlorides and Cu1(bpy)nCl*, **Macromolecules**, 28, 7970, 1995.
23. Ando, T.; Kamigaito, M.; Sawamoto, M. *Iron(II)chloride complex for living radical polymerization of methyl methacrylate*, **Macromolecules**, 30, 4507, 1997.
24. Nishikawa, T.; Ando, T.; Kamigaito, M.; Sawamoto, M. *Evidence for living radical polymerization of methyl methacrylate with ruthenium complex: Effects of protic and radical compounds and reinitiation from the recovered polymers*, **Macromolecules**, 30, 2244, 1997.
25. Wei, M.; Wayland, B.B. *Quasi-living radical polymerization of acrylates by an organocobalt porphyrin complex at room temperature*, **Polymer Preprints, American Chemical Society, Division Polymer Chemistry**, 38, 681, 1997.
26. Sawamoto, M.; Kamigaito, M. *Transition metal-mediated living radical polymerization: Recent advances*, **Polymer Preprints, American Chemical Society, Division Polymer Chemistry**, 38, 740, 1997.

27. Percec, V.; Barboiu, B. *Metal catalyzed "living" radical polymerization initiated with sulfonyl halides*, **Polymer Preprints, American Chemical Society, Division Polymer Chemistry**, 38, 733, 1997.
28. Ando, T.; Kato, M.; Kamigaito, M.; Sawamoto, M. *"Living" radical polymerization of methyl methacrylate with ruthenium complex: Formation of polymers with controlled molecular weights and very low distributions*, **Macromolecules**, 29, 1070, 1996.
29. Wei, M.; Matyjaszewski, K.; Patten, T.E. *Model studies of slow termination process in the polymerization of styrene by atom transfer radical polymerization*, **Polymer Preprints, American Chemical Society, Division Polymer Chemistry**, 38, 683, 1997.
30. Grimaud, T.; Matyjaszewski, K. *Controlled "living" radical polymerization of ethyl methacrylate by atom transfer radical polymerization*, **Macromolecules**, 30, 2216, 1997.
31. Qui, J.; Matyjaszewski, K. *Polymerization of substituted styrenes by atom transfer radical polymerization*, **Macromolecules**, 30, 5643, 1997.
32. Wang, J-S.; Matyjaszewski, K.; *Controlled "living" radical polymerization. Halogen atom transfer radical polymerization promoted by a Cu(I)/Cu(II) redox process*, **Macromolecules**, 28, 7901, 1995.
33. Haddleton, D.M.; Waterson, C.W.; Derrick, P.J.; Jasieczek, C.B.; Shooter, A.J. *Monohydroxy terminally functionalized poly(methyl methacrylate) from atom transfer radical polymerisation*, **Chemical Communications**, p. 683, 1997.
34. Patten, T.; Xia, J.; Abernathy, T.; Matyjaszewski, K.; *Polymers with very low polydispersities from atom transfer radical polymerization*, **Science**, 272, 866, 1996.
35. Matyjaszewski, K.; Gaynor, S.; Wang, J-S. *Communications to the editor: Controlled radical polymerizations: The use of alkyl iodides in degenerative transfer*, **Macromolecules**, 28, 2093, 1995.
36. Gaynor, S.; Wang, J-S.; Matyjaszewski, K. *Controlled radical polymerization by degenerative transfer: Effect of the structure of the transfer agent*, **Macromolecules**, 28, 8051, 1995.
37. Gaynor, S.; Wang, J-S.; Matyjaszewski, K. *Well defined polymers obtained through the use of controlled radical polymerization: The use of alkyl iodides as degenerative transfer reactions*, **Polymer preprints, American Chemical Society, Division Polymer Chemistry**, 36, 467, 1995.

38. Solomon, D.H.; Looney, M.G. *Structural control by living radical polymerization*, **Plastics Engineering, New York**, 40, 15, 1997.
39. Doi, T.; Matsumoto, A.; Otsu, T. *Elucidation of mechanism for living radical polymerization of styrene with N,N-diethyldithiocarbamate derivatives as iniferters by the use of spin trapping technique*, **Journal of Polymer Science Part A: Polymer Chemistry**, 32, 2241, 1994.
40. Otsu, T.; Tazaki, T. *Living radical polymerization in homogeneous system with phenylazotriphenylmethane as thermal iniferter*, **Polymer Bulletin**, 16, 277, 1986.
41. Otsu, T.; Matsumoto, A.; Tazaki, T. *Living radical polymerization of methyl methacrylate with tetraphenylsuccinodinitrile as a thermal iniferter*, **Memoirs, Faculty of Engineering, Osaka City University**, 27, 137, 1986.
42. Otsu, T.; Matsumoto, A.; Yoshioka, M. *Macromolecular design by living radical polymerization using iniferter technique*, **Indian Journal of Technology**, 31, 172, 1993.
43. Moad, G.; Solomon, D.H. **The Chemistry of Free Radical Polymerisation**. Elsevier Science Inc., Australia, p. 249, 1995.

## CHAPTER 3

### THE CONTROL OF MOLECULAR MASSES AND MOLECULAR MASS DISTRIBUTIONS BY CHAIN TRANSFER AGENTS

#### 3.1 INTRODUCTION

In radical reactions, termination is the most important chain stopping reaction that can occur. These termination reactions do not only influence the average molecular mass of the polymer but the MMD as well. A wide MMD is usually obtained as a result of bi-molecular termination. The molecular mass and MMD are important factors in the macroscopic properties of a polymer, such as: film formation, viscosity, melting point, and softening point, as well as many other properties.<sup>1</sup> It is most important to be able to control the molecular mass of the synthesised polymers in emulsion free-radical polymerisation.

The addition of conventional CTAs in emulsion polymerisation has been used to control the molecular mass of polymers and the nature of the polymer end-groups.<sup>2</sup> These CTAs create new active centres and terminate the original active radical at a decreased molecular mass and result in lower molecular mass polymers.<sup>3</sup> The resulting free radical on the CTA can initiate another radical chain to allow further polymerisation, depending on the reactivity of the newly formed radical. Conventional CTAs can be used in emulsion polymerisation to control the molecular mass of the polymers. These CTAs do not influence the amount of bi-molecular termination that takes place. As a result a wide distribution of molecular masses are obtained, making it difficult to control the MMD of the polymer molecules that are produced.

In recent years the use of CTAs with a “living” character was introduced. The effect of these special CTAs on the molecular masses of polymers has been investigated extensively.<sup>4-8</sup> The DP of the polymers produced in “living”/controlled radical polymerisation is equal to the ratio of the monomer to catalyst, while the MMD is Poisson in character.<sup>9</sup> In most of the cases where a CTA with a “living” character was used,  $M_w/M_n$

of the polymer was much less than the  $M_w/M_n$  in conventional radical polymerisation. These low values could until recently only be obtained through anionic and cationic polymerisation.

## 3.2 OBJECTIVES

In this part of the study an investigation was made of the effects of different variables on the molecular mass of polystyrene synthesised by a seeded emulsion polymerisation. The variables that were investigated included the type of CTA, CTA concentration, type of initiator, initiator concentration and monomer concentration. The effect of the first-order interactions of the variables were also considered.

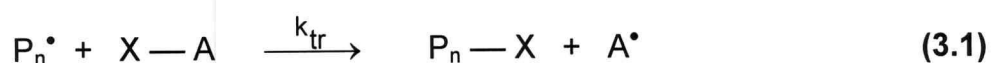
Other responses investigated were particle size, conversion of monomer to polymer and the  $T_g$  of the polymer. All of these responses are a direct consequence of the molecular mass and MMD of the polymer.

In the discussion that follows symbols and abbreviations are used that are explained in the List of Symbols and the List of Abbreviations.

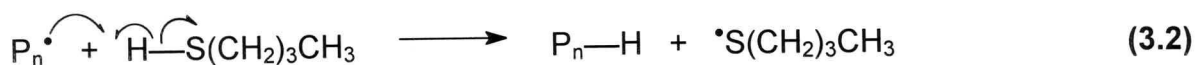
## 3.3 THEORY

### 3.3.1 Chain transfer in radical polymerisation reactions

Conventional chain transfer refers to the reaction between a polymer radical  $P_n^\bullet$  and a chemical species  $XA$ , known as the transfer agent, present in the polymerisation system. A labile group or atom is transferred from  $XA$  to  $P_n^\bullet$ , with the start of a new radical  $A^\bullet$ , as shown in eq. 3.1.<sup>10</sup> The newly formed radical  $A^\bullet$  may reinitiate polymerisation to form  $P_n^\bullet$ .



CTAs may include a monomer, initiator, solvent, polymer or a species that was deliberately added to the reaction mixture. A thiol is an example of a CTA used, see eq. 3.2.



Transfer reactions influence the average degree of polymerisation ( $\overline{DP}$ ), defined as:<sup>11</sup>

$$\overline{DP} = \frac{\text{rate of growth of the polymer}}{\text{total rate of termination}} \quad (3.3)$$

The total rate of termination in eq. 3.3 is the rate of bi-molecular termination as well as the rate of chain transfer.  $\overline{DP}$  is an indication of the extent of polymerisation as well as the molecular mass of the polymer. Eq. 3.3 shows that transfer leads to a reduction in  $\overline{DP}$ , except where XA is a terminated polymer chain.

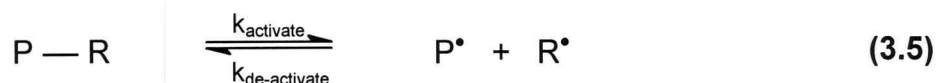
The probability of transfer taking place, P, is given by eq. 3.4.

$$P = \frac{[\text{CTA}]k_{\text{tr,CTA}}}{[\text{CTA}]k_{\text{tr,CTA}} + [\text{M}]k_p} \quad (3.4)$$

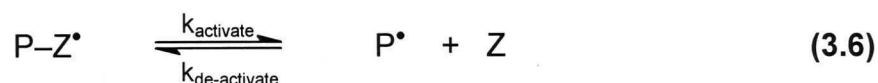
### 3.3.2 Chain transfer agents used in “living”/controlled radical polymerisation

In conventional living polymerisation by ionic or co-ordination mechanisms, all chains are initiated at the beginning of the reaction and grow until all monomer is consumed. “Living”/controlled radical polymerisation becomes possible in the presence of chemical species which reversibly terminate chains. These chemical species reduce the concentration of the propagating species. As a result termination is reduced, giving a quasi-living character to the polymerisation.<sup>12</sup>

There are three mechanisms leading to “living”/controlled radical polymerisation. In the first place a covalent adduct (P — R) homolytically cleaves to form two radicals, R• and P• (see eq. 3.5). The one radical, R•, has a low probability of reacting with the monomer but has a high probability of reacting with the active radical (P•). Recombination of P• and R• can be re-activated and therefore the reaction is reversible. An example of a covalent adduct used as a CTA is the use of nitroxides, as was discussed in section 2.3.1.<sup>13</sup>



The second mechanism involves the reversible reaction between a growing radical P• and a chemical species Z, to produce a stabilised radical P•–Z. An example where a stabilised radical is formed is the reversible complex formed on the active chain ends by persistent radicals, as was proposed in the “living” radical polymerisation mediated by stable nitroxide radicals such as TEMPO. The reaction is shown in eq. 3.6.<sup>14</sup>



The third mechanism is a non-radical species that provides reversible, dormant radicals. Here the role of the radical scavenger is played by a neutral chemical species. A stable adduct with an odd number of electrons is reversibly formed as shown in eq. 3.1 or eq. 3.7.<sup>13</sup>



An example of a non-radical species used as a CTA is the use of a degenerative transfer reaction with alkyl halides such as IAN and PEI as CTAs discussed in section 2.3.4.<sup>13</sup>

### 3.3.3 Control of molecular masses with chain transfer agents

The importance of controlling molecular masses has been discussed earlier (see section 3.4.1). Yoshida showed that the addition of CTAs to radical polymerisations resulted in a molecular mass decrease with an increase in the CTA concentration.<sup>15</sup> Unlike ordinary radical polymerisation, the molecular mass of polymers produced via catalytic chain transfer is not determined by the concentration of the initiator but by the concentration of the CTA. Previous studies showed that even low concentrations of the CTA lead to very low molecular masses of the polymer. The reason for the low molecular masses is the large concentration of active polymer chains consisting of propagating radicals as well as dormant chains. From this follows that an increase in the CTA concentration leads to a further reduction in the molecular mass of the polymer. It was also found that the higher the rate coefficient of transfer of the CTA, the lower is the molecular masses.<sup>4</sup>

The main function of the CTA in both cases discussed earlier (see section 3.3.2), was the formation of stable, dormant polymer chains that can re-initiate. The possibility of re-initiation ensures that polymerisation continues resulting in an increase in the molecular masses of the polymers. The presence of the propagating radicals as well as the dormant chains result in a high concentration of growing chains. Yet, the concentration of chains that are able to terminate through bimolecular termination (propagating chains) remains low. This leads to a low termination rate compared to the rate of propagation. "Living" CTAs also increase the concentration of the polymer chains that are formed. The concentration of polymer chains is equal to the concentration of the CTA and initiator added. The result is low molecular mass polymers with molecular masses decreasing as the CTA concentration increases.

### 3.3.4 Control of molecular mass distributions with chain transfer agents

A polymer with a narrow MMD can be obtained with a CTA that allows "living"/controlled polymerisation. To obtain polymers with low MMDs all the polymer chains must be about the same length on completion of the reaction. To ensure this, all the chains have to start their growth simultaneously and have a similar probability of growth until the end of the polymerisation reaction. Therefore, initiation should be fast, compared to propagation and

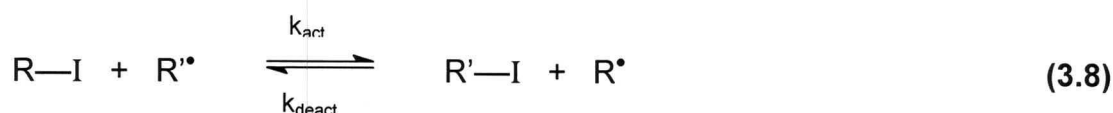
chain stopping events should be negligible.<sup>6</sup> These features conflict with ordinary radical polymerisation where initiation is slow, compared to propagation, and chain stopping events occur continuously.

During “living”/controlled radical polymerisation the CTA and the active radical form dormant chemical species. Because re-initiation of the dormant chemical species is possible, it is still considered as a growing radical chain. These dormant groups do not undergo termination. This leads to a decrease in the termination rate compared to the propagation rate. If transfer of the radical to the CTA has a higher probability than transfer to any other compound, polymerisation will proceed with no termination or transfer reactions, except to the CTA. In this way a pseudo “living” polymer chain is created, leading to the ability to control molecular mass.

### 3.3.5 Chain transfer by means of degenerative transfer reactions

A specific type of chain transfer reaction is degenerative transfer. Here the reactivity of the newly formed radical  $A^\bullet$  towards monomer molecules is far less than that of  $P_n^\bullet$  (see eq. 3.1). In the presence of a degenerative transfer agent, the concentration of  $A^\bullet$  increases and the chance of it taking part in reversible termination also increases. This leads to a reduction in the concentration of reactive species involved in propagation, resulting in a decrease in the rate of polymerisation and  $\overline{DP}$ .<sup>16</sup>

The use of degenerative transfer as a means of “living”/controlled radical polymerisation is discussed in section 2.3.4 and is well documented in literature.<sup>17-20</sup> The CTA that is generally used for degenerative transfer is an alkyl iodide. The alkyl group should be a stabilising group to allow transfer of the iodine atom and stabilisation of the formed radical. The transfer reaction is illustrated in eq. 3.8.<sup>19</sup>



$R^*$  and  $R'^*$  are active chains while the end-capped  $R-I$  and  $R-I'$  are dormant chains. The dormant chains can be re-initiated by another radical after which it can continue to polymerise. Initially the number of polymer chains, equal to the concentration of the CTA added, are formed. The transfer reaction that takes place is thermodynamically neutral. This means that the transfer of the iodine atom between the dormant and the active chain does not involve a loss nor gain of free energy. To accomplish a thermodynamically neutral transfer, the alkyl group should resemble the end-group of the propagating chain. This allows the transfer constant for activation and deactivation to be similar in magnitude.

Although termination does occur it is kept low, restricted to 10 – 30 % of the total concentration of polymer chains present.<sup>17</sup> The low termination rate follows from the low concentration of active radicals present. Yet, a large concentration of chains that are able to propagate is available. When deactivation of an active chain takes place, the chains are end-capped with an iodine atom that prohibits termination. The result is the reversible deactivation of the active, propagating radical chain which leads to the desired decrease in termination reactions taking place in relation to the concentration of polymer chains present.

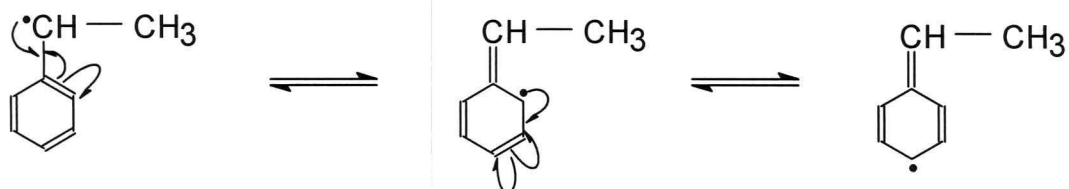
The alkyl iodides do not generate radicals but only participate in the bimolecular exchange of the iodine atom. Conventional initiators like potassium persulphate (KPS) and azobis(isobutyronitrile) (AIBN) can be used to produce the initial radicals. To create effective chain-end properties of the polymer produced, an excess of the CTA in relation to the initiator should be present.

### **3.3.6 Iodoacetonitrile and 1-phenylethyl iodide as degenerative chain transfer agents**

The two CTAs that were used in the present investigation were IAN and PEI. The two CTAs were chosen to resemble the monomeric radical. Both the nitrile and the phenyl group act effectively as radical stabilising groups, allowing easy transfer of the iodine atom. One of their features that makes them such effective CTAs for “living”/controlled radical polymerisation is their resonance stabilisation, shown in Figures 3.1 and 3.2.

**Figure 3.1:**

**Resonance stabilisation of the radical after chain transfer to IAN.**

**Figure 3.2:**

**Resonance stabilisation of the radical after chain transfer to PEI.**

## 3.4 EXPERIMENTAL

### 3.4.1 Planning

The statistical planning as well as the statistical analysis of the designed experiments is discussed in Appendix A. A  $2^{5-1}$  Box, Hunter and Hunter<sup>21</sup> fractional factorial design, produced by STATISTICA (see Appendix A.4), was used to plan and analyse the experimental runs. The design generator for this fractional factorial design is  $E = ABCD$ . The variables A, B, C, D and E are defined in Table 3.1. The high and low levels of each factor are also given Table 3.1. The factor levels for the different runs are given in Table 3.2 and the confounded interactions for the design is given in Table 3.3.

**Table 3.1:**

**Variables investigated in the fractional factorial design to determine the main effects on the different responses with their respective high and low values.**

Variable	Low level (-1)	High level (+1)
A Monomer (styrene)	15%	35%
B Type of initiator	AIBN	K <sub>2</sub> S <sub>2</sub> O <sub>8</sub>
C Initiator concentration	0.0125 mol/dm <sup>3</sup>	0.125 mol/dm <sup>3</sup>
D Type of CTA	1-PEI	IAN
E CTA concentration	0.025 mol/dm <sup>3</sup>	0.125 mol/dm <sup>3</sup>

**Table 3.2:**

**The factor levels for a 16 run fractional factorial design.**

Randomised run number	A	B	C	D	E
1	+1	+1	+1	+1	+1
2	-1	+1	+1	+1	-1
3	+1	+1	-1	+1	-1
4	-1	-1	-1	+1	-1
5	+1	-1	+1	-1	+1
6	+1	-1	+1	+1	-1
7	-1	+1	-1	-1	-1
8	-1	+1	-1	+1	+1
9	-1	+1	+1	-1	+1
10	-1	-1	+1	+1	+1
11	-1	-1	+1	-1	-1
12	+1	+1	-1	-1	+1
13	+1	-1	-1	+1	+1
14	+1	-1	-1	-1	-1
15	+1	+1	+1	-1	-1
16	-1	-1	-1	-1	+1

**Table 3.3:**

**Confounding interactions for a 16-run fractional factorial design.**

Variables and interactions	Confounded interactions
	ABCDE
A	BCDE
B	ACDE
C	ABDE
D	ABCE
E	ABCD
AB	CDE
AC	BDE
BC	ADE
AD	BCE
BD	ACE
CD	ABE
AE	BCD
BE	ACD
CE	ABD
DE	ABC

### 3.4.2 Synthesis of 1-phenylethyl iodide

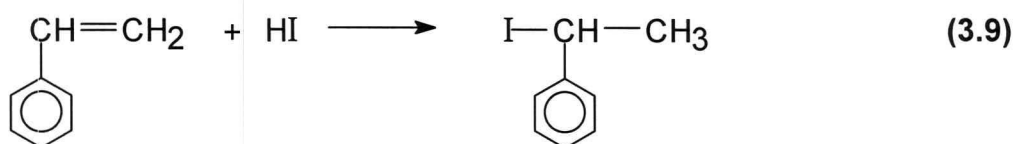
According to the method of Gaynor<sup>17</sup> 1-phenylethyl iodide was prepared via the Markovnikov addition of HI to styrene in the presence of a phase transfer agent.

The following reagents were used:

- Industrial styrene supplied by PLASCON was washed with a 0.3 mol·dm<sup>-3</sup> KOH solution to remove any stabilisers before it was distilled under reduced pressure and dried overnight with CaCl<sub>2</sub> before use. The distilled styrene was kept at 0°C. H<sup>1</sup>-NMR (nuclear magnetic resonance) confirmed that the product was pure.
- An aqueous solution of 47% HI from Aldrich was used as is.
- A phase transfer agent, N-acetyl-N,N,N-trimethylammoniumbromide from UniLab.

A bi-phase mixture of a 1.0 mol·dm<sup>-3</sup> styrene to 3 – 4 mol·dm<sup>-3</sup> of HI-solution was prepared with stirring. 0.1 mol·dm<sup>-3</sup> N-acetyl-N,N,N-trimethylammoniumbromide was added to the mixture. The reaction was carried out at 40 °C over a period of 8h. After completion of the reaction, the organic and aqueous layers were separated. The aqueous layer was washed with three portions of 25 ml of CH<sub>2</sub>Cl<sub>2</sub> and kept. The organic layers were combined and washed with 25 ml of water, three portions of 25 ml of a saturated aqueous CaCO<sub>3</sub>-solution, and then with three portions of 25 ml of H<sub>2</sub>O before the organic layers were again combined.

The product was dried overnight with CaCl<sub>2</sub>. The solvent was evaporated under reduced pressure at 40°C. The product, a dark red oil, was purified by chromatography with hexane as mobile phase and silica gel as stationary phase. After the hexane was evaporated a yellow oil was obtained which was light sensitive. The product was stored below 0°C. The synthesis reaction is illustrated in eq. 3.9.



$H^1$  NMR confirmed that the product was 1-phenylethyl iodide and that no impurities were present.

### 3.4.3 Particle size analysis of the latex particles<sup>22,23</sup>

Particle size analyses were done by photon correlation spectroscopy (PCS). After electron microscopy, this is the best method to study particle sizes at a sub micron level. PCS measure Brownian motion and relates this to the size of the particles. The larger the particles, the slower the particles move, and an accurate indication of the size of the particles can be obtained.

The velocity of the particles is defined by the diffusion coefficient  $D$ , as given in eq. 3.10, referred to as the Stokes–Einstein equation:

$$d(H) = kT/3\pi\eta D \quad (3.10)$$

A Malvern Zetasizer 4 was used to determine the particle size of the latex particles. The instrument compares the amount of light scattered by the latex particles to that scattered by the solvent using a correlator. The Brownian movement of larger particles is less than that of smaller particles. A relation between the amount of scattered light and the velocity at which the particles are moving is obtained which can be transformed by eq. 3.10 to obtain the volume of the latex particles.

Two analyses methods could be used to measure the particle sizes of the latex particles. One is mono-modal, in which the graph that is plotted does not represent any implied distribution. The other is multi-modal which is a standard size distribution analysis. Both these methods gave results for the polydispersity of the particle sizes in terms of the width of the peak obtained.

The coefficient of variation (COV) of the distribution of the particles was provided by the Malvern Zetasizer 4. The COV and the polydispersity index (PDI) is related by the formula in eq. 5.3.<sup>24</sup>

$$\text{PDI} = \left[ 1 + \frac{\sigma^2}{\mu^2} \right]^{1/2} \quad (5.3)$$

with  $\mu$  the number average diameter. The PDI always being lower than 1.

All samples were diluted with a one millimolar NaCl until each of the photo-multipliers counted 1000 photons per second.

#### 3.4.4 Preparation of the seed latex

The following equipment was used: a cylindrical flat-bottomed 2L-glass reactor, a twin blade stirrer and a water bath.

The reactor was charged with the following reagents:

- 21g of an industrial surfactant, Polystep B27, with a sulphate end-group. The surfactant has the general formula  $R\text{---}SO_3^-Na^+$  and is an anionic surfactant, with R being nonylphenoxypolyethyleneoxyethanol. Stepan, Northfield, Illinois, supplied the surfactant. The surfactant is specifically suitable for styrene and butadiene emulsion polymerisation.
- 1150g of distilled and de-ionised water (DDI).
- 600g of distilled styrene that was dried overnight over  $CaCl_2$  (see section 3.4.2)
- 2g KPS, the initiator.

The charged reactor was heated to 90 °C. The added styrene was emulsified while the mixture was stirred at a stirring speed of 300 rpm and purged for 1 h with  $N_2$ . During the rest of the reaction the reactor was kept under a  $N_2$  atmosphere. 2g of the initiator was dissolved in 100g of DDI water and heated separately to 90 °C before it was added to the emulsified styrene at 90°C. The reaction proceeded for 3 h.

Analysis by the Malvern Zetasizer 4 revealed a latex particle size of 104.7nm. This particle size is small enough to allow either one or zero radicals per latex particle (“zero-one” kinetics).<sup>25</sup> Only one peak appeared showing that no secondary nucleation took place. The width of the peak indicated a monodisperse particle size.

### 3.4.5 Latex purification procedure

The prepared styrene latex was cleaned by serum replacement using a 100 000 nominal molecular mass cut-off Ultra Sep membrane (Micron Separations Incorporated, MSI). The serum replacement cell used was similar to the one used by Ahmed.<sup>26</sup> 100g of the seed-latex was placed in the cell and 200g of DDI water was added at the start. The conductivity of the supernatant was determined until it remained constant, and similar to the conductivity of the DDI water.

### 3.4.6 The seeded emulsion polymerisation of styrene in the presence of degenerative reacting chain transfer agents

The following equipment was used: a 250 cm<sup>3</sup> three-neck round bottomed flask, a single blade Teflon stirrer and a water bath.

The previously prepared cleaned seed latex (see sections 3.4.4 and 3.4.5) was diluted with DDI water to give a constant solid content of 10% for all the experiments. A 10% solids content was used to enable GC analysis to be made; preventing clogging of the needle. The conversion of monomer to polymer was determined gravimetrically by measuring the solids contents of the latex with a Mettler HR73 Hologen Moisture Analyser. A standard drying program was used to determine the dry content of the synthesised emulsion. A sample mass of 1 – 2g was placed on an aluminium pan and subjected to infrared-radiation at 180°C. The Mettler HR73 Hologen Moisture Analyser has an estimated error of  $\pm 0.2\%$  in this mass range.

The ingredients for the seeded emulsion polymerisation of styrene were as follows:

- 100g of the styrene seed latex (prepared as described in sections 3.4.4 and 3.4.5).
- 3% (m/m) sodium dodecyl sulfate to act as surfactant.
- 0.06 moles of sodiumbicarbonate to act as buffer.
- Different concentrations of the monomer, styrene (see Table 3.1).
- Different concentrations of either IAN or PEI as CTA (see Table 3.1).
- 2g of either KPS or AIBN, the initiator (see Table 3.1).

Although it was the intention of the present experimental runs to only vary the five chosen variables, two different mechanisms had to be followed resulting from the different natures of the initiators used:

- a) When the water-soluble initiator, KPS, was used, only the CTA and the monomer, styrene was added to the seed latex. The solution was stirred for 24 h at 450 rpm to allow the seed to swell with monomer and CTA. After the seed latex was swelled with monomer and CTA, the emulsion was purged with N<sub>2</sub> for half an hour before the temperature was raised to 70°C before the initiator, separately heated to 70°C, was added. After the initiator was added, the reaction was continued for 4 h. The entire reaction was done in an inert N<sub>2</sub>-atmosphere.
- b) When the water-insoluble initiator, AIBN, was used, the initiator was dissolved in the monomer, styrene. This CTA was added to the monomer-initiator solution and added to the seed latex. The emulsion with the monomer, initiator and CTA was stirred for 24 h in the absence of light, to allow the seed latex particles to swell with monomer, preventing premature polymerisation. The swelled latex was then purged for half an hour before the temperature was raised to 70 °C for initiation to take place. 50g of DDI water, pre-heated to 70°C, was added to ensure that the volumes of the experimental runs for the water-soluble and water-insoluble initiator were the same. The reaction was continued for 4 h.

Analysis by the Malvern Zetasizer 4 revealed that the particle sizes of the seed latex, after it was swelled with monomer, increased at different rates depending on the concentration of monomer etc. added. Upon analysis in multi-modal mode, only one peak appeared. This indicated that no new micelles were formed during the swelling of the original seed latex. After the polymerisation was complete, analysis by the Malvern Zetasizer 4 revealed only one peak in multi-modal mode, indicating that no secondary nucleation of latex particles had occurred during polymerisation. The increase in the particle sizes after polymerisation shows that possible coagulation of the latex particles took place. This could be the result of the increase in the ionic strength of the emulsion during the possible formation of HI that led to an increase in the pH of the latex.

### 3.4.7 Molecular mass and molecular mass distribution determinations

Analysis by GPC revealed both molecular mass and MMD results of the synthesised polystyrene. The GPC had the following features:

- Waters 610 liquid chromatograph equipped with four Phenogel columns obtained from Phenomex.
- The columns were placed in series in order from  $10^3\text{\AA} \rightarrow 10^4\text{\AA} \rightarrow 10^5\text{\AA} \rightarrow 10^6\text{\AA}$  (in the direction of the flow of the continuous phase).
- A Waters 410 differential refractometer was used as detector.
- The system was controlled by a Waters 600E system controller.
- Samples were injected with a Waters Autosampler 717 Plus.

Calibration of the GPC column was done using narrow molecular mass polystyrene standards. The samples that were used are summarised in Table 3.4.

**Table 3.4:**

**Molecular masses of the styrene standards used to calibrate the GPC columns.**

$M_n$	$M_w$	$M_p$	$M_w/M_n$	Company
3967	4136	4000	1.06	Pressurechemical
16700	17200	17600	1.03	Waters
30013	30740	30256	1.06	Pressurechemical
41000	42000	43000	1.03	Waters
198250	207750	198400	1.06	Pressurechemical
392000	400000	402100	1.06	Pressurechemical
892000	942000	949000	1.06	Pressurechemical
1524000	1921000	2161000	1.30	Pressurechemical

The standards and samples to be analysed were dissolved in tetrahydrofuran (THF) to a concentration of 3mg/ml and then filtered through a 0.22  $\mu\text{m}$  Teflon filter from Millex-HV, supplied by Millipore. The settings on the instrument were as follow:

- The pressure was kept constant at 204 psi.
- The temperature at 30°C.
- The flow rate was 0.6ml/min.
- Both the solvent and mobile phase was THF.
- The runtime through the column was approximately 90 minutes.

### 3.4.8 Glass transition temperature determinations

A Pyris 1 Differential Scanning Calorimeter (DSC) from Perkin Elmer was used to determine the  $T_g$  of the synthesised styrene polymers. The sample to be analysed was heated in two phases. First the temperature was raised from  $-50^{\circ}\text{C}$  to  $150^{\circ}\text{C}$  at a rate of  $20^{\circ}\text{C}/\text{min}$ . Then the sample was cooled to  $0^{\circ}\text{C}$  and again heated to  $150^{\circ}\text{C}$  at  $20^{\circ}\text{C}/\text{min}$ .

### 3.4.9 Determining the distribution for 1-phenylethyl iodide and iodoacetonitrile between the water and oil phase

A  $2^2$ -factorial design was used to produce a regression model of the solubility of the two CTAs in the water and oil phase. The variables A and B are defined in Table 3.5 giving the high and low levels of each factor.

**Table 3.5:**

**Variables investigated in the  $2^2$ -factorial design to determine the distribution for the CTAs between the water and oil phase.**

	Variable	High level (+1)	Low level (-1)
A	Styrene concentration	15g	7.5g
B	CTA concentration	1.25g	0.35g

**Table 3.6:**

**The factor levels for  $2^2$ -factorial design to determine the distribution for the CTAs between the water and oil phase.**

RUN NUMBER	A	B
1	-1	-1
2	+1	-1
3	-1	+1
4	+1	+1

The factor names as well as the high and low levels of each factor are also shown in Table 3.5. The factor levels for the different experimental runs are given in Table 3.6. Two separate factorial runs were conducted for both IAN and PEI.

The following equipment was used: a water bath, a single blade Teflon stirrer and a 200ml separating funnel. The chemicals used are the same as summarised in section 3.4.4. The separating funnel was charged with 50g of DDI water and the measured amounts of the CTA and styrene as is depicted in the Tables 3.5 and 3.6. The mixture was well shaken to allow the oil phase to form a suspension in the water phase before it was placed in the water bath at 70°C for 1h. The two phases were separated and the water phase analysed by GC by the internal standard method of quantitative gas chromatogram evaluation via peak area to determine the concentration of the CTA in the water phase.

#### **3.4.10 The internal standard method of quantitative gas chromatogram evaluation via peak area<sup>27</sup>**

An AutoSystem GC from Perkin Elmer with the following specifications were used:

- For PEI and styrene a Quadrex methyl silicone fused silica capillary column with a column length 65m and film thickness 0.2µm.
- For IAN a Quadrex phenyl silicone fused silica capillary column with a column length 45m and film thickness 0.2µm.

The settings on the GC were as follow:

- The injection temperature was 270°C
- The oven temperature was 95°C
- The flame ionisation detector's (FID) temperature was set at 300°C.
- The carrier flow rate was 40ml/min.
- Hydrogen was used as carrier gas.
- The samples were manually injected.

The concentrations of the CTAs were measured with the quantitative evaluation of the chromatograms via peak areas relative to an internal standard, N,N–dimethylformamide

(DMF). The first step was to determine the response factors for the CTAs ( $f_i$ ) using eq. 3.11. A mixture with known concentrations of DMF and each of the CTAs were injected and the peak areas evaluated.

$$f_i = \frac{A_{st} \cdot G_i}{A_i \cdot G_{st}} \cdot f_{st} \quad (3.11)$$

where  $A_{st}$  is the area of DMF,  $G_{st}$  the mass of DMF,  $G_i$  is the mass of the sample being either IAN or PEI,  $A_i$  the area of either IAN or PEI and  $f_{st}$  the response factor for DMF taken arbitrarily as one.

In the second step, the concentrations of the CTAs can be calculated with eq. 3.12 by adding a known amount of DMF to each of the samples that were prepared as discussed in a previous section (see section 3.4.9).

$$G_i = G_{st} \frac{A_i \cdot f_i}{A_{st} \cdot f_{st}} \quad (3.12)$$

The mass of IAN or PEI ( $m_i$ ) can now be calculated with eq. 3.13:

$$m_i = \frac{G_i}{G_s} G_T \quad (3.13)$$

where  $G_s$  is the mass of the sample the DMF was added to and  $G_T$  the total mass of the mixture placed in the separating funnel.

### 3.5 RESULTS AND DISCUSSION

In Table 3.7 a summary of all the responses of all the variables that were investigated in the  $2^{5-1}$ -fractional factorial design is shown.

The molecular mass values, as response, were not randomly distributed around the mean. To be able to analyse the results statistically, it was necessary to transform the responses with a logarithmic function. For this purpose the natural logarithm ( $\ln [M_n]$ ) was used.

The randomised run numbers indicating the sequence in which the experimental runs were conducted are shown in Table 3.7.

In the succeeding sections, the effects of the five variables on the different responses will be discussed. Response surface plots not discussed in these sections are given in Appendix B.

**Table 3.7:**

**Responses measured for the 16–run fractional factorial design.**

No.	A	B	C	D	E	$M_n$	$M_w$	$\ln(M_n)$	$M_w/M_n$	Particle Size	Fractional conversion	$T_g$ (°C)
1	-1	-1	-1	-1	+1	8844	10524	9.09	1.19	141.9	45.16	19.096
2	+1	-1	-1	-1	-1	56030	66115	10.93	1.18	130.7	98.47	98.556
3	-1	+1	-1	-1	-1	318654	1019693	12.67	3.2	110.1	54.66	68.597
4	+1	+1	-1	-1	+1	19492	29433	9.88	1.51	116.3	97.62	84.165
5	-1	-1	+1	-1	-1	23701	35552	10.07	1.5	135	59.05	63.108
6	+1	-1	+1	-1	+1	16578	30006	9.72	1.81	154.5	96.44	88.271
7	-1	+1	+1	-1	+1	663577	1074995	13.41	1.62	113	99.85	107.573
8	+1	+1	+1	-1	-1	42830	218005	10.66	5.09	133	88.10	68.167
9	-1	-1	-1	+1	-1	4174	5885	8.34	1.41	142.4	30.48	79.41
10	+1	-1	-1	+1	+1	744	1533	6.61	2.06	158	98.66	32.966
11	-1	+1	-1	+1	+1	325	650	5.78	2	114.2	95.41	54.123
12	+1	+1	-1	+1	-1	8916	12393	9.1	1.39	166	52.96	111.601
13	-1	-1	+1	+1	+1	476	728	6.17	1.53	141.4	76.14	52.332
14	+1	-1	+1	+1	-1	11067	13723	9.31	1.24	166.2	98.05	94.566
15	-1	+1	+1	+1	-1	1882	3199	7.54	1.7	131.3	99.97	73.563
16	+1	+1	+1	+1	+1	156	459	5.05	2.94	131.3	95.11	76.251

### 3.5.1 Effects of the response molecular mass of the polymer

A significant change in the molecular masses of the synthesised polystyrene (PS) was evident; ranging from 156 to 663 577. The transposed molecular masses vs. the individual run numbers are given in Figure 3.3.

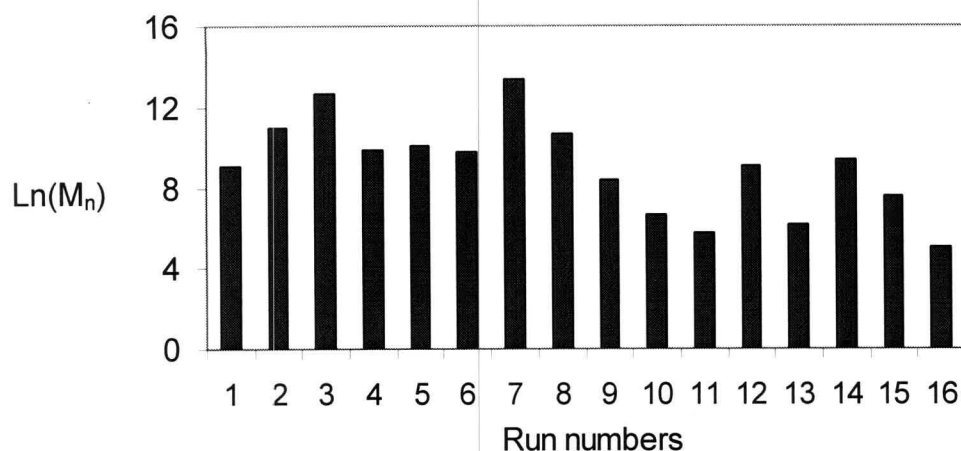


**Figure 3.3:**

**Ln (M<sub>n</sub>) for the 16 runs in the fractional factorial design.**

The Pareto chart of the variables (see Appendix C, Figure C.1) as well as the probability plot of the variables (see Appendix D, Figure D.1) that influence Ln (M<sub>n</sub>) show that the response is mainly influenced by the type of CTA used (variable D). The CTA concentration (variable E) also influenced the results, but to a lesser extent. This is confirmed in the ANOVA table (see Table 3.8). Only the variables and combination of variables that have a significant influence on this response are given in Table 3.8.

**Table 3.8:**  
**ANOVA table of the main effects on the response  $\ln(M_n)$ .**

VARIABLE	SS	df	MS	F	p
Type of CTA: D	50.89	1	50.89	73.15	<<1
CTA concentration: E	10.45	1	10.45	15.02	<<1
Type of initiator and type of CTA: BD	5.96	1	5.96	8.57	0.02
Type of CTA and CTA concentration: DE	4.43	1	4.43	6.36	0.03
Monomer concentration and type of initiator: AB	3.63	1	3.63	5.22	0.05
Initiator concentration and CTA concentration: CE	2.58	1	2.58	3.71	0.09
Error	6.26	9	0.7		
Total SS	84.2	15			

In Figure 3.4, a surface plot of the combination effects of the type of CTA and the CTA concentration on the molecular mass, can be seen. Looking at the contour lines, it is clear that the use of PEI (variable D) as CTA resulted in a larger molecular mass on average than using IAN (variable E), as CTA. Further, an increase in the concentration of the CTA leads to a reduction in the molecular mass of the polymer in the case of IAN. This difference was not that explicit in the case of PEI.

The fact that IAN is more water-solubility than PEI is postulated to lead to a higher exit rate when IAN was used as CTA. This would then increase the amount of termination taking place in the water phase. This increase in the termination rate is believed to be the main reason for the higher molecular masses when IAN was used, compared PEI.

The decrease of molecular mass with an increase in the concentration of the CTA is consistent with a previous discussion on the influence of CTAs on the molecular mass of polymers (see section 3.3.3).

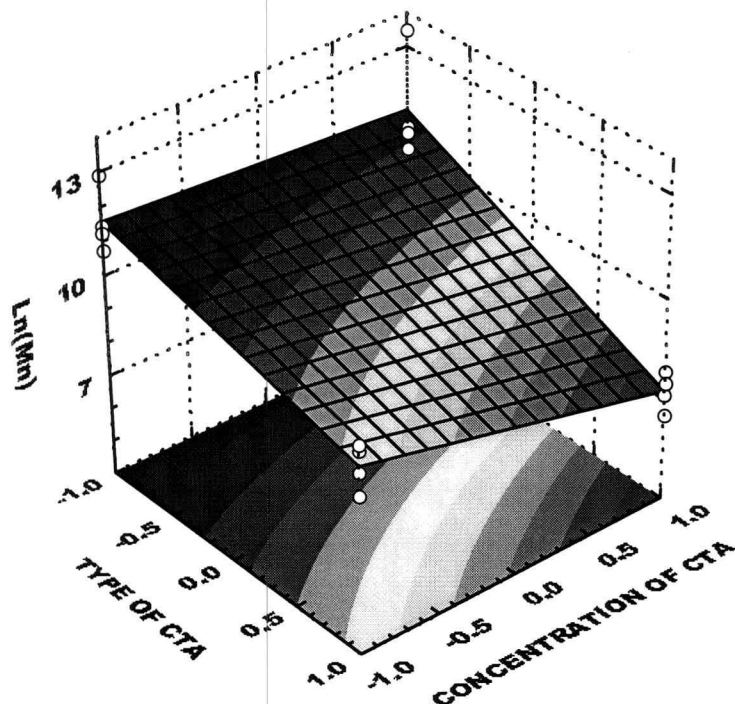
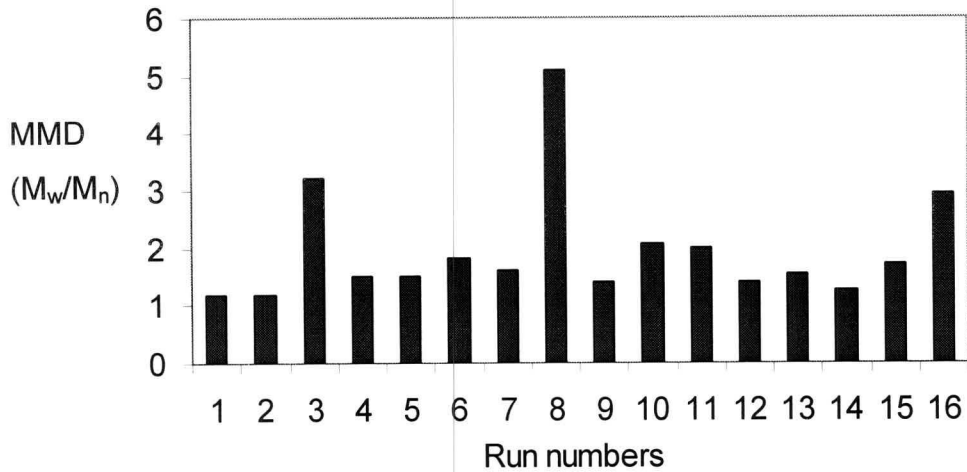


Figure 3.4:

Response surface plot of the concentration of CTA and type of CTA for the response  $\ln(M_n)$ .

### 3.5.2 Effects on the response molecular mass distributions of the polymer

The MMDs obtained from the 16-run fractional factorial design are given in Figure 3.5. These values effectively exclude the effect of the styrene seed peak, which appeared at an earlier elution volume during the GPC analysis. The  $M_w/M_n$  values were on average  $< 2$ . A minimum value of 1.18 for  $M_w/M_n$  was obtained which is a very narrow distribution. This is especially noteworthy for a free radical polymerisation reaction. This observation confirms that a high degree of control can be obtained in the presence of alkyl iodides as CTA in a seeded emulsion polymerisation of styrene.

**Figure 3.5:**

**M<sub>w</sub>/M<sub>n</sub> for the 16 runs of the fractional factorial design.**

**Table 3.9:**

**ANOVA table of the main effects on the response M<sub>w</sub>/M<sub>n</sub>.**

VARIABLE	SS	df	MS	F	p
Type of CTA and CTA concentration: ED	3.62	1	3.62	16.66	<< 1
Type of initiator: B	3.53	1	3.53	16.28	<< 1
Monomer concentration and initiator concentration: AC	2.57	1	2.57	11.83	0.01
Type of initiator and CTA concentration: BE	1.30	1	1.3	5.99	0.04
Type of initiator and type of CTA: BD	0.97	1	0.97	4.49	0.07
Initiator concentration: C	0.76	1	0.76	3.50	0.10
Monomer concentration: A	0.59	1	0.59	2.74	0.14
Type of initiator and initiator concentration: BC	0.56	1	0.56	2.59	0.15
Error	1.52	7	0.22		
Total SS	15.43	15			

The Pareto chart of the variables (see Appendix C, Figure C.2) as well as the probability plot of the variables (see Appendix D, Figure D.2) show that the response  $M_w/M_n$  is mainly influenced by the combination of the type of CTA and the CTA concentration (variables D and E). The other main factor that influenced the MMD is the type of initiator that was used (variable B). The ANOVA table (see Table 3.9) confirms this. Only the variables and combination of variables that have a significant influence on the response,  $M_w/M_n$ , are given in Table 3.9.

In Figure 3.6, the surface plot of the combination of the type of initiator and the CTA concentration on the molecular mass can be seen, showing that the initiator AIBN gave a low MMD.

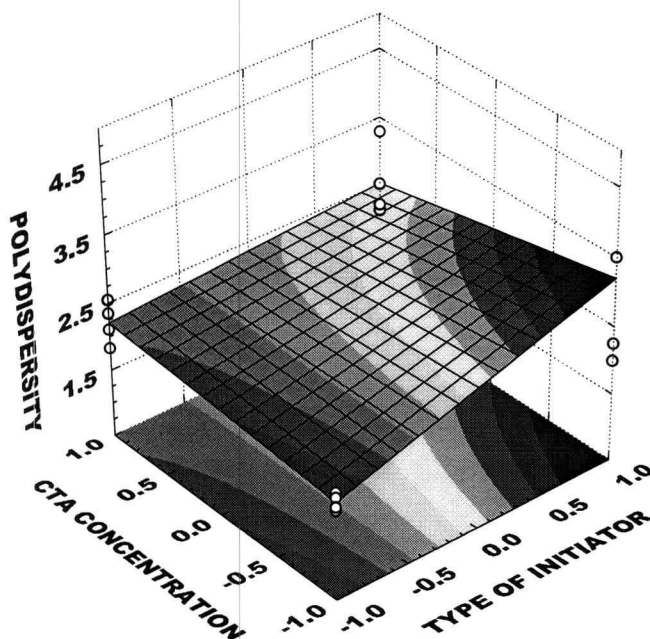


**Figure 3.6:**

**Response surface plot of the concentration of CTA and type of initiator for the response  $M_w/M_n$ .**

In Figure 3.7, the surface plot of the interaction between the type of CTA and the CTA concentration on the molecular mass can be seen. The contours indicate that there are two separate cases to be considered. The first is when PEI is used. In this case a high

concentration of CTA yields a narrow MMD. In the second case when IAN is used, the opposite is found. In this case a low concentration of the CTA is necessary to obtain a narrow MMD. Further, a narrow MMD is obtained when AIBN is used as the initiator.

The  $M_w/M_n$  of polymers produced with AIBN is lower than those produced by KPS. The postulation correlates with effects on molecular mass and MMD that occurs with IAN and PEI. That is, there are two phases, the polymer phase and the aqueous phase. In the aqueous phase polymerisation is negligible but transfer and termination are facile. Therefore, the more water-soluble the active species are, the more termination is expected. This means that both KPS and IAN lead to lower radical concentrations in the particles and in turn this leads to broader  $M_w/M_n$  and or higher molecular mass.

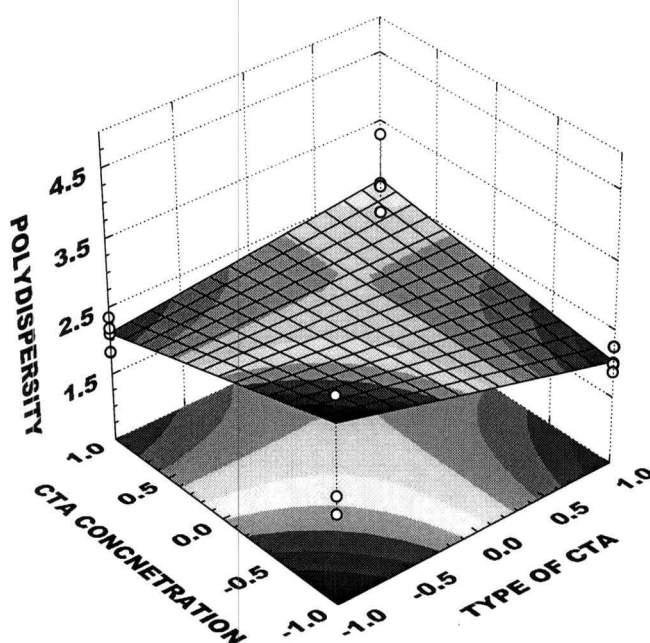


Figure 3.7:

Response surface plot of the concentration of CTA and type of CTA for response  $M_w/M_n$ .

The other important variable that influenced  $M_w/M_n$  of the polymers was the interaction between the type of CTA and the CTA concentration. In their investigation of “living” radical polymerisation with MTEMPO, Yoshida *et al*<sup>28</sup> found no definite relation between the concentration of the catalyst and  $M_w/M_n$  of the polymers produced above a critical concentration of the CTA. In our investigation an increase in the PEI concentration led to

a reduction in  $M_w/M_n$  of the polymers. The increase in the PEI concentration decreases the amount of radical termination, resulting in a reduction of  $M_w/M_n$  of the polymers produced. On the other hand, a low concentration of IAN compared to PEI, produced a low value for  $M_w/M_n$ . This is believed to be the result of the high water solubility of the IAN. Transfer to IAN leads to a high probability of exit of the radical from the particle. As a result the termination reactions; believed to occur in the soap layer and water phase, increases when IAN is used compared to the cases when PEI is used. The chance of all polymer molecules growing with the same statistical probability is reduced and this leads to a higher  $M_w/M_n$  value as the concentration of IAN increases.

### 3.5.3 Effects on the response particle size of the latex particles

Analysis by the Malvern Zetasizer 4 revealed that the particle size of the original seed latex was 104.7nm. On completion of the reaction, the increase in particle size was measured. Results are given in Figure 3.8.

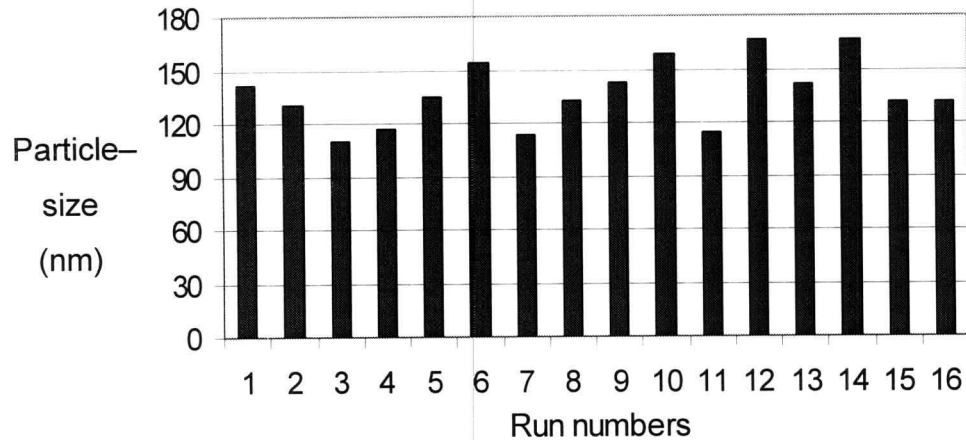
The Pareto chart of the variables (see Appendix C, Figure C.3) as well as the probability plot of the variables (see Appendix D, Figure D.3) show that the response is mainly influenced by the monomer concentration (variable A) and the type of initiator (variable B). The ANOVA table (see Table 3.10) confirms this.

In Figure 3.9, the surface plot of the effect of the combination of the monomer concentration and the type of initiator can be seen. The surface plot indicates that a high monomer concentration leads to a larger ultimate particle size. It is also clear that the use of AIBN as initiator leads to a larger particle size.

The seed latex that was previously prepared (see section 3.4.4) had all its excess surfactant removed (see section 3.4.5). This resulted in no secondary nucleation taking place; confirmed analysis with the Malvern Zetasizer 4, which showed only one, narrow peak. Under these circumstances, an increase in the monomer concentration will lead to an increase in the polymer particle sizes as conversion of monomer to polymer takes place. This is confirmed by the results seen in Figure 3.8.

**Figure 3.8:**

**Particle sizes of the latex particles for the 16 runs of the fractional factorial design.**

**Table 3.10:**

**ANOVA table of the main effects of the response particle size.**

Variable	SS	df	MS	F	p
Type of initiator: B	1499.63	1	1499.63	28.51	<< 1
Monomer concentration: A	1003.31	1	1003.31	19.07	<< 1
Type of CTA: D	845.36	1	845.36	16.07	<< 1
Monomer concentration and CTA concentration: AE	474.15	1	474.15	9.01	0.01
Type of CTA and CTA concentration: DE	379.28	1	379.28	7.21	0.02
Monomer concentration and type of CTA: AD	208.08	1	208.08	3.96	0.08
Error	473.43	9	52.6		
Total SS	4883.22	15			

The other variable influencing the particle sizes was the type of initiator used. AIBN, as a hydrophobic initiator, resulted in a larger latex particle size than those latex particles formed from the hydrophilic KPS. This is probably because of the difference in the

efficiencies of the two initiators. AIBN is the more efficient of the two, leading to a higher conversion and therefore to a larger particle size.<sup>29</sup>

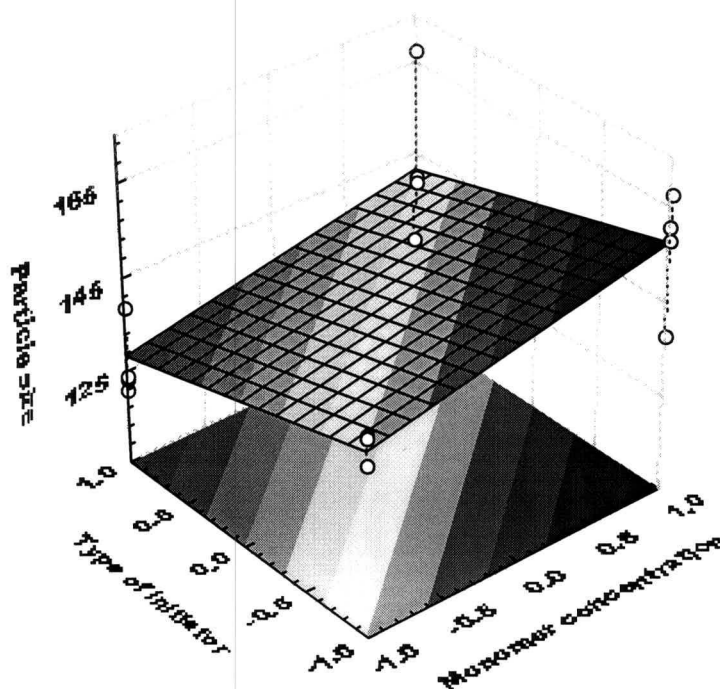


**Figure 3.9:**

**Response surface plot of the concentration of monomer and type of initiator for the response particle size.**

#### **3.5.4 Effects on the response fractional conversion of monomer to polymer**

The fractional conversion of monomer to polymer obtained after a reaction time of 4 h varied between 30% and 100%. The results are given in Figure 3.10.

The Pareto chart of the variables (see Appendix C, Figure C.4) as well as the probability plot of the variables (see Appendix D, Figure D.4) show that the fractional conversion is mainly influenced by the type of initiator (variable B) and the CTA concentration (variable E). The ANOVA table (see Table 3.11) confirms this.

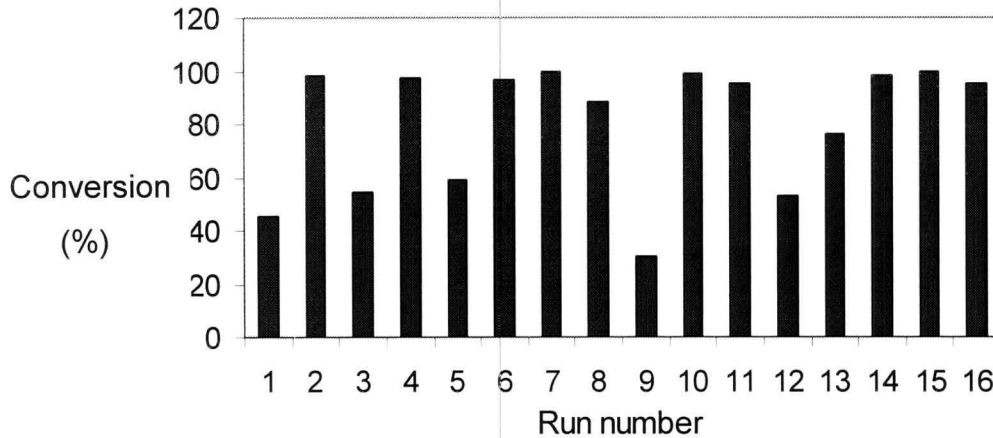


**Figure 3.10:**

**Fractional conversion of monomer to polymer for the 16 runs of the fractional factorial design.**

**Table 3.11:**

**ANOVA table of the main effects of the response conversion.**

Variable	SS	df	MS	F	p
Type of initiator: B	3577.37	1	3577.37	46.14	<< 1
CTA concentration: E	1907.95	1	1907.95	24.61	<< 1
Type of initiator and CTA concentration: BE	822.89	1	822.89	10.61	0.01
Monomer concentration and CTA concentration: AE	780.95	1	780.95	10.07	0.01
Type of initiator and type of CTA: BD	331.58	1	331.58	4.28	0.07
Initiator concentration and type of CTA: CD	291.56	1	291.56	3.76	0.08
Error	697.72	9	77.52		
Total SS	8410.02	15			

In Figure 3.11, the surface plot of the effect of the interaction of the type of initiator and the CTA concentration can be seen. It appears that the use of AIBN as initiator leads to higher conversion and that a low CTA concentration also leads to higher conversion.

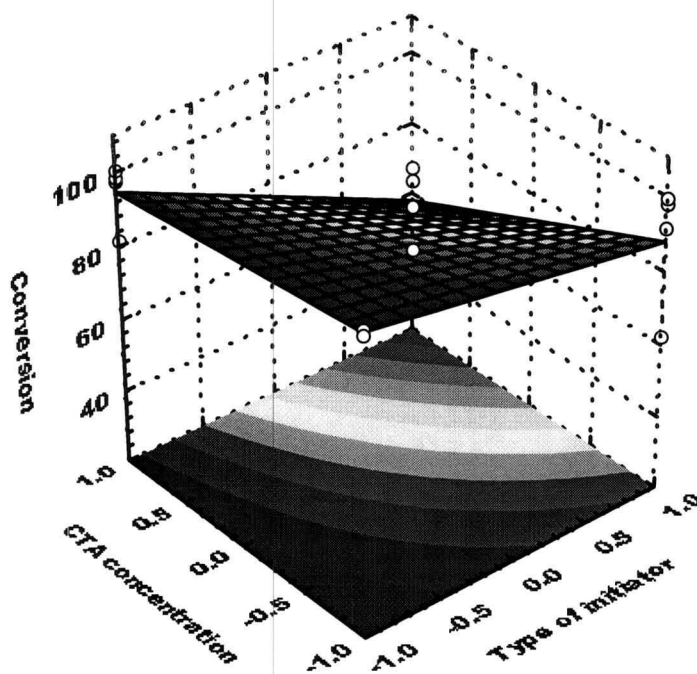


**Figure 3.11:**

**Response surface plot of the concentration of monomer and type of initiator for the response fractional conversion of monomer to polymer.**

One variable that influenced the conversion was the type of initiator. The use of AIBN, as with the response particle size, resulted in a higher fractional conversion than KPS. Again it is believed to be the effect of the difference in the efficiencies of the two initiators, with AIBN being the more efficient of the two, leading to a higher fractional conversion.

The other variable having a major effect on the fractional conversion was the CTA concentration. Scott *et al*<sup>19</sup> found that an increase in the CTA concentration led to a lower conversion. They believed that this was due to the generation of a small amount of  $I_2$  that would inhibit propagation by forming a stable complex with the radical. A possible mechanism for the formation of  $I_2$  is given in Figure 3.12. In the first step the very weak

covalent bond between the iodine atom and the carbon atom is activated either by heat or light.

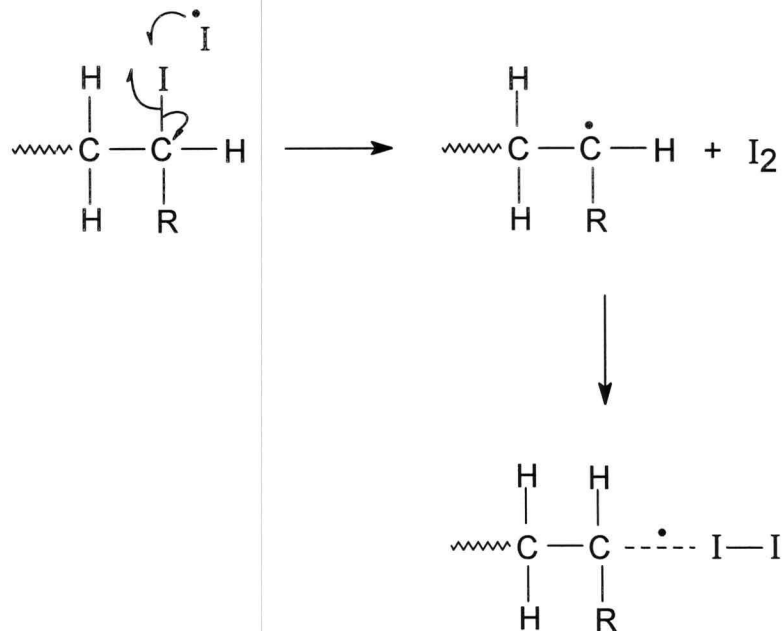


Figure 3.12:

Possible mechanism for the formation of I<sub>2</sub> from a polymer or CTA with an iodine chain-end

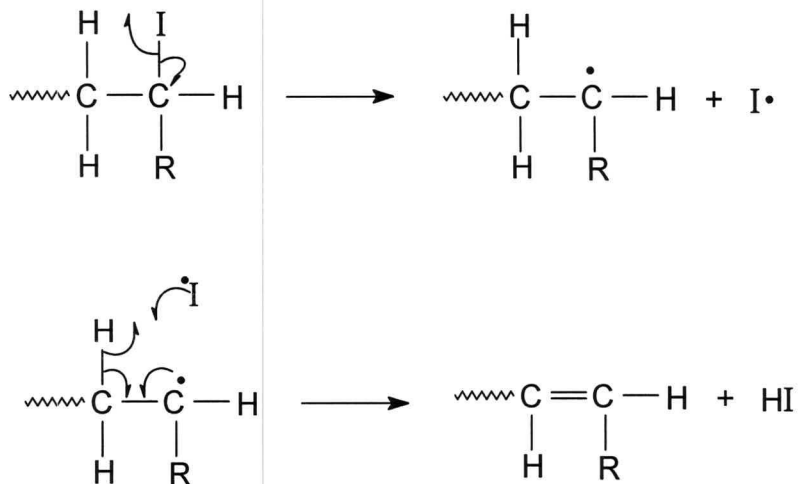


Figure 3.13:

Possible mechanism for the formation of HI from a polymer or CTA with an iodine chain-end.

Extremely low pH values (< pH 3) of the prepared seed led us to believe that the iodine radical abstracted an hydrogen atom from the same molecule to form HI. A possible

mechanism for the reaction is shown in Figure 3.13. The low pH led to instability in the emulsion that caused premature coagulation of the latex particles in some cases. This was confirmed when a yellowish precipitant was observed when  $\text{AgNO}_3$  was added to the supernatant of the centrifuged emulsion. (See Appendix G for relation between conversion and particle size)

### 3.5.5 Effects on the response glass transition temperature

Analysis by DSC revealed that the change in the  $T_g$  of the synthesised polymers corresponded with that of the molecular masses of the polymers. The results can be seen in Figure. 3.14.

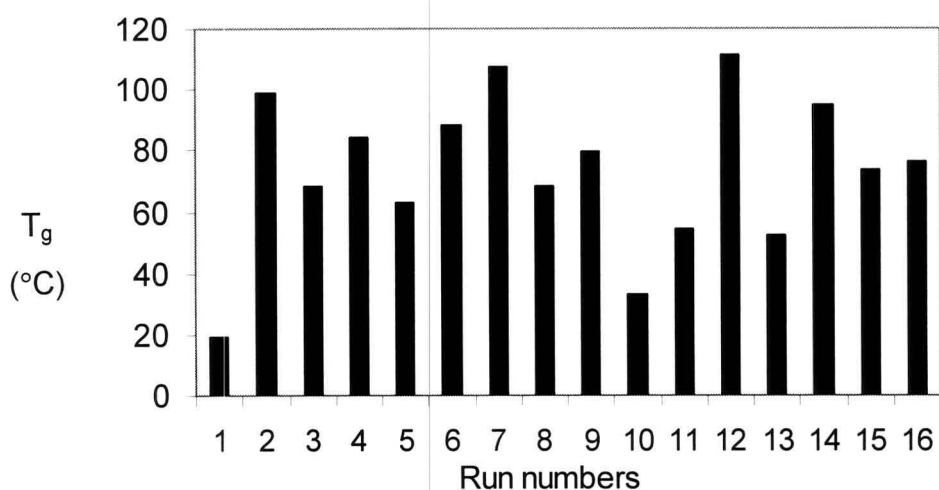


**Figure 3.14:**

#### **$T_g$ of the polymers for the 16 runs of the fractional factorial design**

The Pareto chart of the variables (see Appendix C, Figure C.5) as well as the probability plot of the variables (see Appendix D, Figure D.5) show that the  $T_g$  is mainly influenced by the interaction between the initiator concentration (variable C) and the CTA concentration (variable E). The ANOVA table (see Table 3.12) confirms this.

In Figure 3.15 the surface plot of the effect of the interaction of the initiator concentration and the CTA concentration can be seen. It appears that the use of a low CTA concentration result in a high  $T_g$  while a high CTA concentration is influenced by the

initiator concentration. At a high CTA concentration, low initiator concentration results in a low  $T_g$  while a high initiator concentration results in a high  $T_g$ .

**Table 3.12:**

**ANOVA table of the main effects on the response  $T_g$  of the polymers.**

Variable	SS	df	MS	F	p
Initiator concentration and CTA concentration: CE	2324.13	1.00	2324.13	21.66	<< 1
Initiator concentration and type of CTA: DE	1298.61	1.00	1298.61	12.10	0.01
Type of initiator and CTA concentration: BE	1280.91	1.00	1280.91	11.94	0.01
CTA concentration: E	1274.33	1.00	1274.33	11.88	0.01
Monomer concentration: A	1168.63	1.00	1168.63	10.89	0.01
Type of initiator: B	837.16	1.00	837.16	7.80	0.03
Monomer concentration and initiator concentration: AC	355.16	1.00	355.16	3.31	0.11
Initiator concentration: C	354.54	1.00	354.54	3.30	0.11
Error	751.18	7	107.31		
Total SS	9644.65	15			

The low  $T_g$  at a high CTA concentration confirms the results in section 3.5.1 where a high CTA concentration produced low molecular mass polymers. Because  $T_g$  relates to molecular motion, low molecular mass polymers, having a greater free volume, would have a low  $T_g$ .<sup>30</sup> It is our belief that the reason for the high  $T_g$  at high initiator concentrations, even at high CTA concentration, is the increase in the amount of radicals capable of irreversible termination.

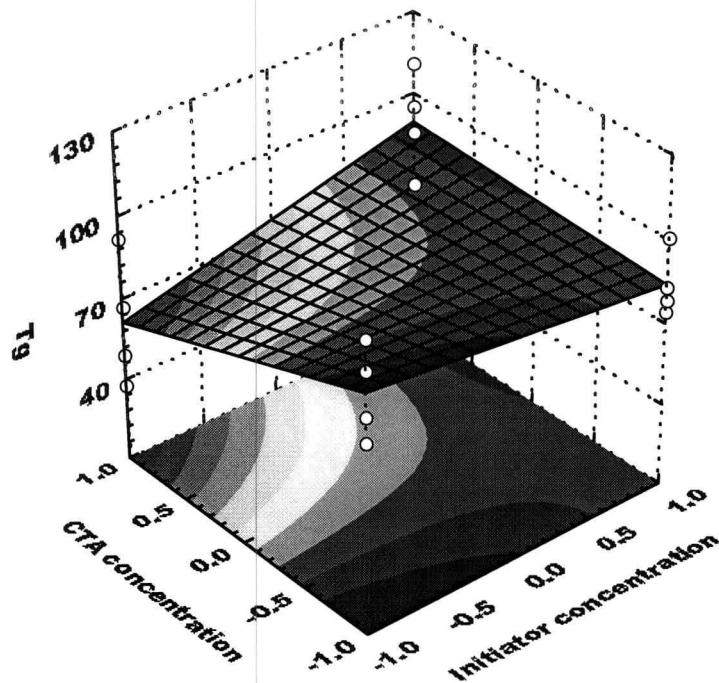


**Figure 3.15:**

**Response surface plot of the concentration of initiator and concentration of CTA on for response  $T_g$ .**

### **3.5.6 The distribution of 1-phenylethyl iodide and iodoacetonitrile between the water and oil phase**

The result of the two  $2^2$ -factorial design is given in Table 3.13. It was not possible to achieve efficient separation between PEI and styrene because of the resemblance in their structures, therefore, the PEI results can not be accepted as reliable. A summary of the stepwise regression of the  $2^2$ -factorial design of the distribution for IAN between the water and oil phase is given in Table 3.14.

**Table 3.13:**

**Results of the two 2<sup>2</sup>-factorial designs to determine the distribution for IAN and PEI between the water and oil phase.**

	CTA	Styrene	PEI	IAN
1	-1	-1	0.0073	0.0124
2	-1	1	0.0263	0.0059
3	1	-1	0.0263	0.0021
4	1	1	0.1348	0.0141

**Table 3.14:**

**A summary of the stepwise regression of the 2<sup>2</sup>-factorial design for the distribution of IAN between the water and oil phase.**

Variable	Step	Multiple R <sup>2</sup>	F	p
Interaction between styrene and IAN concentration: AB	1	0.91	19.22	0.14
Styrene concentration: A	2	0.99	6.30	0.24

The regression model for the 2<sup>2</sup>-factorial design for the distribution of IAN between the water and oil phase is given in eq. 3.14.

$$Y = 0.0045A + 0.0021AB \quad (3.14)$$

This is a clear indication that IAN is present in high concentrations in the water phase.

### 3.6 CONCLUSIONS

The following are the main conclusions drawn from the study described in this chapter:

- Addition of IAN or PEI as CTA to the seeded emulsion polymerisation of styrene leads to a decrease in the molecular mass of the synthesised styrene polymers.
- It is possible to control the molecular masses of polymers produced in the seeded emulsion polymerisation of styrene by selection of both the type of CTA used and the concentration of the CTA.
- Use of water-insoluble initiators result in polymers with a lower MMD than would otherwise be the case with a water-soluble initiator.
- When a high concentration of PEI as CTA is used, polymers with low MMD are obtained but when a high concentration of IAN as CTA is used, polymers with a high MMD are obtained.
- Addition of a CTA does not have a significant effect on the particle sizes of the latex particles after polymerisation.
- Addition of the CTAs investigated led to a lower conversion of monomer to polymer.
- Using a high CTA concentration led to low  $T_g$  polymers.
- The  $T_g$  of the polymers produced in the presence of CTAs can be controlled by selection of different initiator concentrations.
- IAN is unequally divided between the water and oil phases with the highest concentration in the water phase.
- The CTA IAN is in high concentrations present in the water phase.
- Different concentrations of IAN and PEI can be used to regulate the molecular mass,  $T_g$ , and MMD of polymers.

### 3.7 RECOMMENDATIONS FOR FUTURE STUDIES

The following recommendations for future studies are made:

- It was found that the carbon-iodine bond has an extremely low dissociation energy, resulting in the possible formation of  $I_2$  and HI. An investigation should be carried out to determine the effect that temperature has on the strength of the bond, and the contribution of side reactions

- To overcome the problem of long reaction times, the effect of the addition of catalysts that would enhance the reaction rate should be investigated.
- Better control of the pH of the latex should be investigated. This would help to prevent premature coagulation of the latex particles.
- An investigation to find better surfactants to stabilise the low pH latex should also be carried out.
- Other types of CTAs should also be investigated. RAFT seems to be an especially effective method to obtain well-defined polymer molecules in a latex.
- Investigate proper separation between styrene and the CTA PEI to obtain the distribution of PEI between the water and oil phase.

### 3.8 BIBLIOGRAPHY

1. Seymour, R.B.; Carraher, C.E. **Polymer Chemistry, an Introduction**, Marcell Dekker Inc, New York, p. 87, 1981.
2. Moad, G.; Solomon, D.H. **The Chemistry of Free Radical Polymerisation**, Elsevier Science Inc., Australia, p. 234, 1995.
3. Allen, G; Bevington, J.C. **Comprehensive Polymer Science: The Synthesis, Characterization, Reactions & Applications of Polymers**, Pergamon Press, Oxford, 3, p. 171, 1989.
4. Suddaby, K.G.; Haddleton, D.M.; Hastings, J.J.; Richards, S.N.; O'Donnell, J.P. *Catalytic chain transfer for molecular weight control in the emulsion polymerization of methyl methacrylate and methyl methacrylate-styrene*, **Macromolecules**, 29, 8083, 1996.
5. Patten, T.; Xia, J.; Abernathy, T.; Matyjaszewski, K.; *Polymers with very low polydispersities from atom transfer radical polymerization*, **Science**, 272; 866, 1996.
6. Greszta, D.; Mardare, D.; Matyjaszewski, K. *"Living" radical polymerization. 1. Possibilities and limitations*, **Macromolecules**, 27, 638, 1994.
7. Nakagawa, Y.; Gaynor, S.; Matyjaszewski, K. *The synthesis of end functional polymers by "living" radical polymerization*, **Polymer Preprints, American Chemical Society, Division Polymer Chemistry**, 37, 577, 1996.

8. Solomon, D.H.; Looney, M.G. *Structural control by living radical polymerization*, **Plastics Engineering, New York**, 40, 15, 1997.
9. Benedicto, A.D.; Claverie, J.P.; Grubbs, R.H. *Molecular weight distribution of living polymerization involving chain-transfer agents: Computational results, analytic solutions, and experimental investigations using ring-opening metathesis polymerization*, **Macromolecules**, 28, 500, 1995.
10. Allen, G; Bevington, J.C. **Comprehensive Polymer Science: The Synthesis, Characterization, Reactions & Applications of Polymers**, Pergamon Press, Oxford, 3, p. 171, 1989.
11. Mark, H.F.; Bikales, N.M.; Overberger, C.G.; Menges, G.; Kroschwitz, J.I. **Encyclopedia of Polymer Science and Engineering**, John Wiley & Sons, New York, 3, p. 288, 1985.
12. Moad, G.; Solomon, D.H. **The Chemistry of Free Radical Polymerisation**. Elsevier Science Inc., Australia, p. 335, 1995.
13. Matyjaszewski, K. *From "living" carbocationic to "living" radical polymerization*, **Journal of Macromolecular Science, Pure and Applied Chemistry**, A 31, 989, 1995.
14. Mardare, D.; Matyjaszewski, K. *"Living" radical polymerization of vinyl acetate*, **Macromolecules**, 27, 645, 1994.
15. Yoshida, E.; Okada, Y. *Control of molecular weight by living radical polymerization with a nitroxyl radical*, **Polymer Preprints, American Chemical Society, Division Polymer Chemistry**, 34, 3631, 1996.
16. Allen, G; Bevington, J.C. **Comprehensive Polymer Science: The Synthesis, Characterization, Reactions & Applications of Polymers**, Pergamon Press, Oxford, 3, p. 181, 1989.
17. Matyjaszewski, K.; Gaynor, S.; Wang, J-S. *Communications to the editor: Controlled radical polymerizations: The use of alkyl iodides in degenerative transfer*, **Macromolecules**, 28, 2093, 1995.
18. Gaynor, S.; Wang, J-S.; Matyjaszewski, K. *Controlled radical polymerization by degenerative transfer: Effect of the structure of the transfer agent*, **Macromolecules**, 28, 8051, 1995.
19. Gaynor, S.; Wang, J-S.; Matyjaszewski, K. *Well defined polymers obtained through the use of controlled radical polymerization: The use of alkyl iodides as degenerative*

- transfer reactions*, **Polymer Preprints, American Chemical Society, Division Polymer Chemistry**, 36, 467, 1995.
20. Gaynor, S.; Wang, J-S.; Matyjaszewski, K. *Well defined polymers obtained through the use of controlled radical polymerization: The use of alkyl iodides as degenerative transfer reactions*, **Polymer Preprints, American Chemical Society, Division Polymer Chemistry**, 36, 467, 1995.
21. Box, G.E.P.; Hunter, W.G; Hunter, J.S. **Statistics for Experimenters: An Introduction to Design, Data Analysis and Model Building**, Wiley, New York, 1978.
22. Malvern instruments, PCS training course, Version 1.26 software, 1996.
23. Schnablegger, H.; Glatter, O. *Simultaneous determination of size distribution and refractive index of colloidal particles from static light-scattering experiments*, **Journal of Colloid and Interface Science**, 158, 228, 1993.
24. Reimers, J.L.; Schork, F.J. *Predominant droplet nucleation in emulsion polymerization*, **Journal of Applied Polymer Science**, 60, 251, 1996.
25. Gilbert, R.G. **Emulsion Polymerisation, a Mechanistic Approach**, Academic Press, London, p. 144, 1995.
26. Ahmed, S.M.; El-Aasser, M.S.; Pauli, G.H.; Poehlein, G.W.; Vanderhoff, J.W. *Cleaning latexes for surface characterization by serum replacement*, **Journal of Colloid and Interface Science**, 73, 388, 1980.
27. Schomburg, G. **Gas Chromatography, a Practical Course**, VCH publishers, pp. 111 – 121, 1990.
28. Yoshida, E.; Takamasa, F. *Synthesis of well-defined polychlorostyrenes by living radical polymerisation with 4-methoxy-2,2,6,6-tetramethylpiperidine-1oxyl*, **Journal of Polymer Science, Part A: Polymer Chemistry**, 35, 2371, 1997.
29. Moad, G.; Solomon, D.H. **The chemistry of free radical polymerisation**. Elsevier Science Inc., Australia, p. 55 – 56, 1995.
30. Billmeyer, F.W. **Textbook of Polymer Science**, 3<sup>rd</sup> ed., Wiley & Sons, New York, p. 321, 1984.

## CHAPTER 4

# KINETICS OF THE SEEDED EMULSION POLYMERISATION OF STYRENE IN THE PRESENCE OF AN ALKYL IODIDE CHAIN TRANSFER AGENT

### 4.1 INTRODUCTION

The effect which IAN, as a degenerative CTA, has on the kinetics of an emulsion system was studied, and reported here. The kinetics of an emulsion free-radical polymerisation is very complex as a result of its heterogeneity. An emulsion is heterogeneous because it consists of many different phases and substances, all of which have been discussed in section 2.1. If a seed latex is used, the complex equations involved in particle nucleation can be ignored. Understanding the effect that the CTA has on the kinetics of emulsion polymerisation will enable further investigations to be carried out towards optimising a system where CTAs are used to control the molecular mass and MMD of polymers produced in emulsion.

For the purpose of this study the assumptions that Smith and Ewart<sup>1</sup> made will also be applied; they are as follows:

- The locus of chain propagation is in the monomer-swollen particles.
- Radicals entering from the water phase into the latex particles initiate polymerisation.
- It is assumed that the polymerising seed latex is mono-disperse in size.
- No new nucleation of latex particles takes place.

### 4.2 OBJECTIVES

The aim of the investigation was firstly to determine the average number of radicals per latex particle,  $\bar{n}$ . These values would then be compared to values obtained in previous experiments reported in literature.<sup>2</sup> If any discrepancies occurred then a feasible qualitative

model that would explain these differences would be proposed. The second part of the investigation would focus on finding the transfer rate coefficient,  $k_{tr,CTA}$ , for the two CTAs IAN and PEI.

In the following paragraphs an explanation of the intended study follow. All symbols or abbreviations that were used are summarised in the List of Symbols and the List of Abbreviations.

## 4.3 THEORY

### 4.3.1 Emulsion polymerisation

The progress of the emulsion polymerisation can be divided into three distinct intervals. This theory is the most recent and is proposed by Gilbert<sup>3</sup> and Gardon<sup>4</sup>.

Interval I:

This distinct interval is at the beginning of an emulsion polymerisation, where particle nucleation takes place. All the possible nucleation steps are illustrated in Figure 4.1.<sup>5</sup>

During Interval I the latex particles are formed and grow in the presence of monomer droplets and emulsifier or surfactant molecules. Polymerisation will commence in only 0.1% of the originally formed micelles. The other nucleating species are formed in the aqueous phase and polymerisation continues until a hydrophobic oligomer with a degree of polymerisation of  $z$  is reached. For styrene  $z$  is a value of 2–3 repeat units.<sup>6</sup> These oligomeric radicals ( $z$ -mers) migrate from the aqueous phase into micelles or form primary particles. Micelles are groups of surfactant molecules that aggregate with their hydrophobic ends orientated to the inside, away from the aqueous phase, in order to obtain a state of lower energy. When the  $z$ -mer enters a micelle it polymerises further due to the monomer molecules present in the micelle. At this stage the micelle ceases to exist and is now called a latex particle.

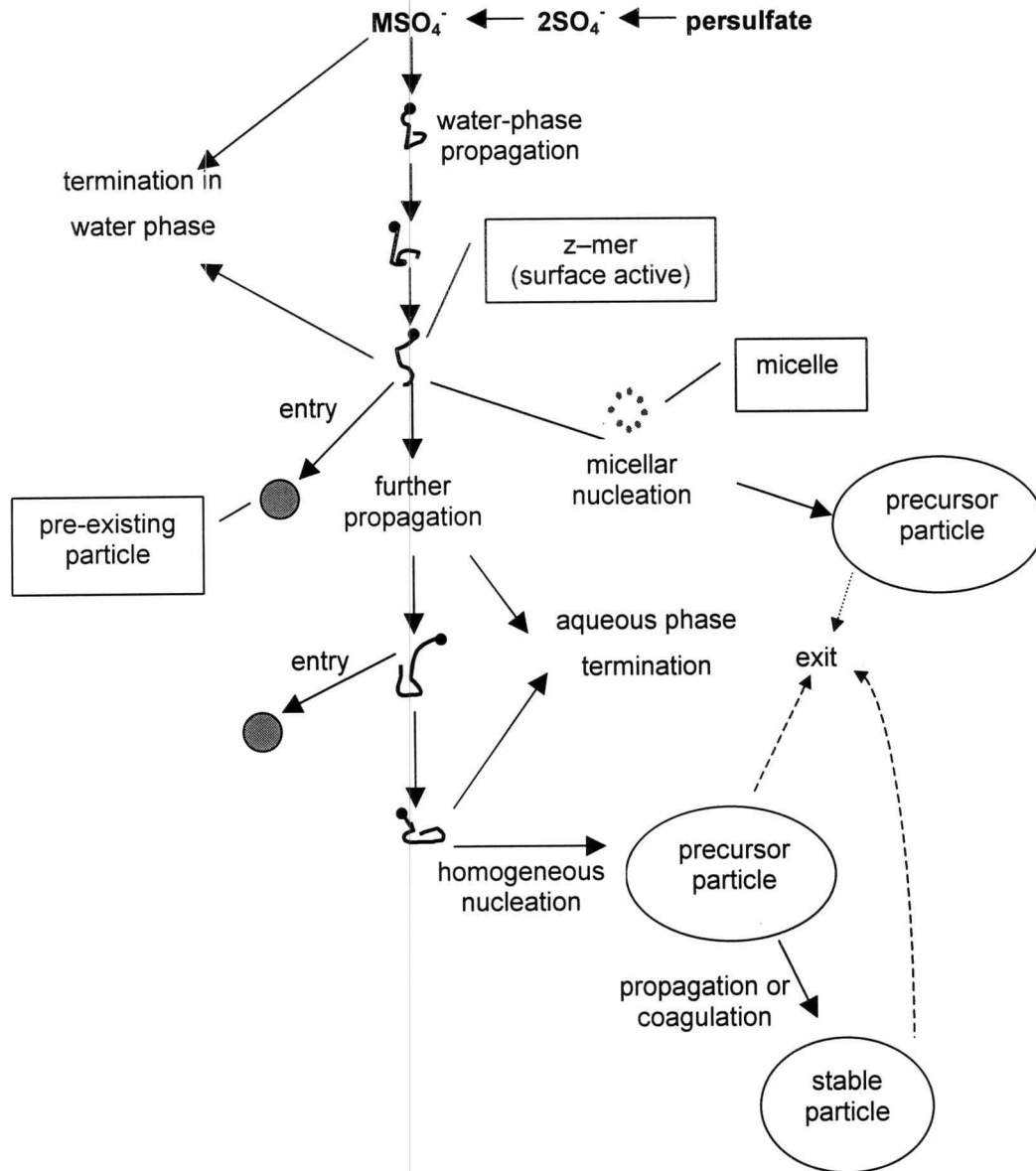


**Figure 4.1:**

**All the possible reactions that can take place in an emulsion polymerisation.**

All particle nucleation stops once the end of Interval I is reached.

Interval II:

In this stage no particle nucleation takes place. During this interval the latex particles grow in the presence of monomer droplets that act as a reservoir for monomer. Monomer from the monomer droplets diffuses through the aqueous phase into the latex particles. The concentration of monomer in the particles remains more or less constant. The reason for this is the balance between the free energy of mixing and the surface free energies. As

diffusion continues, the size of the monomer droplets decrease and as conversion proceeds, these droplets will eventually disappear at the beginning of Interval III.

Interval III:

In this interval no monomer droplets are present. Polymerisation of monomer residing in the particles continues at a decreased rate.

As was previously mentioned in section 4.1, the heterogeneity of emulsion polymerisation makes the mechanism of emulsion polymerisation complex. For this reason the steady state assumption for Interval II will now be applied. This implies that the initiation rate and the termination rate are equal.

The number of radicals in a particle in Interval II is only dependant on the entry and exit rate of the radicals in and out of the swollen particle and on the rate of termination of the radicals in the latex particle.<sup>1,4</sup> This radical balance is given by eq. 4.1 and eq. 4.2 with  $N_n$  the number of latex particles containing  $n$  free radicals.

$$\frac{dN_n}{dt} = \text{entry} + \text{exit} + \text{termination} \quad (4.1)$$

$$\begin{aligned} \frac{dN_n}{dt} = \frac{\rho}{N} (N_{n-1} - N_n) + k_0 \frac{a}{v} [(n+1)N_{n-1} - nN_n] \\ + \frac{k_t}{v} [(n+1)(n+2)N_{n-2} - n(n-1)N_n] \end{aligned} \quad (4.2)$$

Three possible case scenarios exist that can be made from eq. 4.2:

Case I:

The exit rate of radicals out of the particle is much higher than their entry rate. This would lead to a situation where  $\bar{n}$  is smaller than unity.

**Case II:**

The entry rate of radicals into the particle is much higher than their exit rate but is less than their rate of termination. In such a case  $\bar{n}$  would be approximately 0.5. It is assumed that radicals that are formed in the water phase lead to the formation of oligomeric radicals that enter the micelles. Once inside the micelle the radical is incapable of returning to the water phase. When another radical enters the micelle, termination of the existing radical is immediate. Should another radical enter the micelle this would lead to a new propagating polymer chain. On average there are 0.5 radicals in a polymer particle. This is referred to as “zero-one” kinetics and refers to only one or zero living radicals within a polymer particle.<sup>7</sup>

In the case of “zero-one” kinetics, the kinetic equations are less complex. For this reason most case studies are conducted during Interval II. During Interval II secondary nucleation is prevented by using a seed latex from which all excess surfactant has been removed. In such a system the particle number, particle size, particle surface characteristics and other variables are kept constant.

**Case III:**

The entry rate of radicals into the particle is much greater than the rate of termination. In this case,  $\bar{n}$  is larger than unity. This is referred to as “pseudo-bulk” kinetics.<sup>7</sup> Here the kinetics is chain length dependent as a result of termination being chain length dependent.

**4.3.2 The kinetics of emulsion polymerisation**

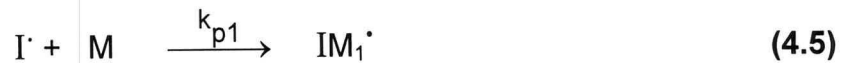
A styrene emulsion system gives a good reference-model against which the results of the current investigation can be tested. In this model it is assumed that instantaneous termination takes place, resulting in a “zero-one” system. The kinetics of the sequence of events in a styrene emulsion polymerisation, in Interval II and III, can be described as follows:<sup>8</sup>

**Initiator decomposition:**

with the first-order rate equation for dissociation of the initiator:

$$-\frac{2d[I_2]}{dt} = \frac{d[I^*]}{dt} = 2fk_d[I_2] \quad (4.4)$$

**Initial propagating step:**



with the first-order rate equation for the initial propagation step:

$$-\frac{d[I^*]}{dt} = \frac{d[IM_1^*]}{dt} = k_{p1}[I^*][M] \quad (4.6)$$

**Propagation:**

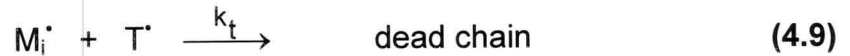


with the first-order rate equation for propagation:

$$-\frac{d[IM_i^*]}{dt} = \frac{d[IM_{i+1}^*]}{dt} = k_p[IM_i^*][M] \quad (4.8)$$

**Termination:**

Two bi-molecular, irreversible termination reactions can occur. One is possibly through disproportionation and the other through recombination.<sup>9</sup> In emulsion polymerisation, as in other radical polymerisation reactions, termination is diffusion controlled and the termination coefficient is chain length dependent.<sup>10,11</sup> The termination reaction is given in eq. 4.9.



with the second-order rate equation for the bi-molecular termination in the particle:

$$-\frac{d[IM_i^{\bullet}]}{dt} = k_t [IM_i^{\bullet}] [T^{\bullet}] \quad (4.10)$$

### Transfer:

When it is assumed that the main transfer reaction that occurs is transfer to the CTA, and all other transfer reactions are negligible. The transfer reaction is given in eq. 4.11:

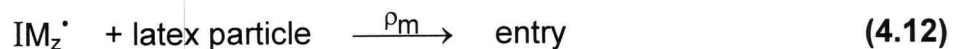
In principle, CTAs do not influence the kinetics of a free radical polymerisation of



monomers in homogeneous or bulk solutions but only reduce the molecular mass of the polymer formed.<sup>12</sup>

### Entry:

At a certain chain length,  $z$ , the oligomer formed in the aqueous-phase becomes surface active. This allows the oligomer to enter into the particle,



where the pseudo-first-order rate coefficient ( $\rho_m$ ) for entry of the  $z$ -mer into the particle is given by eq. 4.13.<sup>13</sup>

$$\rho_m = \frac{2k_d [I_2] N_A}{N_c} \quad (4.13)$$

The re-entry of exited radicals is not taken into account.

The presence of a CTA can influence the rate of entry of radicals into the latex particle. In the case of a hydrophobic CTA, transfer to CTA molecules present in the aqueous phase and subsequent propagation would lead to a z-mer with a lower DP. Although the concentration of a hydrophobic CTA in the aqueous phase is negligible, this can lead to an increase in the entry rate of radicals into the particles. An equation for the entry rate coefficient as a result of z-mers as well as CTA radicals is given in eq. 4.14.<sup>14</sup>

$$\rho = \rho_m + \rho_{\text{CTA}} = \frac{2k_d[I]N_A}{N_c} \left( \frac{k_{t,\text{aq}}[T^*] + k_{\text{tr,CTA}}C_{\text{CTA, aq}}}{k_{p,\text{aq}}C_{m,\text{aq}}} + 1 \right)^{1-z} + \frac{N_A}{N_c} k_{\text{tr,CTA}}C_{\text{CTA, aq}}[T^*] \quad (4.14)$$

In the case of a hydrophilic CTA, transfer to the CTA would not result in immediate entry into the latex particle. Only after propagation to a critical length does the newly formed active radical become surface active. This is confirmed by the solubility of acetonitrile, propanenitrile and n-butanenitrile in water at 25 °C, given in Table 4.1.<sup>15</sup>

**Table 4.1:**

**Water solubility of chemical species resembling the propagating radical after transfer of the radical to the hydrophilic CTA.**

Chemical species	Mass percentage dissolved in the water phase (%)
acetonitrile	> 99
propanenitrile	10.3
n-butanenitrile	3.3

It is clear that the solubility of the active radical decreases rapidly as propagation commences. The solubility is given as a mass percentage of the solute over the total mass. No extreme change in the entry rate is expected in such a case.

#### Exit:

The exit model for radicals from a latex particle is postulated to be the transfer of the radical to a lower molecular mass molecule. This monomeric radical can escape into the aqueous phase if it diffuses away from the particle before it propagates. The exit rate coefficient ( $k_{\text{ex}}$ ) is given by eq. 4.15:<sup>16</sup>

$$k_{\text{ex}} = k_{\text{tr},m} C_{m,p} \frac{k_{\text{ex},m}}{k_{\text{ex},m} + k_{p1} C_{m,p}} \quad (4.15)$$

with

$$k_{\text{ex},m} = (3D_{m,\text{aq}}/r_s^2) (C_{m,\text{aq}}/C_{m,p}) \quad (4.16)$$

In the presence of a CTA, there is a competition between re-initiation of the CTA and exit of the radical. In the case of a good CTA, re-initiation is fast. Therefore, CTA radical exit is usually not taken into account because it is assumed that it is least likely to occur. When, however, re-initiation is not instantaneous, the competition between re-initiation and exit needs to be taken into account. In the case of a hydrophilic CTA, the re-initiation vs. exit balance that may occur may be shifted, allowing a high exit rate of radicals from the latex particles.

In cases where the exit rate of CTA radicals play a definite role, the total exit rate can be defined as:<sup>16</sup>

$$k_{\text{ex}} = k_{\text{ex},m} + k_{\text{ex,CTA}} = k_{\text{tr},m} C_{m,p} P_{\text{ex},m} + k_{\text{tr,CTA}} C_{\text{CTA},p} P_{\text{ex,CTA}} \quad (4.17)$$

with

$$P_{\text{ex},m} = \frac{k_{\text{ex},m}}{k_{\text{ex},m} + k_p C_{m,p} + k_{\text{tr,CTA}} C_{\text{CTA},p}} \quad (4.18)$$

and

$$P_{\text{ex,CTA}} = \frac{k_{\text{ex},m}}{k_{\text{ex,CTA}} + k_{p,n} C_p} \quad (4.19)$$

and

$$k_{\text{ex,CTA}} = (3D_{\text{CTA},\text{aq}}/r_s^2) (C_{\text{CTA},\text{aq}}/C_{\text{CTA},p}) \quad (4.20)$$

### 4.3.3 Determining second-order rate coefficient for transfer to a chain transfer agent

An established method to determine the chain transfer coefficient to monomer is the Mayo method.<sup>17</sup> The Mayo-equation is given by eq. 4.21.<sup>18</sup>

$$1/P_n = [(1 + \lambda)/2](k_t/k_p^2)(R_p/[M]^2) + C_M \quad (4.21)$$

with:

$$C_M = k_{tr,CTA}/k_p \quad (4.22)$$

Because large errors can be introduced during the extrapolation process, there are problems with the accuracy of this method. An alternative method is based on the chain length distribution in which the following concept is used: the MMD of linear polymer chains produced by emulsion polymerisation not only influences the bulk properties of the resultant polymer sample, but also reflects the molecular events that contribute to polymer growth. The limiting molecular masses of the polymers produced in the presence of CTAs are primarily due to the transfer reaction that takes place. The  $k_{tr,CTA}$  value can be obtained from the transfer dominated region of the chain length distribution which is the number molecular mass distribution.<sup>19-24</sup>

The basic notion is that, for sufficiently high molecular masses and low radical concentrations as a result of low initiator concentrations, the molecular mass distributions that are formed will follow the simple exponential decay given by eq. 4.25.<sup>18</sup>

$$\lim_{M \rightarrow \infty} P_{\text{instant}}(M) = \exp \left\{ - \frac{k_{tr,M}[M] + k_{tr,CTA}[CTA]}{k_p[M]} \frac{M}{M_0} \right\} \quad (4.25)$$

The number molecular mass distribution,  $P(M)$ , is obtained from the calibrated GPC results:<sup>18</sup>

$$\begin{aligned} P(M) &= \frac{\overline{W}(M)}{M} \\ &= \frac{G(V_{el})}{M \cdot \frac{dM}{dv}} \end{aligned} \quad (4.26)$$

where  $G(V_{el})$  is the GPC trace and is  $V_{el}$  the elution volume.

As a result of the nature of the kinetics associated with emulsion polymerisation, as discussed previously (see section 4.3.2), termination is the main chain-stopping event for shorter chains. A plot of the natural logarithm of the number molecular mass distribution against the molecular mass should reveal that  $\ln P(M)$  becomes non-linear as the molecular mass decreases. This is primarily due to the variation in the extent of termination compared to the extent of transfer for the low molecular mass molecules as a result of the change in the mobility of the molecules as their molecular masses increase. The linear region of the  $\ln P(M)$  vs.  $M$  plot is apparent at high molecular masses, where the chain-stopping mechanism is dominated by chain transfer.<sup>18</sup> The gradient of the linear part of the plot of  $\ln P(M)$  vs.  $M$  is given by eq. 4.27.

$$\text{Grad} = -\frac{k_{tr,M}}{k_p M_0} - \frac{k_{tr,CTA}}{k_p M_0} \cdot \frac{[CTA]}{[M]} \quad (4.27)$$

When the slope at each concentration of the CTA is plotted against  $[CTA]/[M]$ , a linear plot with a gradient as given in eq. 4.28 is obtained.

$$\text{Grad}' = -\frac{1}{k_p M_0} \cdot k_{tr,CTA} \quad (4.28)$$

Multiplying the slope by the molecular mass of the monomer, the ratio of  $k_p$  and  $k_{tr,CTA}$  is obtained. In order to reduce other chain length dependant reactions such as termination, a low initiator concentration have to be used to obtain a low conversion. For the purpose of the present study a conversion of less than 10% is considered to be low, and therefore, 10% conversion was used as a cut-off point under which the experimental runs were done.

In a private conversation with my study leader, the method used above was questioned. In the original cases referred to in the literature, CTAs were used that only allowed single step transfers. The character of the alkyl iodides used in this study allowed multiple transfer reactions to take place. For this reason it is suggested that in a further

investigation, an extrapolation to an infinitely high CTA concentration should be made to arrive at a correct single transfer step value.

#### 4.3.4 Determining the initiator concentration to obtain a 10% conversion of monomer to polymer

To reduce chain length dependant reactions, the conversion of monomer to polymer was not allowed to exceed 10%. To obtain a conversion of 10%, initiator concentration necessary to allow the reaction to continue for 0.5 h had to be calculated.

If it is assumed that transfer does not influence the rate of polymerisation and that all the radicals produced by the initiator decomposition are used in further polymerisation reactions, the steady state assumption can be made.<sup>25</sup> The net rate of initiation then becomes equal to that of propagation:

$$2fk_d[I] = 2k_p[M^*]^2 \quad (4.28)$$

This leads to:

$$[M^*] = \left[ \frac{fk_d[I]}{k_{tr,CTA}} \right]^{0.5} \quad (4.29)$$

If eq. 4.29 is substituted into eq. 4.4, the following eq. 4.30 is obtained:

$$-\frac{d[M]}{dt} = k_p \left[ \frac{fk_d[I]}{k_{tr,CTA}} \right]^{0.5} [M] \quad (4.30)$$

If it is believed that the CTA has no effect on conversion (X), but only on the MMD, the conversion can be obtained by integrating eq. 4.30 to give eq. 4.31:

$$X = 1 - \exp - \left\{ 2k_p \left( \frac{f}{k_d k_{tr,CTA}} \right)^{0.5} [I_0]^{0.5} (1 - e^{-k_d t/2}) \right\} \quad (4.31)$$

Using eq. 4.31 it is now possible to determine the initiator concentration to obtain 10% conversion.

## 4.4 EXPERIMENTAL

### 4.4.1 Determining the average number of free radicals per particle

The following equipment was used: a three neck round bottomed flask, a single blade Teflon stirrer and a water bath.

A styrene seed latex (see section 3.4.4) was used for the reaction to allow polymerisation in Interval III. The seed latex was washed in a serum replacement cell (see section 3.4.5). The seed was diluted to give a stock solution of the seed latex with a constant solids content of 10% for all the experiments. A 10% solids content was used to enable GC analysis to be made; preventing clogging of the needle.

The ingredients for the reaction were as follow:

- 100g of the styrene seed latex.
- 3% (m/m) sodium dodecyl sulfate to act as surfactant.
- 0.06 moles of sodiumbicarbonate to act as buffer.
- Different concentrations of IAN as CTA given in Table 4.2.
- 2g of KPS, dissolved in 50cm<sup>3</sup> of DDI water.
- Stirring speed of 400 rpm.
- Temperature of 70°C.
- Monomer

The reagents were stirred for 24 hours to allow the seed latex to be swollen with monomer. Analysis by Malvern Zetasizer 4 revealed an increase in the latex particle size of 51%. The reagents were purged with N<sub>2</sub> for half an hour before the initiator was added. The

reaction was continued for five hours under an inert atmosphere of N<sub>2</sub> at a temperature of 70°C. Four identical reactions were run at different IAN concentrations given in Table 4.2.

**Table 4.2:**

**Different IAN concentrations used to determine the average number of free radicals per particle in a seeded emulsion polymerisation of styrene.**

Run number	[IAN] (mol / 0.336mol styrene)
1 (reference)	0.000
2	0.002
3	0.003
4	0.004

Each sample that was taken was immediately quenched in a 5% (m/v) aqueous hydroquinone solution. Ethylene glycol was added to act as dispersant. DMF was added to act as an internal standard for the GC analysis. The GC analysis revealed the residual styrene concentration of the styrene monomer to allow the fractional conversion of monomer to polymer to be calculated. The internal standard method of quantitative GC evaluation via peak area was used to determine the residual styrene concentration and is explained in section 3.4.10.

#### **4.4.2 Determining the initiator concentration necessary to obtain a 10% conversion to calculate the rate transfer constants for a chain transfer agent**

As was mentioned previously in section 4.3.4, a low conversion was needed to prevent chain dependant reactions taking place in the polymerisation of styrene in the presence of the CTA. Using eq. 4.31 the initiator concentration necessary to reach a 10% conversion of monomer to polymer in 0.5 h, was calculated. A value for  $k_{t,CTA}$  for the transfer of the iodine atom from IAN or PEI to styrene does not exist in literature. Hence, the  $k_{t,CTA}$  value for 2-iodo-propane as chemical homologue was used. The values for the constants used to calculate the time necessary to reach 10% conversion is given in Table 4.3.

**Table 4.3:**

**The constants used to calculate the initiator concentration necessary to reach a 10% conversion of styrene monomer to polymer in the presence of chain transfer agents.**

Constant	Value
$k_d^{21}$	$4.19 \times 10^{-5} \text{ s}^{-1}$
$k_p$	484 $\text{dm}^3\text{mol}^{-1}\text{s}^{-1}$
$k_t$	45 $\text{dm}^3\text{mol}^{-1}\text{s}^{-1}$
$f^{26}$	0.7

The initiator concentration was calculated to be  $0.012 \text{ mol}\cdot\text{dm}^{-3}$ .

#### 4.4.3 Determining the rate transfer constants for IAN and PEI

Styrene was distilled and dried as was described in section 3.4.2. A stock solution of styrene containing the initiator, AIBN, was prepared and stored below  $0^\circ\text{C}$ . 3 g of the stock solution was weighed off into specially designed Schlenk-tubes. This corresponds to 0.03 moles of styrene. Both the CTAs that were used in the two separate experiments were added at different concentrations. The concentrations of the CTAs used are given in Table 4.4.

**Table 4.4:**

**Concentrations of the CTAs used for the different runs to obtain  $k_{tr,CTA}$  for IAN and PEI.**

Run number	Concentration of the CTA ( $\text{mol}\cdot\text{dm}^3$ )
1	0.08
2	0.10
3	0.12

The Schlenk-tubes were put through five freeze-thaw cycles to remove any oxygen that was present in the solutions. After the tubes were sealed, they were transferred to a water bath at 70 °C. The polymerisation was continued for half an hour before the tubes were removed. The polymer solution was quenched with a 2.5 % (m/v) mixture of hydroquinone in methanol and cooled in ice.

The quenched polymer solution was dried under reduced pressure at a temperature of 60 °C. The conversion of the retained polymer was measured gravimetrically to ensure that the conversion was below 10%. The dried polymer was dissolved in THF at a concentration of 3 mg/ml. The samples were run on a Waters GPC with Millenium software to determine their molecular masses. The operating temperature was 30 °C while a flow rate of 0.6 ml/min was maintained. The GPC was equipped with a refractive index detector. Eight polystyrene standards were used for calibration (see section 3.4.7).

## 4.5 RESULTS AND DISCUSSIONS

### 4.5.1 Determining the average number of free radicals per particle

The fractional conversion ( $x$ ) of the samples that were drawn from the reactor were calculated with eq. 4.32.

$$x = 1 - \frac{m_M}{m_M^0} \quad (4.32)$$

The data i.e. the fractional conversions were plotted against time. These data points were fitted with a suitable curve using TableCurve for Windows and are given in Appendix F, Figures F.1, F.2, F.3 and F.4 for Runs 1 – 4 respectively. The corresponding equations used to fit the four curves are given in Appendix F Table F.1. TableCurve for Windows is a Jandel Scientific product.

The numerical derivative for the equations that were fitted for Runs 1 – 4 was used to calculate  $\bar{n}$  using eq. 4.33.<sup>27</sup>

$$\bar{n} = \frac{dx}{dt} \frac{n_M^0 N_A}{k_p C_p N_C} \quad (4.33)$$

The monomer concentration within the latex particles ( $C_p$ ) can be calculated with eq. 4.34:<sup>28</sup>

$$C_p = (1-x) \frac{m_M^0/M_0}{m_M^0 V_{SM} + m_p^0 V_{Sp} + x m_M^0 (V_{Sp} - V_{SM})} \quad (4.34)$$

with 
$$V_{SM} = \frac{1}{d_M} \quad (4.35)$$

$$V_{Sp} = \frac{1}{d_p} \quad (4.36)$$

Further, the latex particle density ( $N_c$ ) is calculated with eq. 4.37:<sup>29</sup>

$$N_c = \frac{m_p^0}{4/3 \pi r_u^3 d_p} \quad (4.37)$$

The average number of free radicals per latex particle ( $\bar{n}$ ) over time for the four runs are given in Figure 4.2.

The rate of Run 1 is much higher than that of Runs 2 and 3. A difference in the maximum value of  $\bar{n}$  for the reactions with IAN and the reaction without the CTA can be seen. To explain this and other observations, the reaction is divided into three timed events called phases A, B and C illustrated in Figure 4.3. The curve in Figure 4.3 constructed using the equation for the plots given in Appendix F (see Table F.1) using arbitrarily chosen constants. The graph in Figure 4.3 is not the actual data set but only a sketch to explain the mechanism involved during the seeded emulsion polymerisation of styrene. Figure 4.4 is a plot of the average number of free radicals per latex particle against conversion for the plot in Figure 4.3.

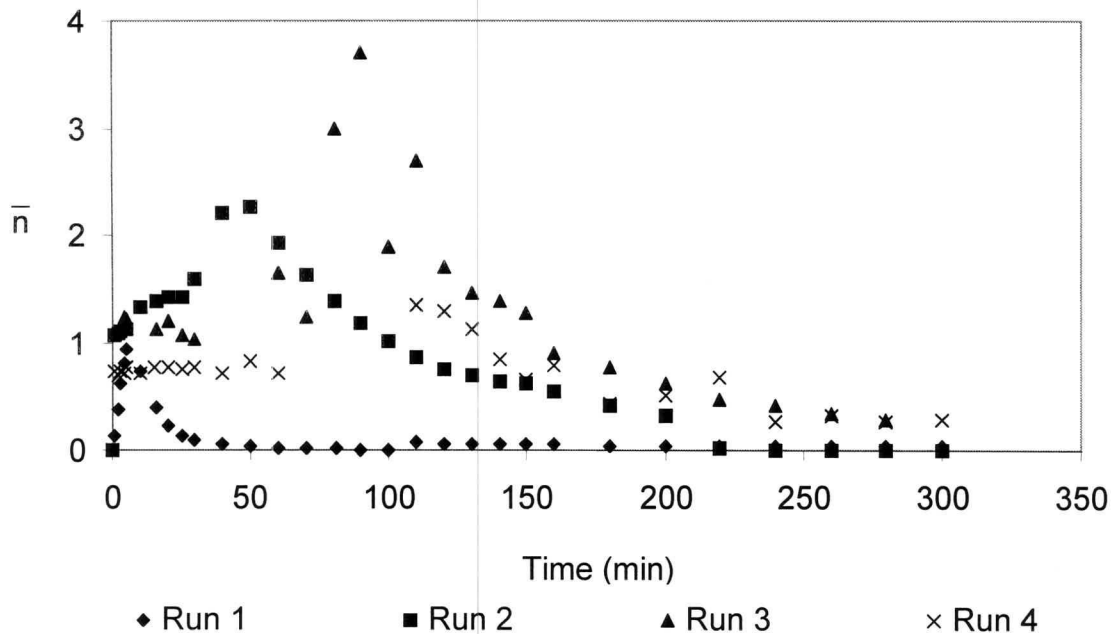


**Figure 4.2:**

**The average number of free radicals per latex particle for Run 1 – 4 over the reaction time.**

### Phase A

Starting at zero radicals, the amount of radicals in the water phase increases during initiation. As polymerisation in the aqueous phase commences, oligomeric radicals reach the critical length,  $z$ . The  $z$ -mers migrate into the particles, increasing  $\bar{n}$ . This phase is the same for the standard seeded emulsion polymerisation of styrene as well as the ones in which IAN was added as CTA. However, the rate of entry in the cases where IAN was added was lower than in the run without the CTA. The reason is believed to be the lower rate of propagation when IAN is present. The decrease in the propagation rate was also observed in literature using PEI and is believed to be the result of  $I_2$  and HI being formed (see section 3.5.4).<sup>30</sup> From the plot given in Figure 4.4 it can be seen that there is an increase in  $\bar{n}$  at low conversion.

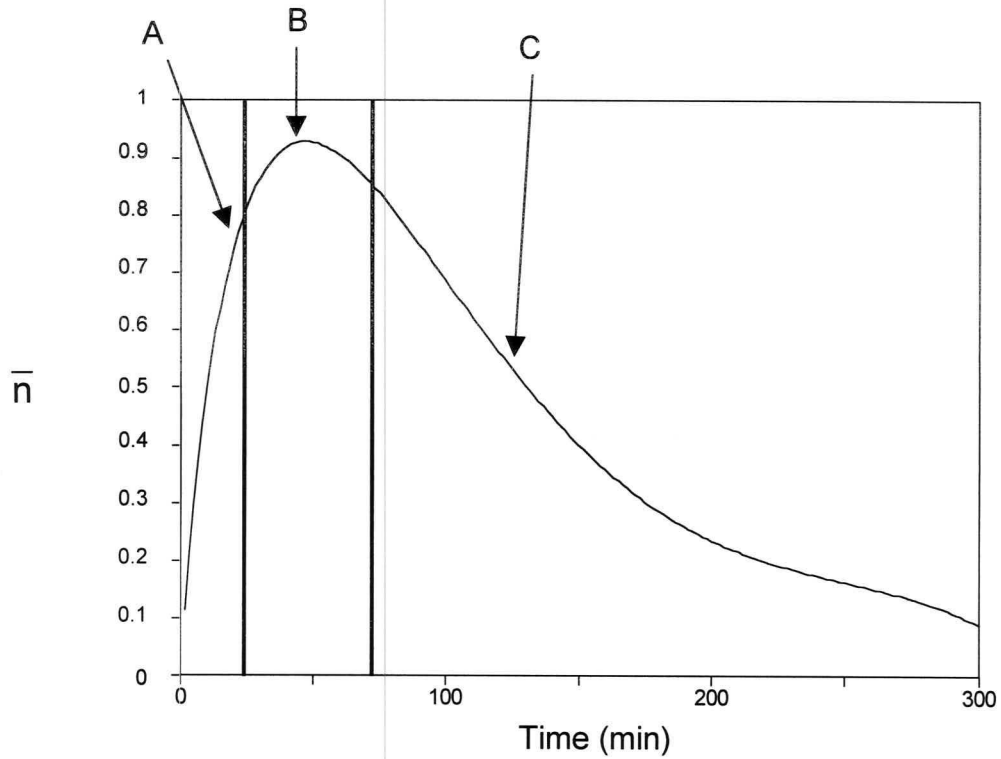


**Figure 4.3:**

**Average number of free radicals over time for the seeded emulsion polymerisation of styrene in the presence of IAN .**

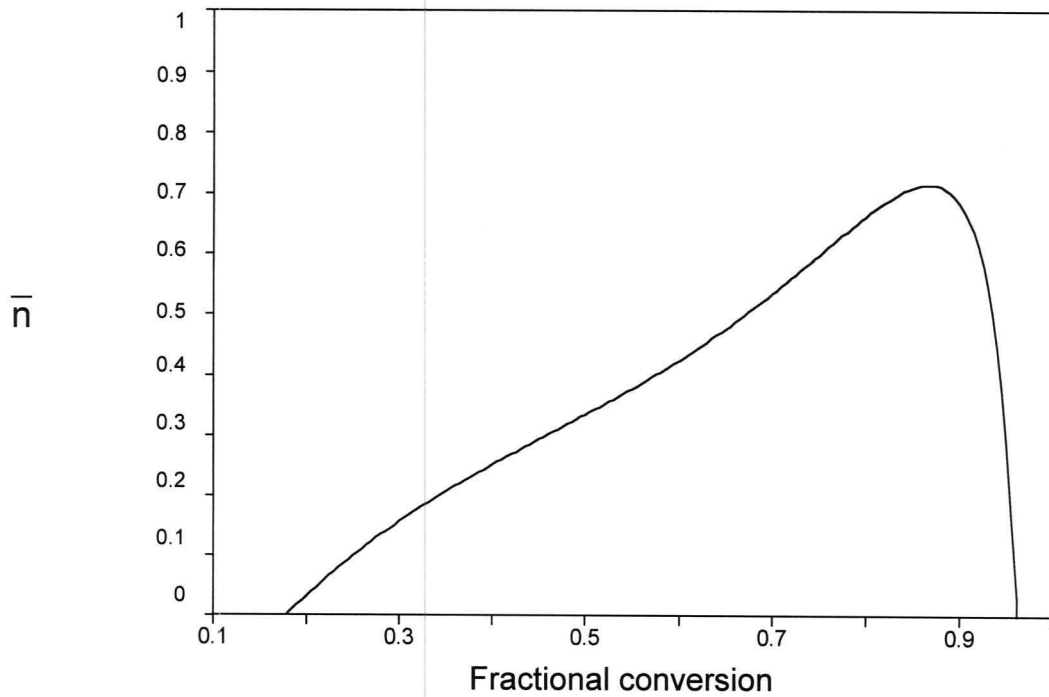


**Figure 4.4:**

**Average number of free radicals against conversion for the seeded emulsion polymerisation of styrene in the presence of IAN.**

## Phase B

A maximum value of  $\bar{n}$  is reached in this phase. For the standard seeded emulsion polymerisation of styrene (Run 1), the maximum value of  $\bar{n}$  is between 0.5 and 1. This value for  $\bar{n}$  increased up to a fractional conversion of 0.9, where it reached a maximum value (see Figure 4.4). This is in concurrence with a “zero–one” system described earlier, in section 4.3.1.<sup>31</sup>

In “zero–one” kinetics, the latex particle size is so small that only one or no radical can be present in the latex particle. In “pseudo–bulk” kinetics, however, more than one radical can be present in a latex particle because the particles are much larger than under normal “zero–one” conditions, leading to a time–dependant termination rate (see section 4.3.1). For Runs 2 – 4, when IAN was used as CTA,  $\bar{n}$  exceeded 1 as if “pseudo–bulk” kinetics is obeyed. This presupposes that the termination rate has decreased to such an extent making it a time–dependant reaction. Assumptions made previously by Matyjaszewski confirm this.<sup>33</sup> Yet, the particle size is well below that used in “pseudo–bulk” kinetics. This would imply that under these conditions it is possible to obtain more than one radical in a latex particle under conditions normally attributing to “zero–one” conditions. The conclusion is that difference between “zero–one” and “pseudo–bulk” is not a definite one, but the change from the one to the other is much more gradual.

## Phase C

At a high conversion, Run 1 has a steady decrease in  $\bar{n}$ , to zero. This is a result of monomer molecules being depleted and, to a lesser extent, termination taking place. The decrease in  $\bar{n}$  is much more obvious with IAN in Runs 2 – 4. At high conversion  $\bar{n}$  decreases drastically. It is believed that transfer to the CTA leads to a high exit rate due to the water–solubility of IAN and this in turn causes the termination of radicals. Both effects are due to the hydrophilic nature of the CTA.

#### 4.5.2 Transfer constants for chain transfer to iodoacetonitrile and 1-phenylethyl iodide

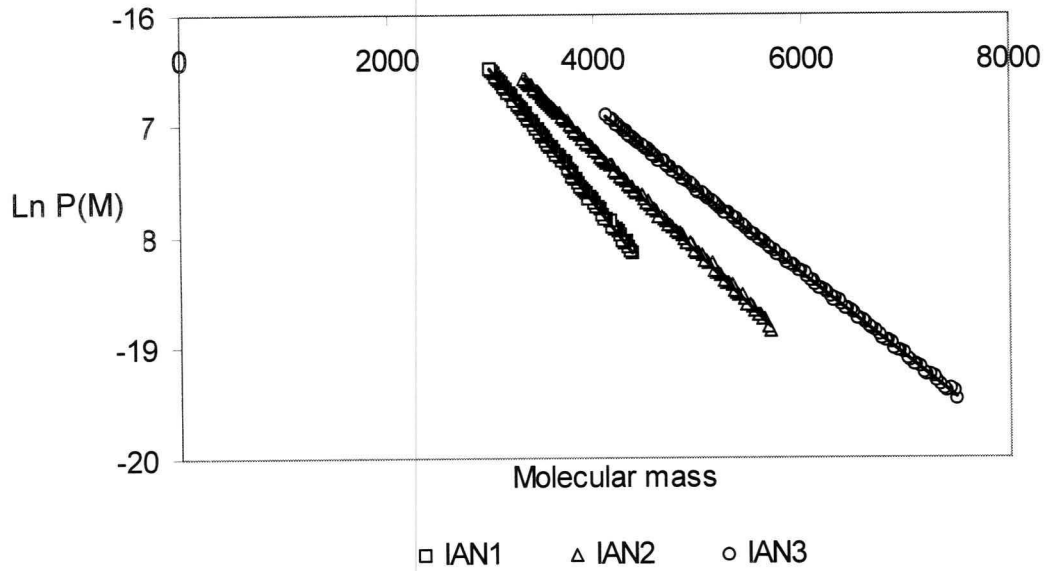
The chain transfer reaction from styrene to IAN or PEI is a degenerative transfer reaction (see section 2.3.4). This is the result of the resonance stabilisation of IAN and PEI. Figure 3.2 illustrates the resonance stabilisation of IAN and Figure 3.3 illustrates the resonance stabilisation of PEI (see section 3.3.6).

**Table 4.5:**

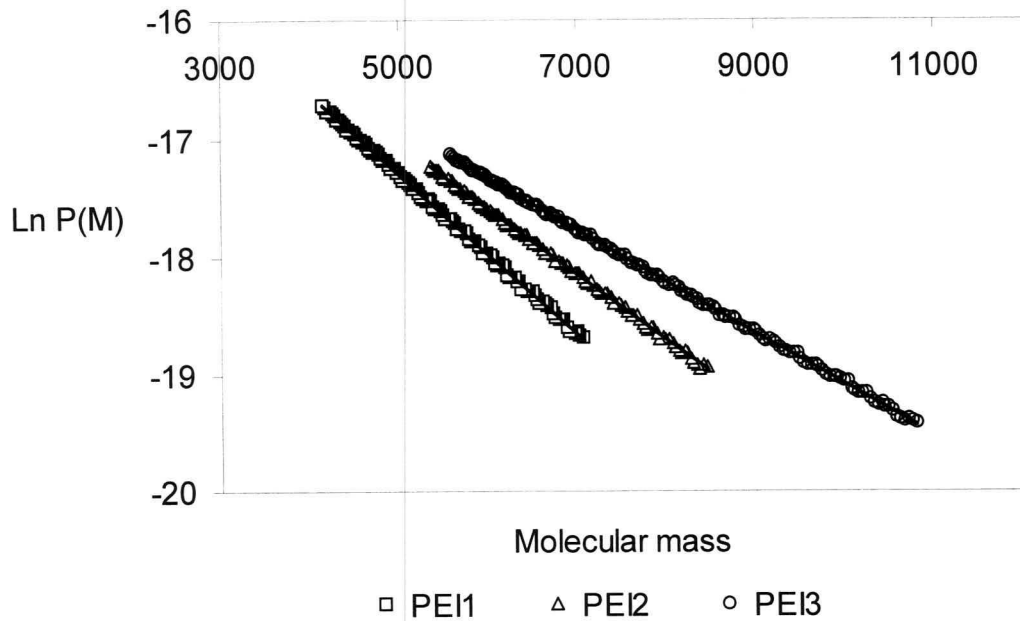
**Table of the gradients of the plots of  $\ln P(M)$  vs.  $M$  for IAN and PEI at different concentrations of the CTA in the bulk polymerisation of styrene.**

Number	Gradient	
	IAN	PEI
1	-0.0012	-0.0007
2	-0.0009	-0.0006
3	-0.0008	-0.0004
Mean	-0.00097	-0.00057
Standard Error	0.00012	8.82E-05
Median	-0.0009	-0.0006
Standard Deviation	0.000208	0.000153

The value for  $k_{tr,CTA}$  was calculated as discussed in section 4.3.3. Figures 4.5 and 4.6 show the linear part of the plot of  $\ln P(M)$  vs.  $M$  of IAN and PEI respectively. The slopes of the linear part of the curve in Figure 4.5 and Figure 4.6 were obtained by linear regression. The gradients of the different runs are given in Table 4.5. The obtained slopes at the different CTA concentrations were then plotted against  $[CTA]/[M]$ . The plots for IAN and PEI respectively are given in Figures 4.7 and 4.8.

**Figure 4.5**

Graph of  $\ln P(M)$  against molecular mass for the chain transfer from styrene to IAN.

**Figure 4.6**

Graph of  $\ln P(M)$  against molecular mass for the chain transfer from styrene to PEI.

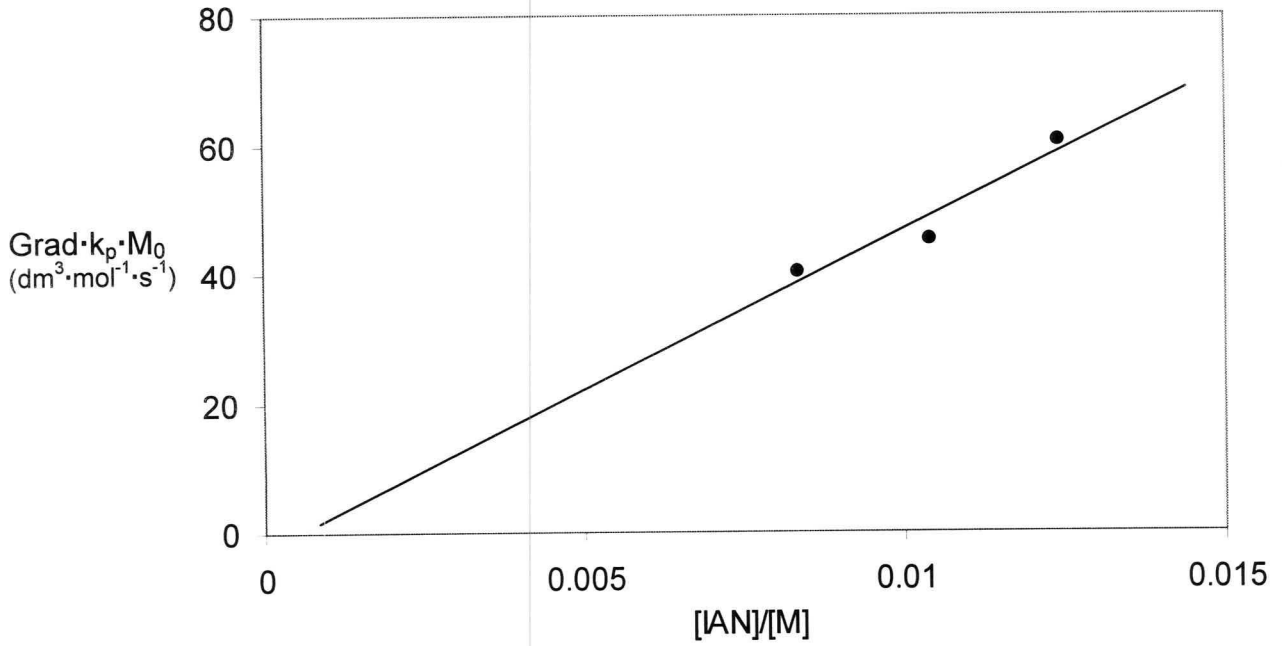


**Figure 4.7:**  
**Plot of the gradient of  $\ln P(M)$  against  $M$  vs.  $[IAN]/[M]$ .**

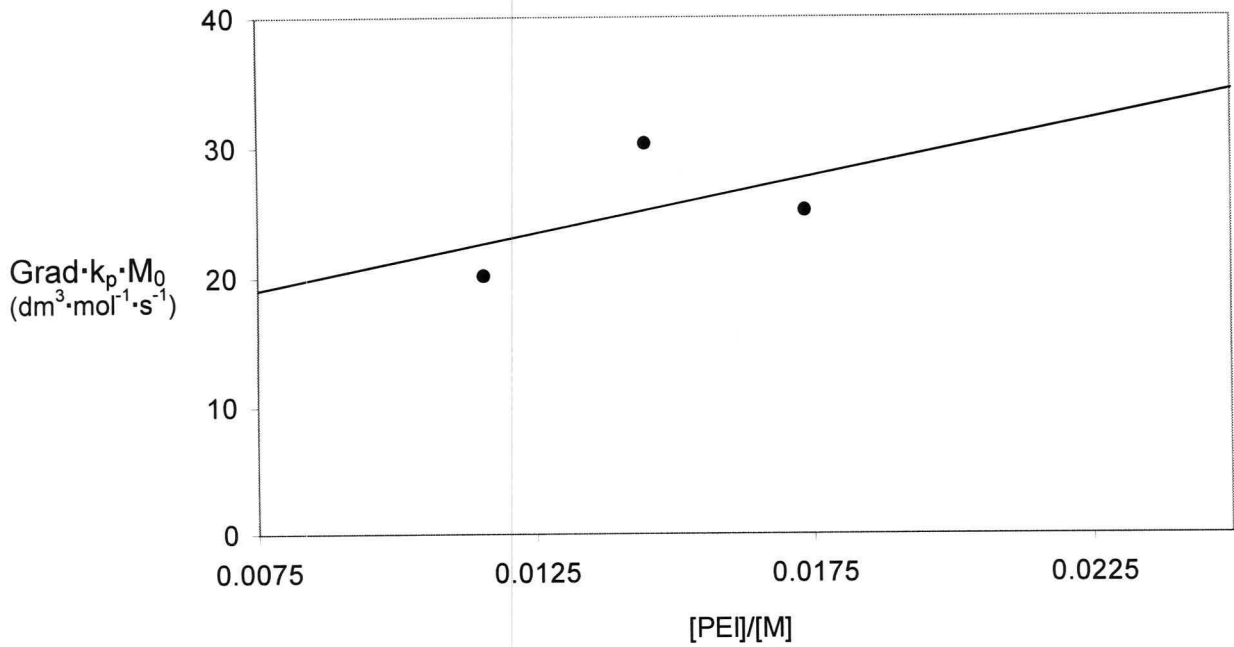


**Figure 4.8:**  
**Plot of the gradient of  $\ln P(M)$  against  $M$  vs.  $[PEI]/[M]$ .**

The slopes of the plot of  $\ln P(M)$  vs.  $M$  for the different concentrations of IAN and especially PEI, showed a large standard deviation and sample variance.

The gradient of the plots in Figures 4.7 and 4.8 (see eq. 4.28) was used to calculate  $k_{tr,CTA}$  for the two CTAs. The second-order rate coefficients for transfer of the radical from styrene to the CTAs are given in Table 4.6.

**Table 4.6:**

**$k_{tr,CTA}$  values for IAN and PEI in the solution polymerisation of styrene.**

CTA	$k_{tr,CTA}$ ( $\text{dm}^3/\text{mol/s}$ )
IAN	4945
PEI	873

The fact that  $k_{tr,CTA}$  for the transfer reaction from styrene to IAN and PEI is much greater than 0.1, shows that both IAN and PEI are effective CTAs.<sup>34</sup> Compared to the chemical homologue, 2-iodo-propane, that was used, IAN and PEI have far greater chain transfer constants. The possibility that IAN and PEI have such high  $k_{tr}$  values as a result of its ability to undergo repeated transfer reactions should be investigated.

## 4.6 CONCLUSIONS

The aim of the investigation was firstly to determine the average number of radicals per latex particle,  $\bar{n}$ . The second part of the investigation focused on finding the transfer rate coefficient,  $k_{tr,CTA}$ , for the two CTAs IAN and PEI. Highlights of the study were the following:

- The rate of entry in the cases where IAN was added was lower than in the run without the CTA. The reason is believed to be the the result of  $I_2$  and HI being formed which inhibits the reaction.
- It is possible to obtain more than one radical in a latex particle under “zero-one” conditions. The conclusion is that difference between “zero-one” and “pseudo-bulk” is not a definite one, but that the change from the one to the other is a gradual one.

- Transfer of the radical from the propagating radical molecule to the hydrophilic CTA IAN leads to fast exit of the radical from the latex particle into the aqueous phase, thus decreasing  $\bar{n}$ ; especially at high conversion.
- IAN and PEI are effective CTAs with an experimentally calculated  $k_{tr,CTA}$  value of 4945 and 873 dm<sup>3</sup>/mol/s respectively.

#### 4.7 RECOMMENDATIONS FOR FUTURE STUDIES

The following recommendations for future studies are made:

- An investigation into the kinetics of particle growth in a seeded emulsion polymerisation to determine the rate parameters for entry, exit and termination in the presence of IAN and PEI should be done.
- The possibility of using catalyst to enhance the reaction rate that is slowed by the addition of a CTA should be investigated.
- A new method to determine the  $k_{tr,CTA}$  values have to constructed that will most probably have to measure the oligomeric fractions, and then, numerically solve the relevant differential equations.
- The investigation that was used to determine the  $k_{tr}$  of the CTAs should be repeated in order to extrapolate the CTA concentration to infinitely low values. This would show if the repeated transfer reactions that are taking place is has an effect on the value for  $k_{tr}$ .

#### 4.8 BIBLIOGRAPHY

1. Smith, W.V.; Ewart, R.H. *Kinetics of emulsion Polymerization*, **Journal of Chemical Physics**, 16, 592, 1948.
2. Gilbert, R.G.; Napper, D.H. **Journal of Macromolecular Science, Reviews, Macromolecular Chemistry and Physics**, C23, 1, 1983.
3. Gilbert, R.G. **Emulsion Polymerisation, a Mechanistic Approach**, Academic Press, London, p. 52, 1995.
4. Gardon, J.L. *Emulsion polymerization. I Recalculation and extension of the Smith–Ewart theory*, **Journal of Polymer Science, Part A–1**, 6, 623, 1968.
5. Gilbert, R.G.: [www.chem.usyd.edu.au/~gilbert/summary.html](http://www.chem.usyd.edu.au/~gilbert/summary.html).

6. Gilbert, R.G. **Emulsion Polymerisation, a Mechanistic Approach**, Academic Press, London, p. 175, 1995.
7. Gilbert, R.G. **Emulsion Polymerisation, a Mechanistic Approach**, Academic Press, London, p. 80, 1995.
8. Billmeyer, F.W. **Textbook of polymer science**, 3<sup>rd</sup> ed., Wiley & Sons, New York, p. 56, 1984.
9. Billmeyer, F.W. **Textbook of polymer science**, 3<sup>rd</sup> ed., Wiley & Sons, New York, p. 52, 1984.
10. Russel, G.T.; Gilbert, R.G.; Napper, D.H. *Chain length–dependant termination rate processes in free–radical polymerization. 1. Theory*, **Macromolecules**, 25, 2459, 1992.
11. Russel, G.T.; Gilbert, R.G.; Napper, D.H. *Chain length–dependant termination rate processes in free–radical polymerization. 2. Modeling methology and application to methyl methacrylate emulsion polymerization*, **Macromolecules**, 26, 3538, 1993.
12. Maxwell, I.A.; Morrison, B.R.; Napper, D.H.; Gilbert, R.G. *Entry of free radicals into the latex particles in emulsion polymerization*, **Macromolecules**, 24, 1629, 1991.
13. Lichti, G; Sangster, D.F.; Whang, B.C.Y.; Napper, D.H.; Gilbert, R.G. *Effects of chain–transfer agents on the kinetics of the seeded emulsion polymerization of styrene*, **Journal of the Chemical Society, Faraday Transcripts** 1. 78, 2129, 1994.
14. Geurts, J.M. **Latices with Intrinsic Crosslink Activity**, *Ph.D. thesis*, Eindhoven University of Technology, Eindhoven, The Netherlands, p 46, 1997.
15. Riddick, J.A. **Organic Solvents: Physical Properties and Methods of Purification**, 4<sup>th</sup> ed., John Wiley & Sons, New York, pp. 582 – 587, 1986.
16. Geurts, J.M. **Latices with Intrinsic Crosslink Activity**, *Ph.D. thesis*, Eindhoven University of Technology, Eindhoven, The Netherlands, p 48 – 49, 1997.
17. Brandrup, J; Immergut, E.H. **Polymer Handbook**, 2<sup>nd</sup> ed., Wiley Interscience, New York, 19
18. Christie, D.I.; Gilbert, R.G. *Transfer constants from complete molecular weight distributions*, **Macromolecular Chemical Physics**, 197, 403, 1996.
19. Lichti, G; Gilbert, R.G.; Napper, D.H. *Molecular weight distributions in emulsion polymerizations*, **Journal of Polymer Science, Polymer Chemistry Edition**, 18, 1297, 1980.
20. Shortt, D.W. *Differential molecular weight distributions in high performance size exclusion chromatography*, **Journal of Liquid Chromatography**. 16, 3371, 1993.

21. Clay, P.A.; Gilbert, R.G. *Molecular weight distributions in free-radical polymerizations. 1. Model development and the implications for data interpretation*, **Macromolecules**, 28, 552, 1995.
22. Clay, P.A.; Gilbert, R.G. *Molecular weight distributions in free-radical polymerizations. 2. Low-conversion bulk polymerization*, **Macromolecules**, 30, 552, 1997.
23. Kukulj, D; Davis, T.P.; Gilbert, R.G. *Catalytic chain transfer in miniemulsion polymerization*, **Macromolecules**, 30, 7661, 1997.
24. Kukulj, D; Davis, T.P.; Gilbert, R.G. *Chain transfer to monomer in the free radical polymerizations of methyl methacrylate, styrene, and  $\alpha$ -methylstyrene*, **Macromolecules**, 31, 994, 1998.
25. Gilbert, R.G. **Emulsion Polymerisation, a Mechanistic Approach**, Academic Press, London, p. 84, 1995.
26. Soh, S.K.; Sundberg, D.C. *Diffusion controlled vinyl polymerization: IV Comparison of theory and experimentation*, **Journal of Polymer Science, Polymer Chemistry Edition**, 20, 1345, 1982.
27. Gilbert, R.G. **Emulsion Polymerisation, a Mechanistic Approach**, Academic Press, London, p. 50, 1995.
28. Gilbert, R.G. **Emulsion Polymerisation, a Mechanistic Approach**, Academic Press, London, p. 62, 1995.
29. Gilbert, R.G. **Emulsion Polymerisation, a Mechanistic Approach**, Academic Press, London, p. 144, 1995.
30. Gaynor, S.; Wang, J-S.; Matyjaszewski, K. Well defined polymers obtained through the use of controlled radical polymerization: The use of alkyl iodides as degenerative transfer reactions, **Polymer Preprints, American Chemical Society, Division Polymer Chemistry**, 36, 467, 1995.
31. Gilbert, R.G. **Emulsion Polymerisation, a Mechanistic Approach**, Academic Press, London, p. 83, 1995.
32. Gilbert, R.G. **Emulsion Polymerisation, a Mechanistic Approach**, Academic Press, London, p. 110, 1995.
33. Matyjaszewski, K. <http://www.chem.cmu.edu/Matyjaszewski.html>.
34. Le, T.P.T.; Moad, G.; Rizzardo, E.; Thang, S.H. **International Patent Application PCT/US97/12540; WO9801478** (Chemical Abstracts 128, 1998: 115390).

## CHAPTER 5

### CO-POLYMERISATION OF A FUNCTIONAL STYRENE SEED WITH BUTYL ACRYLATE

#### 5.1 INTRODUCTION

The ability to produce copolymers from a functional styrene seed synthesised with an alkyl iodide as a CTA in the form of IAN, would prove that they were “living” polymers as the ability to co-polymerise is one of the criteria for a “living” radical polymerisation.<sup>1</sup>

Not only does a “living”/controlled radical polymerisation provide well-controlled polymerisation reactions with products of low MMD, but in degenerative transfer and in ATRP it can result in a functional polymer chain with a halogen end-group. In both cases the polymer chain consists of the backbone with the initiator species on the one end and a halide group on the other end. Iodine groups are extremely reactive and allow not only activation of the carbon halide bond in a second reaction step, but also for subsequent chemical reactions in which the iodine atoms can be substituted through a phase transfer reaction to another functional groups, such as an ester, alcohol, nitrile, amine, mercaptan, etc.<sup>2</sup> Such reactions take place in the absence of any chain-breaking reaction, resulting in the production of well-defined polymers. This eventually makes it possible to produce architectural precise polymers. The importance of such polymers has been discussed in section 1.1.

#### 5.2 OBJECTIVES

The objective of this part of the study was to prove that the polymers produced in the presence of an alkyl iodide CTA have iodine as functional end-groups that can possibly be polymerised in a second polymerisation step to increase the molecular mass of these polymers. This is important in proving that “living” polymerisation did indeed take place. In

the second part the effect that the type of CTA, the CTA concentration and the initiator concentration had on the properties of the copolymer that was formed, were determined.

## 5.3 THEORY

### 5.3.1 The synthesis of block copolymers

The syntheses of block copolymers depend on the existence of an active centre at the end of block A, usually being a cation or an anion. There are three possible ways to obtain this. One is the subsequent addition of monomers to the growing species that are of the same type (cations or anions). A second is by the transformation of active sites (e.g. changing an anion to a cation) and a third is by the coupling of different active sites (e.g. a cation to an anion). Until recently only systems involving anions, cations and organometallic active centres were used to produce Living polymerisation reactions. Recent reports in the literature have, however, described results of a number of investigations on block copolymers that were formed by “living” radical polymerisation.<sup>3-9</sup> Because these latest reactions still involve chain breaking reactions, they are not perfect living systems and therefore, the word “living” is used.

One of the most important requirements for obtaining well-defined copolymers is the ability of the active species to survive the first stages of the polymerisation as well as the subsequent second and even third stages in which blocks are formed. The principle of “living” radical co-polymerisation is the production of a functional polymer or macromer. This process is described in section 3.4. In addition, co-polymerisation is the subsequent addition of co-monomer. The problem of using a free-radical as an active centre in polymerisation reactions is its high reactivity and short lifetime. The high reactivity of polymer-radicals enhance the probability of termination or transfer. This problem can be overcome by the use of CTAs. The discussion on the “livingness” of free-radicals in the presence of degenerative CTAs is presented in section 2.2.

### 5.3.2 Gradient high performance liquid chromatography (G-HPLC)<sup>10</sup>

Different separation modes exist in the liquid chromatography of polymers. Generally porous column packing are used as the stationary phase. High molecular mass solutes can, dependent on their size, partly penetrate into the pores of the column packing and furthermore undergo interactions if an active stationary phase is present. Therefore, two main processes can be distinguished in liquid chromatography of polymers: steric exclusion and adsorption that is an enthalpic interaction as illustrated in Figure 5.1.

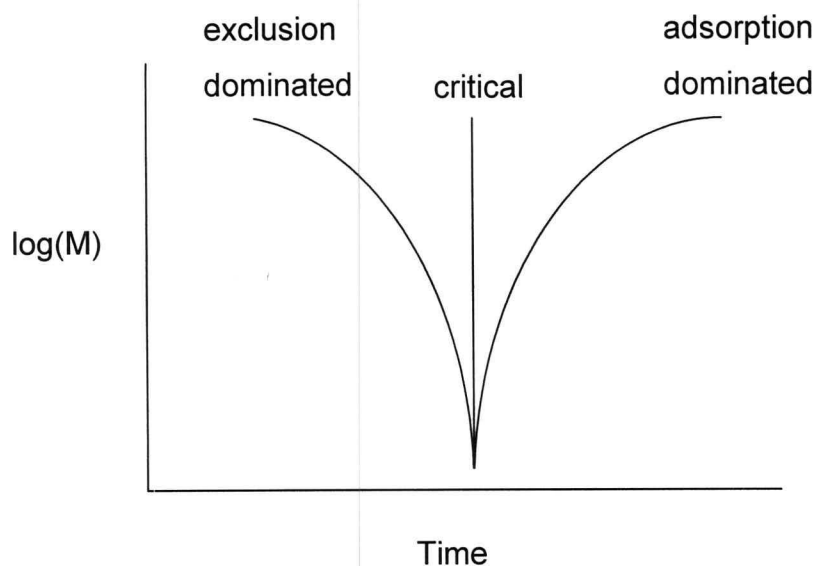


**Figure 5.1:**

**Separation modes in the liquid chromatography of polymers.**

The retention volume,  $V_r$ , is given in eq. 5.1:

$$V_r = V_i + K_{\text{sec}}V_p + K_{\text{ads}}V_s \quad (5.1)$$

In this expression, the retention volume is divided into the interstitial volume  $V_i$ , the pore volume  $V_p$ , and the stationary phase volume  $V_s$ .  $K_{\text{sec}}$  and  $K_{\text{ads}}$  represent the distribution coefficients for steric exclusion and for adsorption the chromatography

A chromatographic distribution coefficient is defined in eq. 5.2:

$$K_D = \frac{c_s}{c_m} = \exp\left(\frac{-\Delta\mu_0}{RT}\right) \quad (5.2)$$

where  $c_s$  and  $c_m$ , represent the concentration of a solute in the stationary and the mobile phase, respectively and  $\Delta\mu_0$  is the standard chemical potential difference for solute molecules in both phases.

In the case that a thermodynamically good solvent for the polymer, which also effectively suppresses enthalpic interactions with the stationary phase is used as the mobile phase,  $K_{ads} = 0$  and retention is governed by entropic exclusion effects. This chromatographic mode is known as Size Exclusion Chromatography (SEC) also known as GPC. When the thermodynamic quality of the solvent is decreased by the addition of a poor solvent,  $K_{ads}$  may increase as enthalpic, absorptive interactions, thus contributing to the total retention. These interactions are in most cases stronger for larger molecules. At a certain critical point  $K_{ads}$  is large enough and retention is dominated by adsorption. Adsorption can be conducted as an isocratic or as a gradient (G-HPLC) experiment.

For the purpose of the present study, G-HPLC was used to prove that a copolymer of styrene and butyl acrylate was formed. An explanation on G-HPLC will now be given:

In contrast to low molecular mass polymers, polymers with large molecular masses have a large number of adsorbable groups. These are all identical in the case of homo-polymers but differ for copolymers. A dissolved polymer was adsorbed from a solution onto a substrate. Enthalpic interactions occur between the polymer and the solvent, the polymer and the substrate and in some cases within the polymer itself by intra-molecular interactions.

Gradient elution of polymers starts with the complete retention of the sample at the initial conditions followed by gradual elution during the subsequently applied gradient. Due to the limited solubility of polymers, the starting mobile phase (eluent) is often, although not necessarily, a non-solvent for at least part of the injected polymer. During gradient elution, the thermodynamic quality of the eluent increases, which leads to the gradual re-dissolution of the polymer. Subsequently, when the chromatographic strength of the

eluent is large enough, the polymer starts migrating.

Both solubility and sorption of polymers depend on chemical composition and molar mass of the molecules. Thus, the final separation is determined by more than one molecular characteristic. Because the solubility of different chemical species differs from each other, the retention times between different homo-polymers as well as the retention time between homo-polymers and copolymers will differ.

## 5.4 EXPERIMENTAL

### 5.4.1 Planning

The statistical planning and the statistical analysis of designed experiments are discussed in Appendix A. A Box, Hunter and Hunter<sup>11</sup> factorial design was used to plan and analyse the experimental runs. The high and low levels of each factor as well as the selected variable names are given Table 5.1. The factor levels for the different runs are given in Table 5.2. No confounding of the interactions took place.

**Table 5.1:**

**Variables investigated in the factorial design with their respective high and low levels.**

VARIABLE	LOW LEVEL (-1)	HIGH LEVEL (+1)
A CTA concentration ( $\text{g}/\text{cm}^3$ )	0.0001	0.001
B BA concentration ( $\text{mol}/\text{dm}^3$ )	0.01	0.08
C Initiator concentration	0.001	0.005

**Table 5.2:**

**The factor levels for the different co-polymerisation runs in the co-polymerisation of styrene and BA.**

Randomised run number	A	B	C
1	-1	-1	-1
2	+1	-1	-1
3	-1	+1	-1
4	+1	+1	-1
5	-1	-1	+1
6	+1	-1	+1
7	-1	+1	+1
8	+1	+1	+1

#### 5.4.2 Preparation of the functional styrene seed

The following equipment was used: a cylindrical flat-bottomed 2L-glass reactor, a twin blade stirrer and a water bath.

The reactor was charged with:

- 21g of an industrial surfactant with a sulphate end-group, named Polystep B27, see section 3.4.4.
- 1150g DDI water.
- 600g distilled styrene that was dried overnight over  $\text{CaCl}_2$  (see section 3.4.2).
- 3g IAN from Aldrich (2% (m/m) on styrene).
- 2g KPS, the initiator.

The charged reactor was heated to 90 °C with only 200g of the original 600g of styrene added. The styrene was allowed to emulsify while the reaction mixture was purged for 1 hour with  $\text{N}_2$ . The chain transfer agent, IAN, was added to the remaining 200g of styrene monomer. The initiator was dissolved in 100g of DDI water. Both the initiator solution and

the CTA solution were added to the reactor over a period of two hours and the reaction was then allowed to proceed for a total of 24 hours at a stirring speed of 300 rpm in an inert atmosphere.

Analysis by the Malvern Zetasizer 4 revealed a latex particle size of 162nm. Only one peak appeared showing that no secondary nucleation took place. The PDI showed that a seed latex with monodisperse particles were created. The details of the particle size analysis are found in section 3.4.3.

A sample of the synthesised functional seed was prepared for GC analysis to determine the concentration of residual monomer in the latex. The samples consisted of the latex, DMF as internal standard and ethylene glycol as bi-phase solvent. The samples were injected in an AutoSystem Perkin Elmer GC, the specifications for the instrument can be found in section 4.4.1. The residual monomer was found to be 4.95%.

The residual monomer could influence further analysis and had to be removed. In order to remove the residual monomer, the seed was first heated to 70°C after which 1% (m/m on solids) of tertiary butylhydroperoxide (TBHP) with a 10 hour  $t_{1/2}$  at 172 C° was added. TBHP was used as monomer scavenger. The residual KPS in the emulsion acted as catalyst to form, with TBHP, a redox system. This reaction is used in the industry as a procedure to mop up residual monomer. The concentration of styrene at the end of the reaction was measured with GC. No evidence of any styrene could be found in at completion of the reaction. Analysis by GPC revealed that there was no observable increases in the molecular mass of the styrene polymers after the TBHP was added. It is therefore assumed that no major grafting took place.<sup>12</sup>

The surfactant was removed from the functional styrene latex by placing the latex in a dialysis tube (pore size 60nm). Placing the tube in boiling water for 1h cleaned the dialyses tube of any chemicals present. The latex was poured into the dialyses tube and placed in distilled water for one week during which time the excess surfactant diffused through the membrane into the distilled water. The water was replaced daily.

### 5.4.3 Co-polymerisation of styrene and butyl acrylate

During the co-polymerisation of styrene and butyl acrylate (BA), 2 gram of the functional seed latex was placed in each of eight polytops. Added to each polytop were the co-monomer BA, in different concentrations varying between 0.01 and 0.08 mol/dm<sup>3</sup>. These concentrations ensured that all the co-monomer was dissolved in the latex particles of the seed. While the mixture was stirred, the seed latex particles were allowed to swell over a period of 24 hours. KPS, as initiator, was added to the swollen seed. After the seed was initially purged with N<sub>2</sub>, for five minutes, the temperature was raised to 70°C to allow co-polymerisation of BA over 24 hours under an inert atmosphere.

The reacted seed was analysed by GC in the same way as was discussed in section 5.4.2 to determine the amount of residual BA monomer. Conversion of BA monomer to polymer was 99%.

### 5.4.4 Gradient high performance liquid chromatography analysis

The previously prepared samples (see section 5.4.3) were analysed by gradient high performance liquid chromatograph (G-HPLC) to determine if co-polymerisation took place. The instrument specifications were:

- Waters Pump, Waters 600S Controller
- Waters Automated Switching Valve
- Waters 490 Programmable Multiwave Detector
- Separations Spark Holland Mistral Column Oven
- Applied Chromatography Systems LTD (ACS 750/14) Evaporative Light Scattering Detector (ELSD)
- A Waters 712 Waters Intelligent Sample Processor (WISP)
- Millenium Software.
- The columns that were used were: a Waters Symmetry C<sub>18</sub>, 3.9x 150 mm column (P/N WAT 046980) and a pre-column (P/N 88084).

The solvents that were used were:

- THF HPLC–S from Biosolve Ltd,
- Acetonitrile (ACN) HPLC–S (Gradient Grade) from Biosolve Ltd and
- Water from Millipore.

The settings of the instrument were as follows:

- ELSD temperature 70°C.
- Column oven temperature 35°C.
- Flow speed 0.5ml/min.
- Sparging of all the solvents were done with He at a flow rate of 10ml/min
- 4% gradient, at which the solvents were introduced, were used and is given in Table 5.3:

**Table 5.3:**

**The gradient used for the different solvents to separate the copolymer from the homo-polymer.**

Time (min)	Flow	Solvent A (THF)	Solvent B (H <sub>2</sub> O)	Solvent D (ACN)
0	0.5	0	50	50
12.5	0.5	0	0	100
37.5	0.5	100	0	0
40	0.5	100	0	0
45	0.5	0	50	50

The standards that were used to calibrate the column are given in Table 5.4 with PS and poly(butyl acrylate) (PBA). The concentration of all the standards and samples used were 1mg/ml in THF, while the PBA was dissolved in toluene.

The previously prepared samples (see section 5.4.3) were also subjected to a GPC analysis to determine the molecular mass and MMD of the polymers. The method is described in section 3.4.7.

**Table 5.4:****Table of the standards used to calibrate the column.**

Name of the standards	Number average molecular mass, $M_n$ ( $\times 10^3$ )	Polidispersity ( $M_w/M_n$ )	Company name
PS1	0.5	1.14	TSK Standard
PS2	2.45	1.05	Polymer Labs
PS3	5.05	1.05	Polymer Labs
PS4	9.2	1.03	Polymer Labs
PS5	66	1.03	Polymer Labs
PS6	570	1.05	Polymer Labs
PS7	1075	1.05	Polymer Labs
PS8	7000	1.11	Polymer Labs
PS9	20000	1.3	Polymer Labs
PBA	$M_w = 61800$	$M_n = 20\ 700$	Scientific polymer Products Inc.

**Table 5.5:****Results of the GPC analysis on the styrene–butyl acrylate copolymers prepared.**

Run number	A	B	C	$M_n$	$M_w$	$M_w/M_n$
1	-1	-1	-1	8685	14677	1.69
2	+1	-1	-1	10066	19254	1.90
3	-1	+1	-1	7251	13124	1.81
4	+1	+1	-1	9341	15692	1.68
5	-1	-1	+1	10166	17180	1.69
6	+1	-1	+1	10876	20990	1.93
7	-1	+1	+1	9994	17089	1.71
8	+1	+1	+1	6906	13052	1.89

## 5.5 RESULTS AND DISCUSSIONS

### 5.5.1 Gel permeation chromatography analysis

The results of the GPC analysis are summarised in Table 5.5. The Pareto charts of the responses  $M_n$ ,  $M_w$  and  $M_w/M_n$  are given in Figures 5.2 and 5.3. None of the variables or first order interactions has any significant effect on any of the responses.

The small increase in molecular mass was the result of low co-monomer concentrations. The variable that had the greatest effect on the molecular masses of the polymers is the co-monomer concentration while the variable that had the greatest effect on  $M_w/M_n$  were the initiator concentration. An increase in the co-monomer would indeed lead to an increase in the molecular masses of the polymers. Further, an increase in the initiator concentration would create new propagating centres that can polymerise the BA to form lower molecular mass PBA homo-polymers, increasing the  $M_w/M_n$ .

### 5.5.2 Gradient high performance liquid chromatography analysis

The plot of the eight styrene-butyl acrylate copolymers named Runs 1 – 8 and the single reference peak consisting of only the original styrene-seed polymer are given in Figure 5.4. The main observation made regarding the outcome of the experiment is the position of the peaks of Run 1 – 8 relative to the reference peak. A definite shift in the peaks of Runs 1 – 8 is visible. The peaks of Runs 1 – 8 exited earlier than the reference peak. This is believed to be result of BA grafting on the styrene seed, thus changing the interaction between the stationary phase and the polymer molecules. The reason why such a small shift was observed was the low BA co-monomer concentrations present.

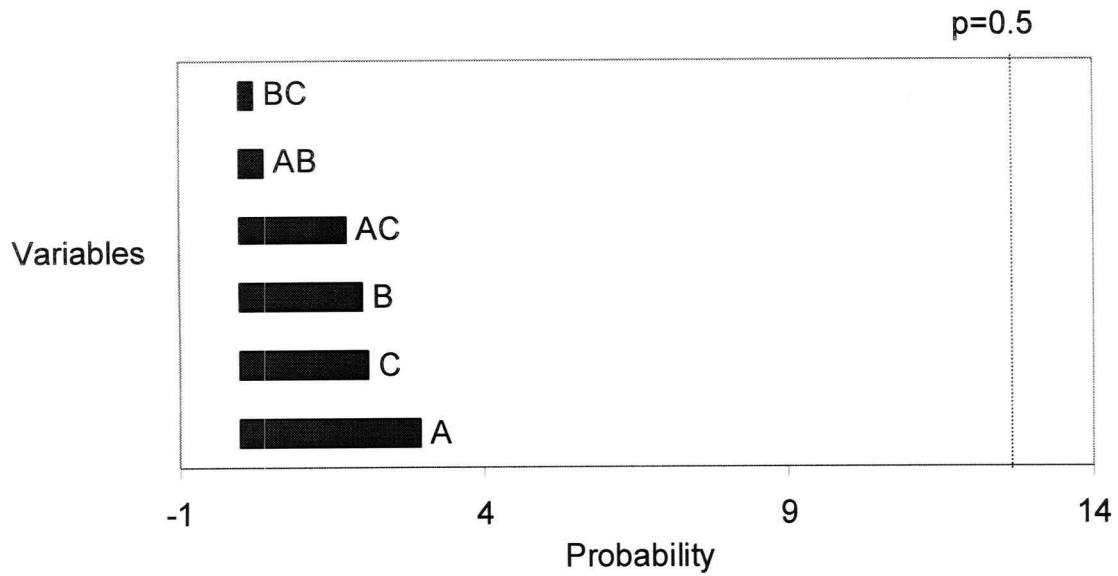


Figure 5.2:

Pareto chart of the main effects of  $M_n$  in the co-polymerisation of styrene and BA.

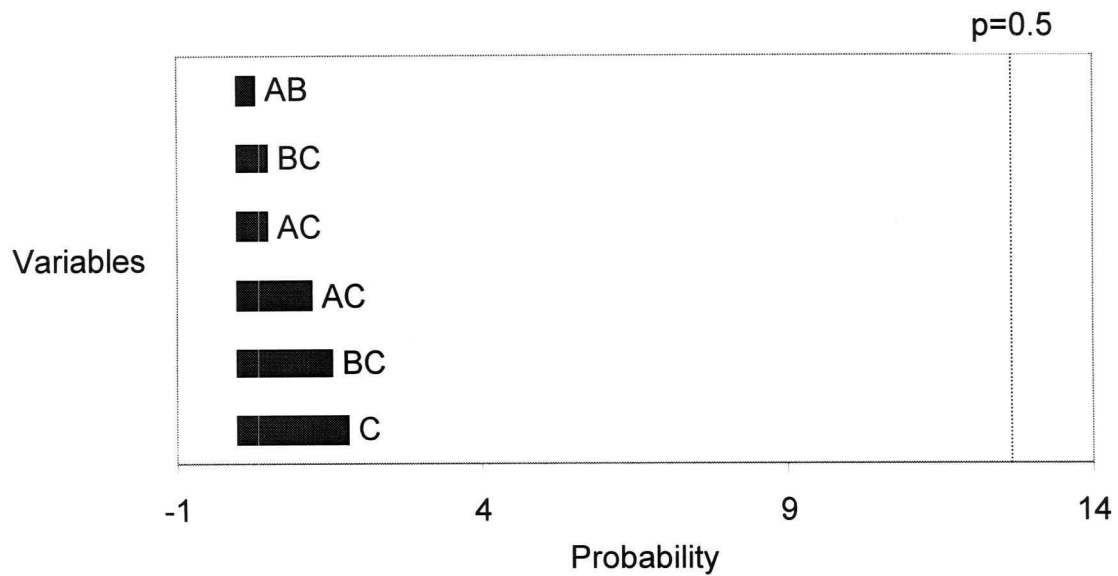
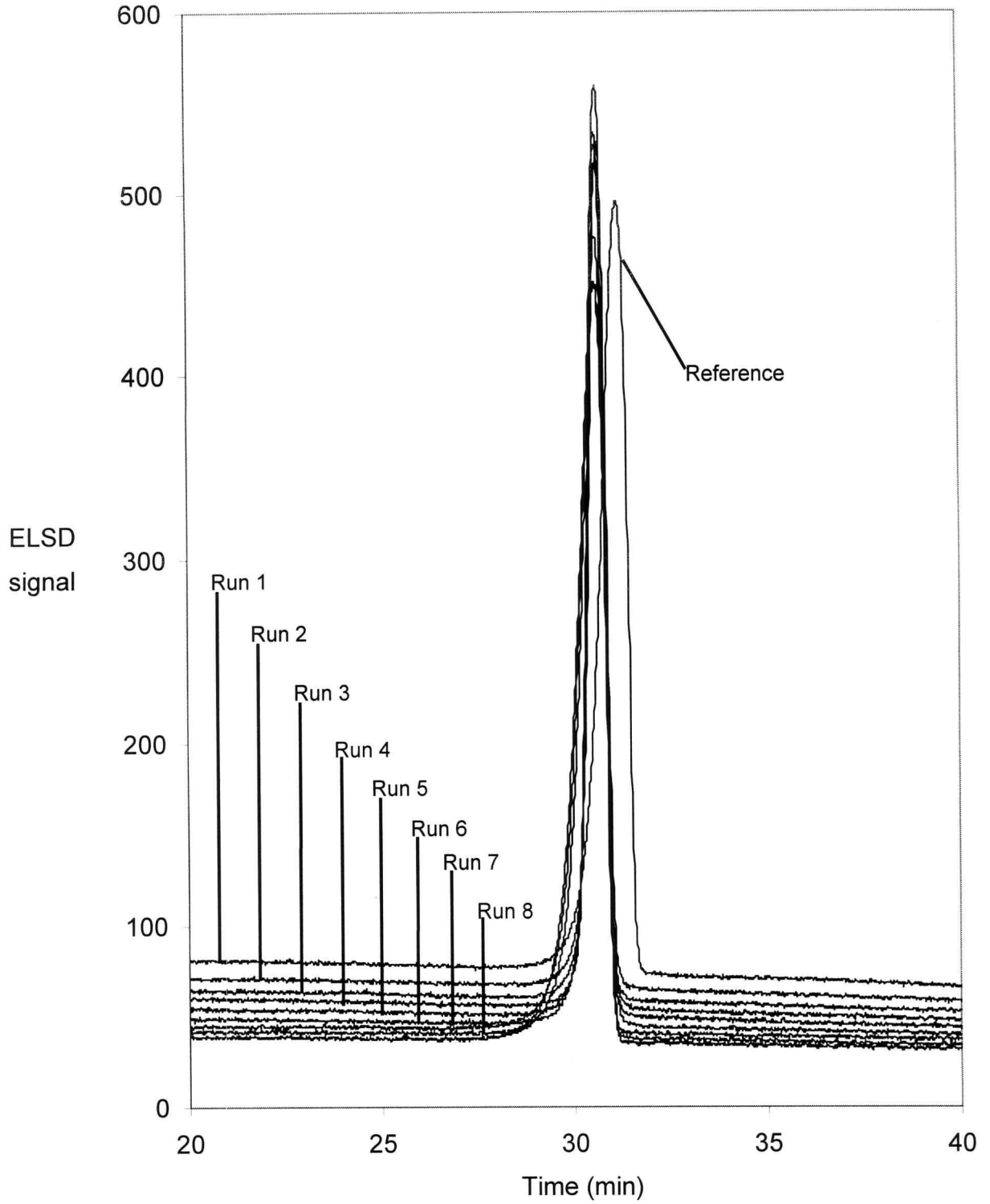


Figure 5.3:

Pareto chart of the main effects of  $M_w/M_n$  in the co-polymerisation of styrene and BA.



**Figure 5.4:**  
G-HPLC analysis of Runs 1 – 8 and the reference using ELSD.

## 5.6 CONCLUSIONS

The main conclusion that can be made from this study is that a styrene–butyl acrylate copolymer was probably formed by co–polymerising a functional styrene seed with BA as co–monomer in a subsequent step. Proof was given that the polymers produced in the presence of an alkyl iodide CTA have iodine as functional end–groups can in a subsequent polymerisation reaction lead to an increase in the molecular mass of these polymers. This showed that “living” polymerisation probably took place.

A second conclusion is that the type of CTA used, the CTA concentration, the initiator concentration nor any interactions of the variables had any significant effect on the molecular mass or  $M_w/M_n$  of the styrene–butyl acrylate copolymers that were formed. This is believed to be the result of a extremely low co–monomer, initiator and CTA concentration in the co–polymerisation reaction. However, the variable that had the greatest effect on the molecular masses of the polymers is the co–monomer concentration while the variable that had the greatest effect on  $M_w/M_n$  was the initiator concentration.

## 5.7 RECOMMENDATIONS FOR FUTURE STUDIES

It is suggested that further investigations into the effects of the variables: initiator concentration, co–monomer concentration and CTA concentration on  $M_n$  and  $M_w/M_n$  as response should be made, using higher concentrations of the different chemical species than were used in this study. The effects of higher concentrations of the chemical species on the G–HPLC analysis should also be investigated.

## 5.8 BIBLIOGRAPHY

1. Le, T.P.T.; Moad, G.; Rizzardo, E.; Thang, S.H. **International Patent Application PCT/US97/12540**; WO9801478 (Chemical Abstract (1998) 128: 115390).
2. Morrison, R.T.; Boyd, R.N. **Organic Chemistry**, 4<sup>th</sup> ed., Allyn and Bacon Inc., Boston, p. 206, 1983.
3. Beers, K.L.; Gaynor, S.G.; Matyjaszewski, K. *The use of "living" radical polymerization to synthesize graft copolymers*, **Polymer Preprints, American Chemical Society Division Polymer Chemistry**, 37, 571, 1996.
4. Greszta, D.; Matyjaszewski, K. *Gradient copolymers – a new class of materials*, **Polymer Preprints, American Chemical Society, Division Polymer Science**, 37, 569, 1996.
5. Gaynor, S.G.; Matyjaszewski, K. *Step-growth polymers as macroinitiators for "living" radical polymerization: Synthesis of ABA block copolymers*, **Macromolecules**, 30, 4241, 1997.
6. Nakagawa, Y.; Gaynor, S.G.; Matyjaszewski, K. *The synthesis of end functional polymers by "living" radical polymerization*, **Polymer Preprints, American Chemical Society Division Polymer Chemistry**, 37, 577, 1996.
7. Li, I.Q.; Howell, B.A.; Dineen, M.T.; Kastl, P.E.; Lyons, J.W.; Meunier, D.M.; Smith, P.B.; Priddy, D.B. *Block copolymer preparation using sequential normal/living radical polymerization techniques*, **Macromolecules**, 30, 5195, 1997.
8. Krstina, J.; Moad, G.; Rizzardo, E.; Winzor, C.L. *Narrow polydispersity block-copolymers by free-radical polymerization in the presence of macromonomers*, **Macromolecules**, 28, 5381, 1995.
9. Heuts, J.P.A.; Kukulj, D.; Forster, D.J.; Davis, T.P. *Copolymerization of styrene and methyl methacrylate in the presence of a catalytic chain transfer agent*, **Macromolecules**, 31, 2894, 1998.
10. Philipsen, H.J.A. **Mechanisms of Gradient Polymer Elution Chromatography and its Application to (Co)polyesters**, *Ph.D. thesis*, Eindhoven University of Technology, Eindhoven, The Netherlands, p. 14 – 23, 1998.
11. Box, G.E.P.; Hunter, W.G; Hunter, J.S. **Statistics for experimenters: An introduction to design, data analysis and model building**, Wiley, New York, 1978.
12. Mark, H.F.; Bikales, N.M.; Overberger, C.G.; Menges, G.; Kroschwitz, J.I. **Polymer Encyclopedia**, Wiley & Sons, New York, Vol. 11, p. 11 & Vol. 15, p. 406, 1985.

# CHAPTER 6

## CONCLUSIONS

To the best of the author's knowledge, results of work carried out in this study offer the first proof that "living"/controlled radical polymerisation of styrene with alkyl iodides as CTAs can be successfully carried out in emulsion. Two alkyl iodides were used namely IAN and PEI. Both functional styrene polymers with iodine end-groups and styrene-butyl acrylate copolymers were produced.

The basic aim of this thesis was to describe the results of the effects of alkyl iodides as CTAs on the seeded emulsion homo- and co-polymerisation of styrene and butyl acrylate. With reference to the original objectives of this study, presented in section 1.4, the following conclusions are given:

First, the effects of selected variables on certain responses were investigated using a  $2^{5-1}$ -fractional factorial design for the design and analysis of the experiments and the following conclusions made:

- The use of alkyl halides as CTAs in the seeded emulsion radical polymerisation leads to a decrease in the molecular mass of the synthesised styrene polymers.
- It is possible to control the molecular masses of polymers produced in radical emulsion polymerisations by selection of both the type of CTA used and the concentration of the CTA.
- Use of a water-insoluble initiator results in a polymer with a lower MMD than would otherwise be the case with a water-soluble initiator.
- The use of a high concentration of PEI as CTA resulted in a polymer with a low MMD, while the use of a low concentration of IAN as CTA led to a polymer with a low MMD.
- Addition of a CTA does not have a significant effect on the particle sizes of the latex particles after polymerisation.
- The conversion of monomer to polymer is negatively influenced by the addition of a alkyl iodide CTAs thus increasing the reaction time.

- Using a high CTA concentration led to low  $T_g$  polymers.
- The  $T_g$  of the polymers produced with a high CTA concentration can be controlled by selection of different initiator concentrations. A high initiator concentration will result in a high  $T_g$  polymer and a low initiator concentration will result in a low  $T_g$  polymer.
- IAN and PEI can be used to regulate the molecular mass,  $T_g$ , and MMD of polymers.

Second, the effect IAN as CTA on the kinetics of a seeded styrene emulsion polymerisation was investigated. Attention was focused on the conversion of monomer to polymer to calculate the change in the average number of radicals per latex particle ( $\bar{n}$ ) and calculation of the second-order rate coefficient of transfer from the propagating radical to the CTA ( $k_{tr,CTA}$ ) and the following conclusions can be made:

- The rate of entry in the cases where IAN was added was lower than in the run without the CTA. The reason is believed to be the result of  $I_2$  and HI being formed which inhibits the reaction.
- It is possible to obtain more than one radical in a latex particle that, because of size would be classified as “zero-one” conditions. The conclusion is that the difference between “zero-one” and “pseudo-bulk” is not a definite one, but that the change from the one to the other is a gradual one.
- Transfer of the radical from the propagating radical molecule to the hydrophilic CTA IAN leads to fast exit of the radical from the latex particle into the aqueous phase, thus decreasing  $\bar{n}$ ; especially at high conversion.
- IAN and PEI are effective CTAs with an experimentally calculated  $k_{tr,CTA}$  value of 4945 and 873  $dm^3/mol/s$  respectively.

Third, the possibility of producing block-copolymers in emulsion with alkyl iodides as CTAs was investigated. Butyl acrylate was added to a functional styrene seed and co-polymerised in a second stage and the following conclusions can be made:

- Analysis by G-HPLC revealed that the product was probably a styrene-butyl acrylate block-copolymer. The production of a block-copolymer acted as proof that the system that was created when styrene was polymerised in the presence of alkyl iodides as CTAs was a “living” system that could be co-polymerised in a second stage.

- Neither the type of CTA used, the CTA concentration, the initiator concentration nor any interactions of the variables had any significant effect on the molecular mass or  $M_w/M_n$  of the styrene–butyl acrylate copolymers that were synthesised. This is believed to be the result of an extremely low co–monomer, initiator and CTA concentration in the co–polymerisation reaction.
- The variable that had the greatest effect on the molecular masses of the polymers is the co–monomer concentration.
- The variable that had the greatest effect on  $M_w/M_n$  was the initiator concentration.

The advantages of producing polymers with pre–determined molecular masses and a narrow MMD to influence macro properties of industrial polymers are numerous. Further, the possible ability of forming an iodine end–functional styrene seed latex can lead to a variety of possibilities that include the production of copolymers, gradient copolymers, star polymers etc. to control the microstructure of polymers produced in emulsion. It is also possible to change the iodine end–functional group to another reactive chemical end–group to allow either ionic– or condensation– or catalysed polymerisation of monomers. Changing the end–functional group of a polymer can also change the intermolecular properties of the polymer towards other compounds.

## APPENDIX A

### EXPERIMENTS BASED ON AN EXPERIMENTAL DESIGN

#### A.1 INTRODUCTION

Examples of experimental optimisation of chemical research by chemists and engineers to increase the efficiency of systems are well documented.<sup>1-5</sup> One way of experimental design is to identify factors or variables that influence the response or effects that are of importance. A factor is defined as any experimental variable that can affect the result of an experiment. e.g. temperature or different concentrations of the reagents.<sup>6</sup> The response is the outcome that is tested e.g. yield. By changing the levels of the  $k$  factors individually, while the other  $k-1$  factors are kept constant, one can obtain a maximum response for each factor. However, these designs are fairly limited for they do not take into account possible interactions between factors. Another disadvantage is that convergence towards an optimum is not rapid. It is also possible that convergence may not be reached.

Another possibility is the use of statistically designed experiments. Montgomery defines statistically designed experiments as the process of planning experiments so that appropriate data can be collected and be analysed by statistical methods to result in valid and objective conclusions.<sup>3</sup> Factorial designed experiments are a good way of judging the relative significance of factors and give a quantitative measure of the contribution of each factor to the overall response. It provides the smallest number of runs with which  $k$  factors can be studied. Two-level factorial designs are a two-way arrangement by means of which two factors and their interactions can be studied. Two-level factorial designs are adequate and their application is a well-established procedure that has been treated in detail.<sup>2,3,4</sup> They are especially useful in the early stages of experimental work when there are likely to be many factors to be investigated.

A cube in space, resulting in an infinitive amount of runs that can be made to represent a design with three factors. In a factorial design, only certain key points called the vertices are chosen as seen in Figure A.1.

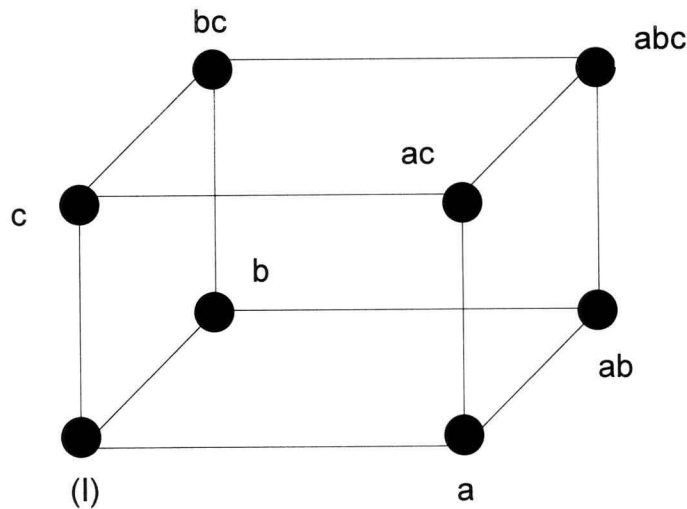


**Figure A.1:**

**Geometric representation of the experimental space and main effects of a  $2^3$  factorial design.**

where “I” represents a treatment with all the factor levels at a low level, “a” represents a treatment with only factor A at a high level, “ab” represent a treatment with factors A and B at a high level, etc.

Factorial designs reduce the number of experimental runs necessary to determine which variables have a significant effect on the measured response. The possibility exists that the design may converge to a point that is not the optimum and it is, therefore necessary to confirm results. Factorial designs are a useful tool to investigate the effect of a set of variables and their interactions on a response, especially at the beginning of an investigation.

All the symbols and abbreviations that will be used in the following discussion is summarised in the List of Symbols and the List of Abbreviations.

## A.2 BASIC STATISTICS

### A.2.1 Definitions

Consider any set of arbitrary data,  $y_i$ , where  $i = 1, 2, 3 \dots n$ .

The **sample mean** ( $\bar{y}$ ) of this data set is:<sup>1,2</sup>

$$\bar{y} = \frac{\sum y}{n} \quad (\text{A.1})$$

For a hypothetical population with a very large number of  $N$  observations, there would be a corresponding **population mean** ( $\eta$ ), also called the **expected value**, seen in eq. A.2.<sup>1,2</sup>

$$\eta = \frac{\sum y}{N} \quad (\text{A.2})$$

A measure of how far any particular observation,  $y$ , is from the mean,  $\mu$ , is the deviation ( $y - \mu$ ). The **variance of the population** ( $\sigma^2$ ) is the mean value of the square of such deviations taken over the whole population:<sup>1,2</sup>

$$\sigma^2 = E(y - \eta)^2 = \frac{\sum (y - \eta)^2}{N} \quad (\text{A.3})$$

A measure of the spread of the data set is  $\sigma$ , the positive square root of the variance. This is called the **standard deviation of the population** ( $\sigma$ ):<sup>1,2</sup>

$$\sigma = \sqrt{V(y - \eta)} = \sqrt{\frac{\sum (y - \eta)^2}{N}} \quad (\text{A.4})$$

In the same way the **variance of the sample** ( $s^2$ ) is:<sup>1,2</sup>

$$s^2 = \frac{\sum (y - \bar{y})^2}{n - 1} \quad (\text{A.5})$$

and the **sample standard deviation** ( $s$ ):<sup>1,2</sup>

$$s = \sqrt{\frac{\sum (y - \bar{y})^2}{(n - 1)}} \quad (\text{A.6})$$

A set of data,  $y$ , is **normally distributed** ( $f(y)$ ) when the probability distribution of  $y$  is given by eq. A.7.<sup>3</sup>

$$f(y) = \frac{1}{\sigma\sqrt{2\pi}} e^{-\frac{1}{2}\left[\frac{(y-\mu)}{\sigma}\right]^2} \quad (\text{A.7})$$

When  $\sigma^2$  and  $\mu$  are 1 and 0 respectively, the data is normally distributed around 0. The notation used for the distribution of data for normally distributed data around the mean (expected value) with a variance of  $\sigma^2$  is  $N(\mu, \sigma^2)$ . A geometric representation of a normally distributed data set is seen in Figure A.2.

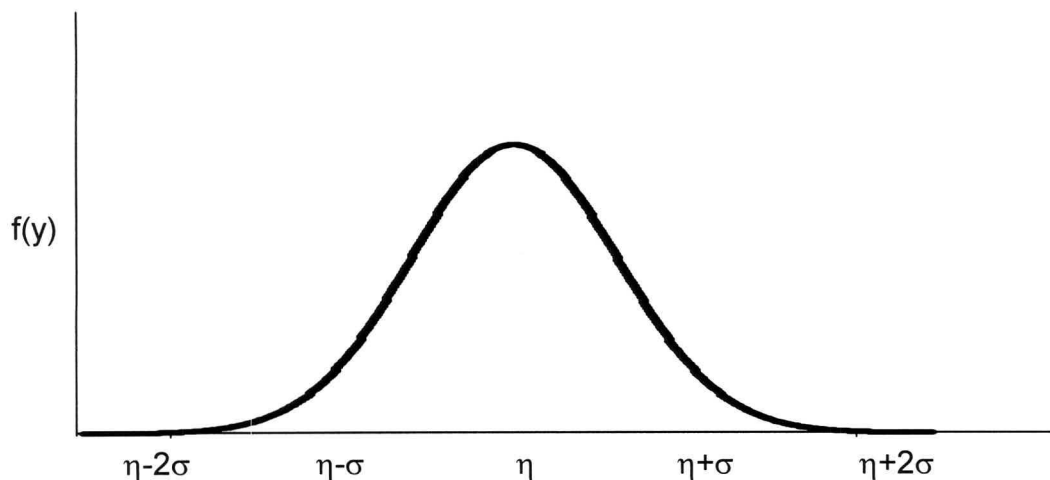


**Figure A.2:**

**Geometric representation of a normally distributed data set.**

It is possible to avoid the use of an extensive external data set in the form of a population to generate a reference distribution. Assuming randomness in the sampling of the data allows one to use eq. A.8 and eq. A.9. Box, Hunter and Hunter gave a full account of the mathematical proof of this relations.<sup>2</sup>

$$E(\bar{y}) = \eta \quad (\text{A.8})$$

and

$$V(\bar{y}) = \frac{\sigma^2}{n} \quad (\text{A.9})$$

### A.2.2 Analysis of results

After a statistical test has been conducted, the experimental results are compared against a statistical norm in a test of significance. If the outcome of this test is such that the results differ from the norm, then it is probable that the differences observed are not solely due to experimental error. This probability is connected to a confidence level of 95% or, customary, it is said to be at a  $\alpha = 5$  level. In general, any outcome that lies outside the confidence interval is rejected. In such cases it is accepted that a true difference between treatments does exist.

Significance testing or hypotheses testing is used to draw conclusions about the significance of data. A hypothesis is a statement about the data. Two types of hypotheses are used. The first hypothesis could state that a given variable has a significant effect. This is called the alternative hypothesis ( $H_1$ ). The second hypothesis is called the null hypothesis ( $H_0$ ). The null hypothesis is a statement contradicting the alternative hypothesis. If the null hypothesis is rejected, a statistically significant difference has been observed.

The critical value,  $\bar{X}$ , that is associated with  $\alpha$  is calculated with eq. A.10, using a z value representing the 5% cut off level.<sup>4,7</sup>

$$z = \frac{\bar{X} - \mu}{\sigma / \sqrt{n}} \quad (\text{A.10})$$

In most cases  $\sigma$  is not known and are hence estimated by the sample standard deviation ( $s$ ). Then the analogue of eq. A.10 would be used. This is called the  $t$ -statistic, shown in eq. A.11.

$$t = \frac{\bar{X} - \mu}{s / \sqrt{n}} \quad (\text{A.11})$$

Thus, for any given distribution of data as seen in Figure A.3,  $t$  corresponds to the level of the test and  $\bar{X}$  give the critical value above which the null hypothesis ( $H_0$ ) is rejected. The value for  $t$  is obtained from the  $t$ -distribution in the  $t$ -table, found either in statistical textbooks or statistical computer packages.<sup>4,6</sup>

Figure A.3 gives a geometric representation of a normally distributed data set showing the critical  $\bar{X}$  value above which  $H_0$  is rejected in the  $t$ -statistic test.

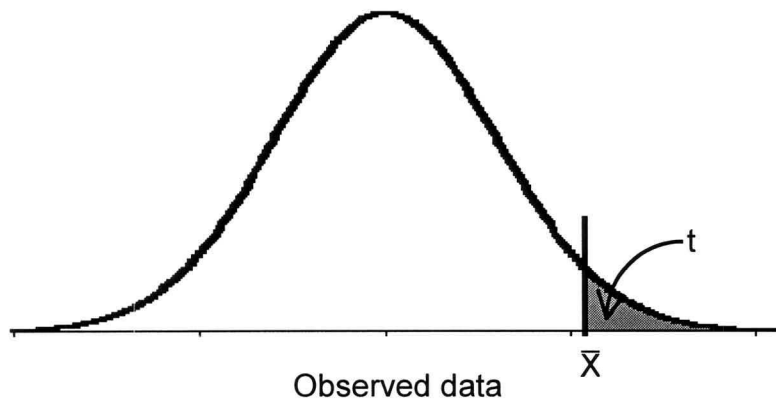


**Figure A.3:**

**Geometric representation of a normally distributed data set showing the critical  $\bar{X}$  value above which  $H_0$  is rejected in the  $t$ -statistic test.**

### A.2.3 Analysis of variance (ANOVA)

When comparing more than two sets of data, it is important to have a strategy by which to establish whether the differences between the means are due to random variation or

whether they result from the effect of a factor on the recorded data. The ANOVA technique is a useful tool with which to make such decisions.

ANOVA gives answers to the following questions that are asked in factorial designs:

- Does a factor have an effect on the response?
- How real is the apparent effect?
- Does the effect of one factor depend on the level of the other factors – does an interaction occur between factors?
- How real is the interaction?
- What are the confidence levels of each of the observed effects?

Suppose any matrix that represents a set of experiments with  $j$  repetitions and with  $i$  runs in each repetition is given in eq. A.12.

$$\begin{array}{cccc}
 y_{11} & y_{12} & \cdots & y_{1j} \\
 \cdot & \cdot & \cdots & \cdot \\
 \cdot & \cdot & \cdots & \cdot \\
 \cdot & \cdot & \cdots & \cdot \\
 y_{i1} & y_{i2} & \cdots & y_{ij}
 \end{array} \tag{A.12}$$

with  $1 \leq i \leq r$  and  $1 \leq j \leq c$ .

In ANOVA the deviation of the observed values are obtained from the partitioning of the **total sum of squares** ( $SS_T$ ) into the **sum of squares of the treatments** ( $SS_{\text{treatments}}$ ) and the **sum of squares of the error** ( $SS_E$ ), given in eq. A.13.<sup>3</sup>

$$SS_T = SS_{\text{treatments}} + SS_E \tag{A.13}$$

with

$$SS_T = \sum_{i=1}^r \sum_{j=1}^c (y_{ij} - \bar{y})^2 \tag{A.14}$$

and 
$$SS_{\text{treatments}} = n \sum_{i=1}^r (\bar{y}_i - \bar{y})^2 \quad (\text{A.15})$$

and 
$$SS_E = \sum_{i=1}^r \sum_{j=1}^c (y_{ij} - \bar{y}_i)^2 \quad (\text{A.16})$$

In ANOVA the null hypothesis states that  $H_0 : \mu_1 = \mu_2$ , implying that the means are equal. The null hypothesis is tested against the alternative that states that  $H_1 : \mu_1 > \mu_2$ . The critical point for rejecting the null hypothesis within a certain confidence interval in ANOVA is determined by the F-ratio. This critical point is calculated according to eq. A.17 with the **mean sum of squares of the treatments** ( $MS_{\text{treatments}}$ ) seen in eq. A.18 and the **mean sum of squares of the error** ( $MS_E$ ) seen in eq. A.19.<sup>3</sup>

$$F_0 = \frac{MS_{\text{treatments}}}{MS_E} \quad (\text{A.17})$$

with 
$$MS_{\text{treatments}} = \frac{SS_{\text{treatments}}}{(a-1)} \quad (\text{A.18})$$

and 
$$MS_E = \frac{SS_E}{(N-a)} \quad (\text{A.19})$$

Comparing the value of  $F_0$  with the corresponding value at a confidence level of  $\alpha = 5$  in a F-distribution table, the null hypothesis will be rejected if  $F_0 > F$ .<sup>3</sup>

### A.3 2-LEVEL FACTORIAL DESIGNS

As was mentioned in section 3.1, a factorial design refers to an experiment in which, in one complete trial, all possible combinations of the levels of all the factors are investigated. In such an experiment each of the factors A, B, etc. will be assigned a maximum and a minimum value that will be referred to as +1 and -1 respectively in the design. These values are called the factor levels. The relationship between the factor values and the

factor levels assigned to them are in a linear relation to each other. The relationship between the factor values ( $x$ ) and the factor levels ( $X$ ) are given in eq. A.20.<sup>8</sup>

$$X = c_1x + c_2 \quad (\text{A.20})$$

The designs that we used were Box, Hunter and Hunter<sup>2</sup>  $2^{k-l}$ -factorial designs. A  $2^{k-l}$ -factorial design is a  $k$ -level factorial design. In the case of a fractional factorial design,  $l$  determines the fraction. Table A.1 show an example of the  $2^3$ -factorial design with factors A, B and C, and has been illustrated in Figure A.1.<sup>3,4,6</sup>

**Table A.1:**  
**The factor levels as well as the treatments for a  $2^3$ -factorial design.**

Treatments	A	B	C
I	-1	-1	-1
a	+1	-1	-1
b	-1	+1	-1
ab	+1	+1	-1
c	-1	-1	+1
ac	+1	-1	+1
dc	-1	+1	+1
abc	+1	+1	+1

### A.3.1 Main effects

The individual effects of each factor and interaction are called the factor's main effect. The main effect of a factor is defined as the change in the response when there is a change in the level of the factor. The main effect of a factor is the difference between the average response at the high level and the average response at the low level of the factor. When the difference in response between the levels of one factor is not the same at all levels of the factor, there is an interaction occurring. As an example the main effect of factor A is determined by eq. 3.21 as illustrated in Figure A.3.<sup>2,3</sup>

$$\begin{aligned}
 A &= \bar{y}_{A^+} + \bar{y}_{A^-} \\
 &= \frac{a + ab + ac + abc}{4n} - \frac{(1) + b + c + bc}{4n} \\
 &= \frac{1}{4n} [a + ab + ac + abc - (1) - b - c - bc] \tag{A.21}
 \end{aligned}$$

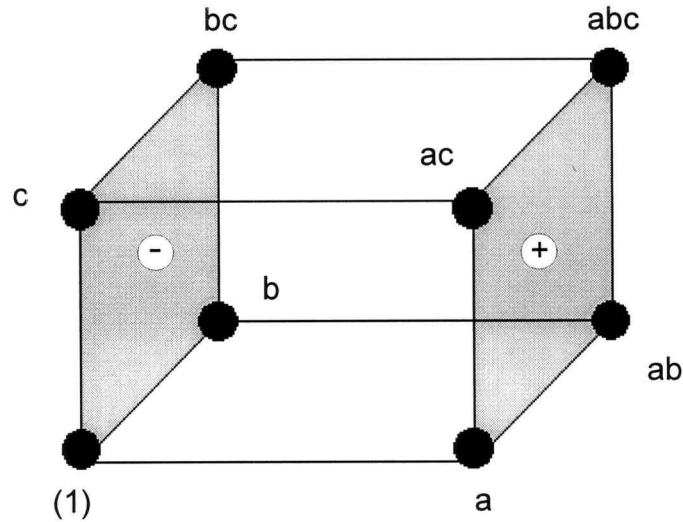


**Figure A.3:**  
**Geometric representation of a 2<sup>3</sup>-factorial design with the contrasting sides representing the main effects of factor A.**

### A.3.2 Statistical analysis

ANOVA is used to determine the magnitude and direction of the main effects to see which factors have the biggest influence on the response. The sum of squares for each of the factors and interactions as well as the total sum of squares can be calculated. The sum of squares for factor A is seen in eq. 3.22 and for the interaction AB in eq. 3.23.<sup>3</sup>

$$SS_A = \frac{1}{bcn} \sum_{i=1}^a y_i^2 - \frac{y^2}{abcn} \tag{3.22}$$

$$\begin{aligned}
 SS_{AB} &= \frac{1}{cn} \sum_{i=1}^a \sum_{j=1}^b y_{ij}^2 - \frac{y^2}{abcn} - SS_A - SS_B \\
 &= SS_{\text{subtotals}(AB)} - SS_A - SS_B \tag{A.23}
 \end{aligned}$$

The total sum of squares is given in eq. 3.24.<sup>3</sup>

$$SS_T = \sum_{i=1}^a \sum_{j=1}^b \sum_{k=1}^c \sum_{l=1}^n y_{ijkl}^2 - \frac{y^2}{abcn} \quad (\text{A.24})$$

The  $SS_E$  is calculated with eq. A.25.<sup>3</sup>

$$SS_E = SS_T - SS_{\text{subtotals}(ABC)} \quad (\text{A.25})$$

The ANOVA table can be expressed in terms of the sum of squares and the mean sum of squares as follow:<sup>2,3</sup>

**Table A.2:**  
**ANOVA of the main factor effects of a 2<sup>3</sup>-factorial design.**

Source of variation	SS	df	MS	F <sub>0</sub>
A	SS <sub>A</sub>	a - 1	MS <sub>A</sub>	$\frac{MS_A}{MS_E}$
B	SS <sub>B</sub>	b - 1	MS <sub>B</sub>	$\frac{MS_B}{MS_E}$
C	SS <sub>C</sub>	c - 1	MS <sub>C</sub>	$\frac{MS_C}{MS_E}$
AB	SS <sub>AB</sub>	(a - 1)(b - 1)	MS <sub>AB</sub>	$\frac{MS_{AB}}{MS_E}$
AC	SS <sub>AC</sub>	(a - 1)(c - 1)	MS <sub>AC</sub>	$\frac{MS_{AC}}{MS_E}$
BC	SS <sub>BC</sub>	(b - 1)(c - 1)	MS <sub>BC</sub>	$\frac{MS_{BC}}{MS_E}$
ABC	SS <sub>ABC</sub>	(a - 1)(b - 1)(c - 1)	MS <sub>ABC</sub>	$\frac{MS_{ABC}}{MS_E}$
Error	SS <sub>E</sub>	abc(n - 1)	MS <sub>E</sub>	
Total	SS <sub>T</sub>	abcn - 1		

where df is the degrees of freedom, SS is the sum of squares and MS is the mean sum of squares of the different variables or interactions whose effect is being measured.

By comparing the  $F_0$  values, as discussed in section 3.2.3, one can predict within a certain confidence level whether a certain factor or interaction has a major effect on the response.

### A.3.3 Regression model

The main effects of all the factors and their interactions are distributed points in the experimental space. A regression model is a mathematical model used to obtain the expected value of the response at specific levels of the factors, as seen in eq. A.26.<sup>3,6</sup>

$$y = \beta_0 + \sum_{j=1}^k \beta_j x_{ij} + \varepsilon \quad (\text{A.26})$$

with  $i = 1, 2, \dots, n$  and  $\beta$  the parameters that must be determined with a least squares estimation.

In the **least squares estimation** the estimates,  $\hat{\beta}_i$  (with  $i = 0, 1, 2, \dots, n$ ), are selected to minimise the sum of the squared deviation between the observed value,  $y$ , and the fitted value,  $\hat{y}$ . This is done with calculus by setting the partial derivatives with respect to  $\hat{\beta}_i$  equal to zero.<sup>6</sup>

**Table A.3:**  
**ANOVA for a linear regression model.**

Source of variation	Variation	df	Variance	F ratio
Explained (by regression)	$\sum (\hat{y}_i - \bar{y})^2$	1	$\hat{\beta}^2 \sum x_i^2$	$\frac{\hat{\beta}^2 \sum x_i^2}{s^2}$
Unexplained (residual)	$\sum (y_i - \hat{y}_i)^2$	n-2	$s^2 = \frac{\sum (y_i - \hat{y}_i)^2}{n-2}$	
Total	$\sum (y_i - \bar{y})^2$	n-1		

The accuracy of the estimates of the regression model can be tested with ANOVA. From this a test for the null hypothesis ( $\hat{\beta}_i = 0$  with  $i = 1, 2, \dots, n$ ) is formulated. The ANOVA table can be summarised in terms of the explained and unexplained variances as seen in Table A.3.<sup>6</sup>

#### A.3.4 Responses surfaces

The surface represented by the eq. A.27 is the regression surface of the regression model (see eq. A.26). The regression surface is also called the response surface.<sup>4</sup>

$$y = \eta(x_1, x_2, \dots, x_q) \quad (\text{A.27})$$

### A.4 STATISTICAL PACKAGE

All the data accumulated in the experiments were statistically analysed with the statistical package STATISTICA, release 5.1 (1997 ed.) by Statsoft Inc.<sup>9</sup>

### A.5 BIBLIOGRAPHY

1. Morgan, E.D. **Chemometrics: Experimental Design**, Wiley, New York, 1995.
2. Box, G.E.P.; Hunter, W.G; Hunter, J.S. **Statistics for Experimenters: An Introduction to Design, Data Analysis and Model Building**, Wiley, New York, 1978.
3. Montgomery, D.C. **Design and Analysis of Experiments**, 4<sup>th</sup> ed., Wiley, New York, 1997.
4. Johnson, N.L.; Leone, F.C. **Statistics and Experimental Design in Engineering and Physical Sciences**, 2<sup>nd</sup> ed., Wiley, New York, 1977.
5. Yang, H–J.; Yang, C–H. *Statistical experimental strategies approach to emulsion copolymerization of styrene and n–butyl acrylate*, **Journal of Applied Polymer Science**, 69, 551, 1998.
6. Morgan, E.D. **Chemometrics: Experimental Design**, Wiley, New York, p. 50, 1995.

7. Wonnacott, T.H.; Wannocott, R.J. **Introductory Statistics**, 3<sup>rd</sup> ed. John Wiley and Sons Inc. 1977.
8. Jacobs, E.P. **Statistical and Numerical Techniques in the Optimization of Membrane Fabrication Variables**, *Ph.D.* thesis, University of Stellenbosch, Stellenbosch, South Africa, 1988.
9. Statsoft Inc. <http://www.statsoft.com>

## Appendix B

### RESPONSE SURFACE PLOTS

The response surface plots for the responses of the variables  $\ln(M_n)$ , MWD, particle size, conversion and  $T_g$  for the  $2^{5-1}$ -fractional factorial design. The response surface plots are a representation of an equation that is obtained through a multiple linear regression of the responses. In all the curves the response is on the vertical axes while the other two axes represent any two variables. All other variables are kept constant at a factor level of zero. In the case of a non-continuous variable such as the type of CTA and type of initiator, the response curve is not an accurate representation of the data. In these cases only the maximum and minimum values on the response surface are of any interest.

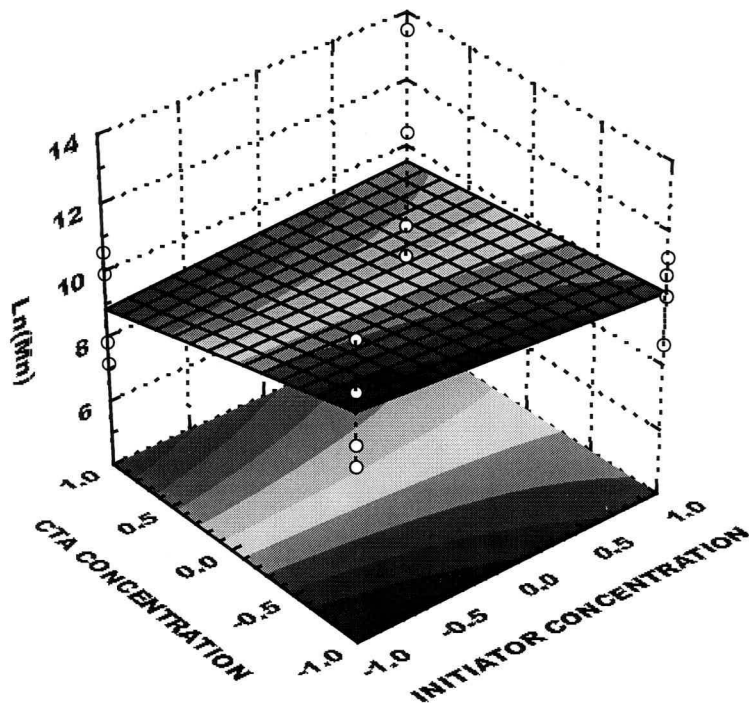
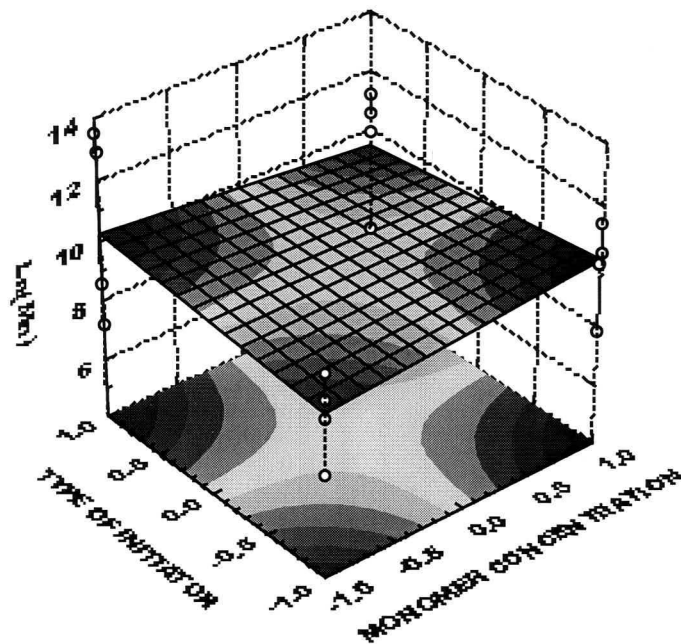
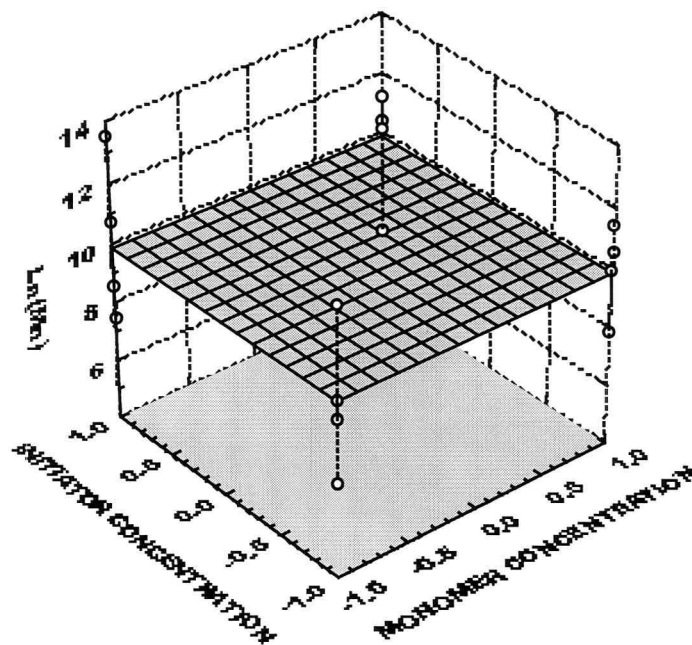


Figure B.1:

Response surface of  $\ln(M_n)$  for the variables Initiator concentration and CTA concentration.



**Figure B.2:**  
Response surface of  $\ln(M_n)$  for the variables monomer concentration and the type of initiator.



**Figure B.3:**  
Response surface of  $\ln(M_n)$  for the variables monomer concentration and initiator concentration.

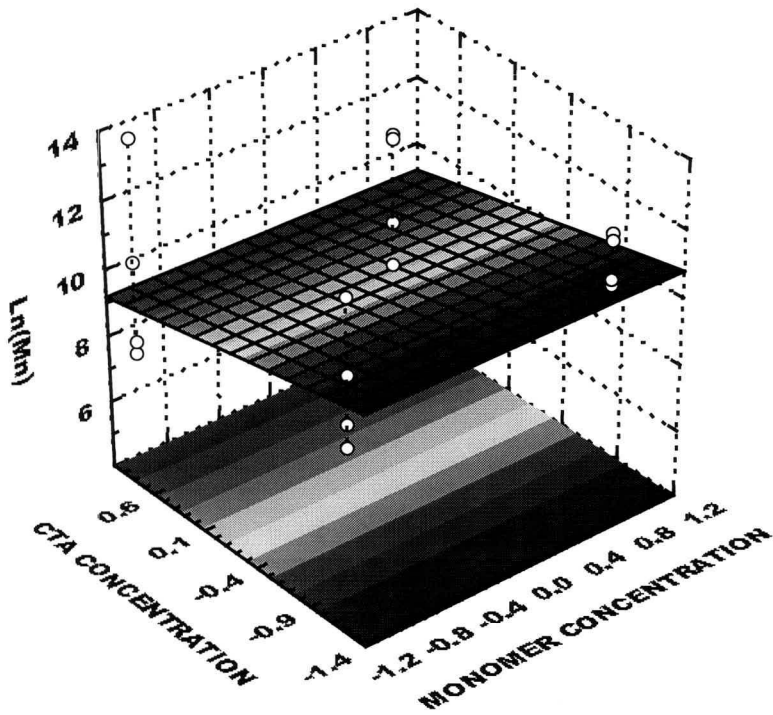


Figure B.4:  
Response surface of  $\ln(M_n)$  for the variables monomer concentration and type of CTA.

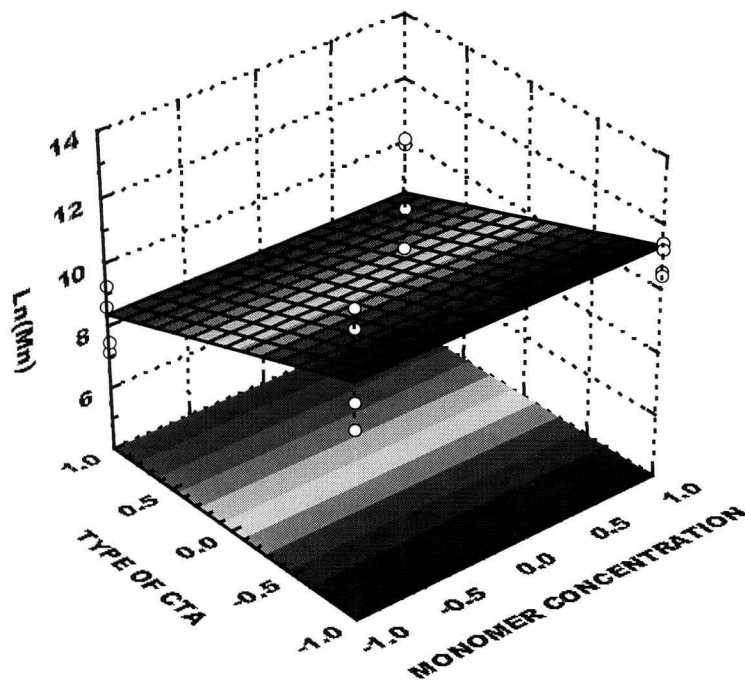


Figure B.5:  
Response surface of  $\ln(M_n)$  for the variables monomer concentration and CTA concentration.

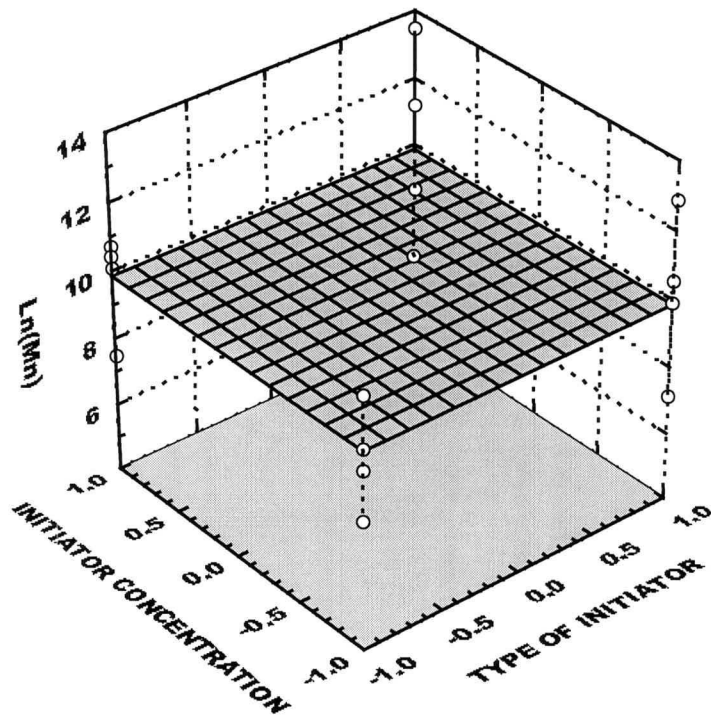


Figure B.6:

Response surface of  $\ln(M_n)$  for the variables Type of initiator and initiator concentration.

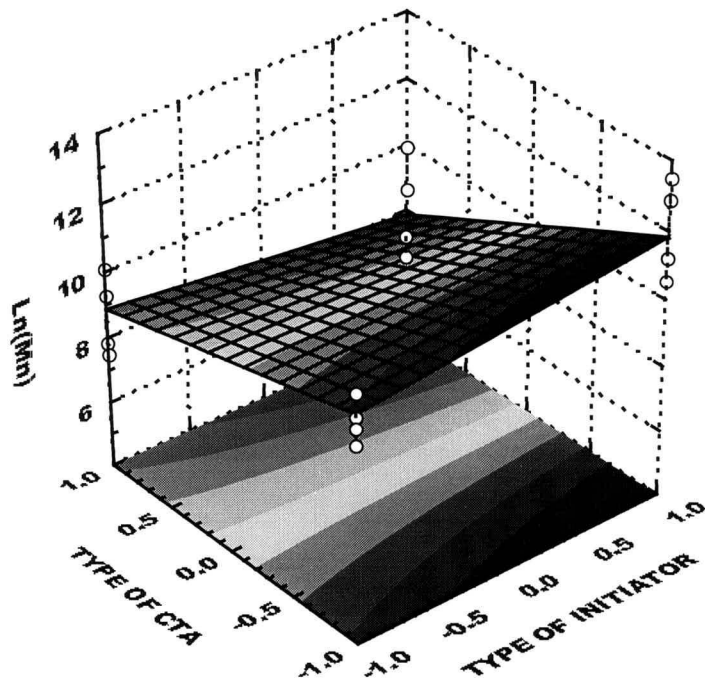


Figure B.7:

Response surface of  $\ln(M_n)$  for the variables type of initiator and type of CTA.

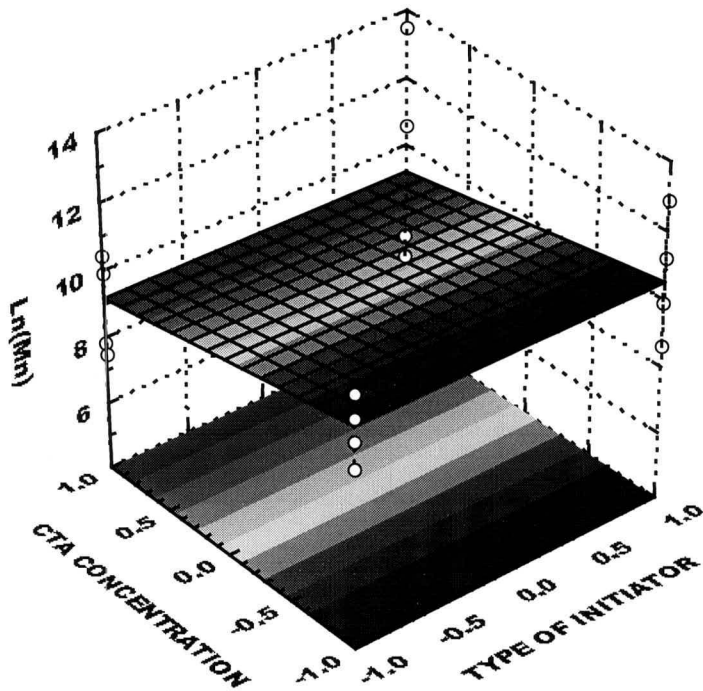


Figure B.8:  
Response surface of  $\ln(M_n)$  for the variables type of initiator and CTA concentration.

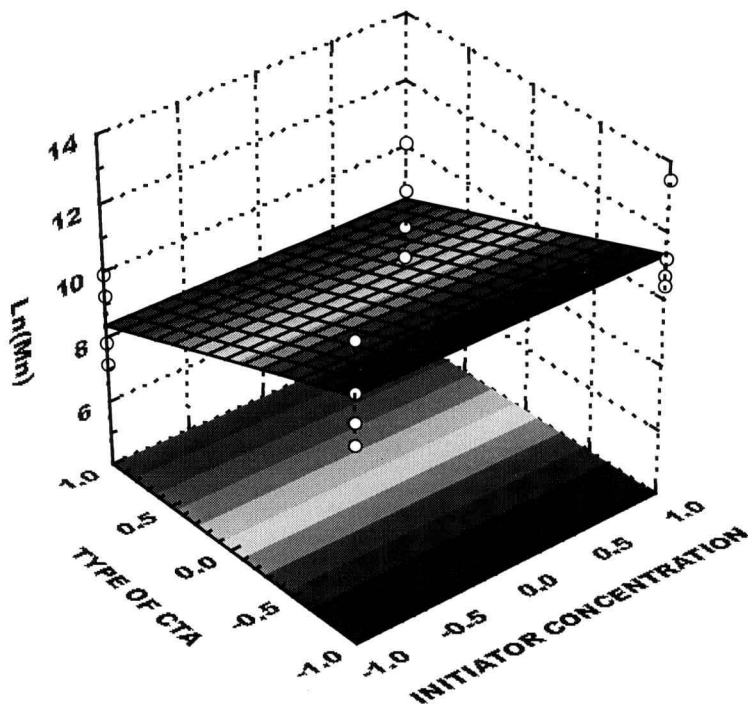


Figure B.9:  
Response surface of  $\ln(M_n)$  for the variables type of initiator and type of CTA.

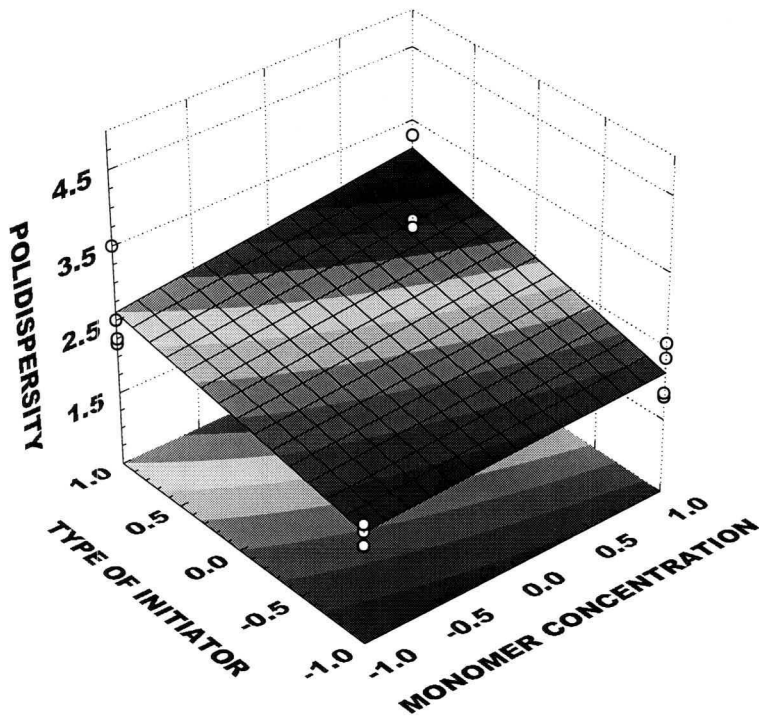


Figure B.10:  
Response surface of  $M_w/M_n$  for the variables monomer concentration and type of initiator.

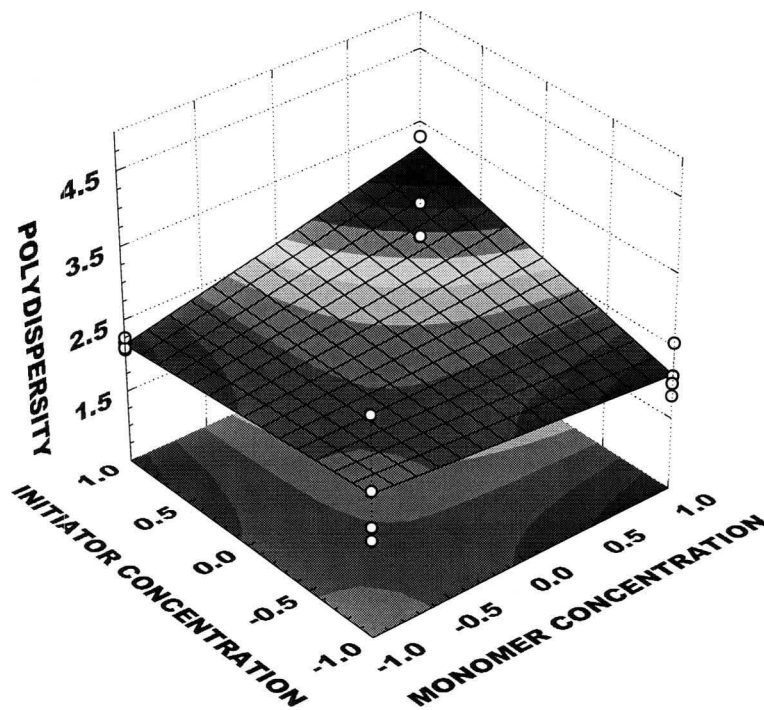


Figure B.11:  
Response surface of  $M_w/M_n$  for the variables monomer concentration and initiator concentration.

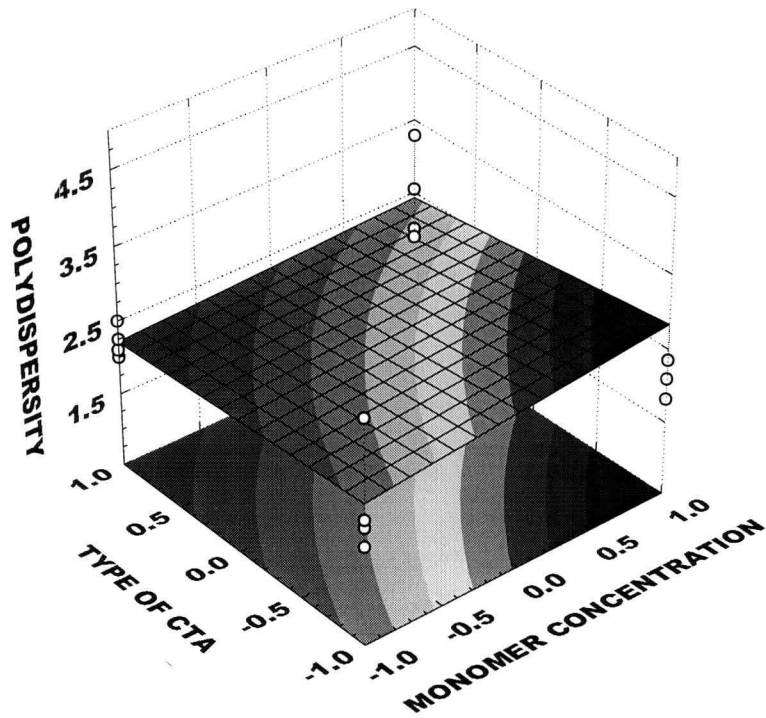


Figure B.12:  
Response surface of  $M_w/M_n$  for the variables monomer concentration and type of CTA.

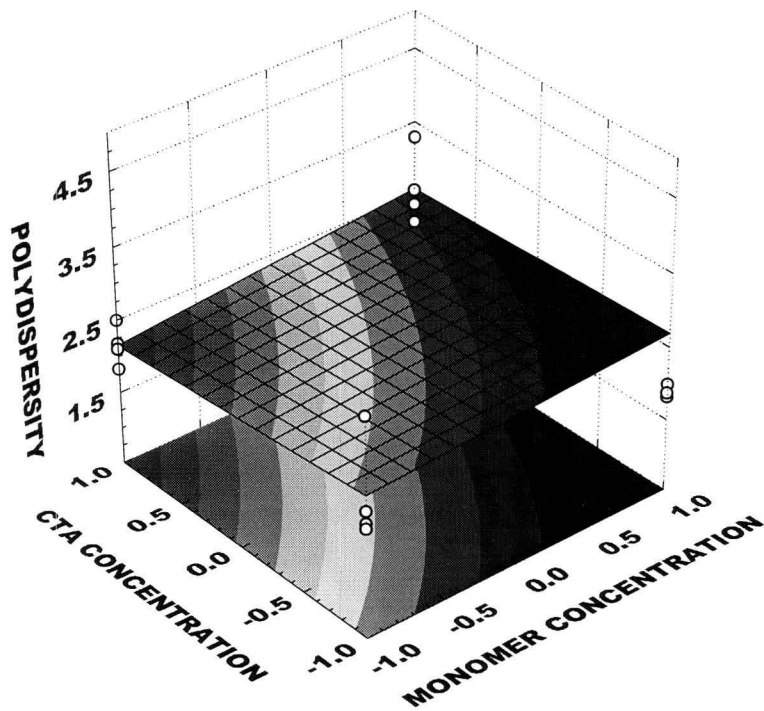


Figure B.13:  
Response surface of  $M_w/M_n$  for the variables monomer concentration and CTA concentration.

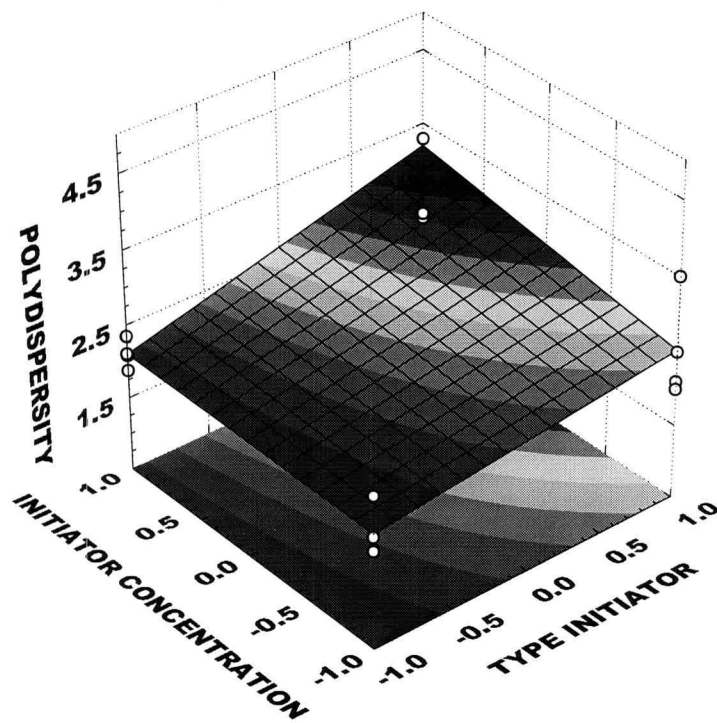


Figure B.16:

Response surface of  $M_w/M_n$  for the variables type of initiator and initiator concentration.

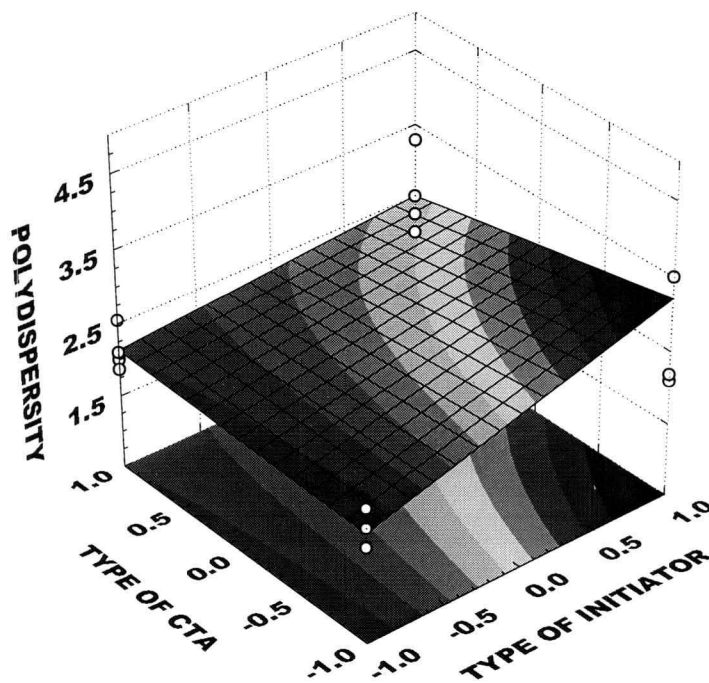


Figure B.17:

Response surface of  $M_w/M_n$  for the variables type of initiator and type of CTA.

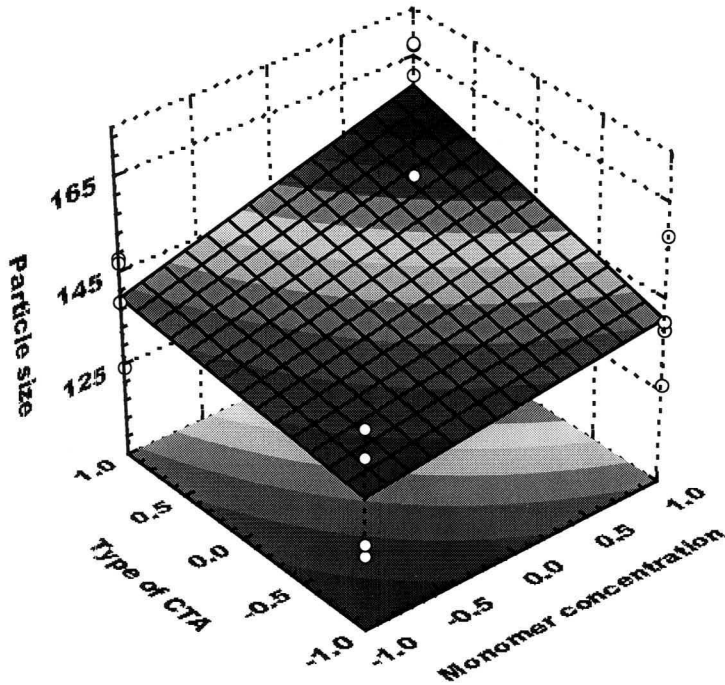


Figure B.18:

Response surface of particle size for the variables initiator monomer concentration and type of CTA.

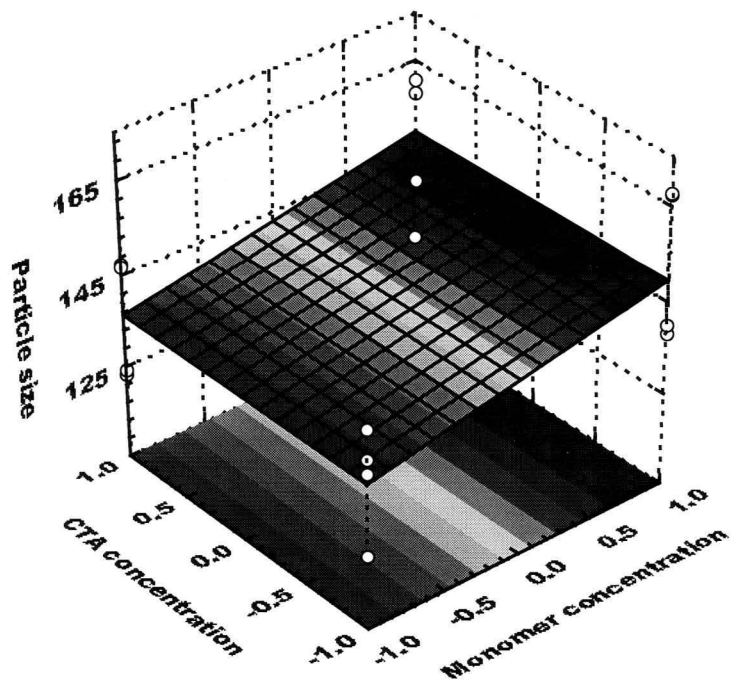


Figure B.19:

Response surface of particle size for the variables Initiator monomer concentration and CTA concentration.

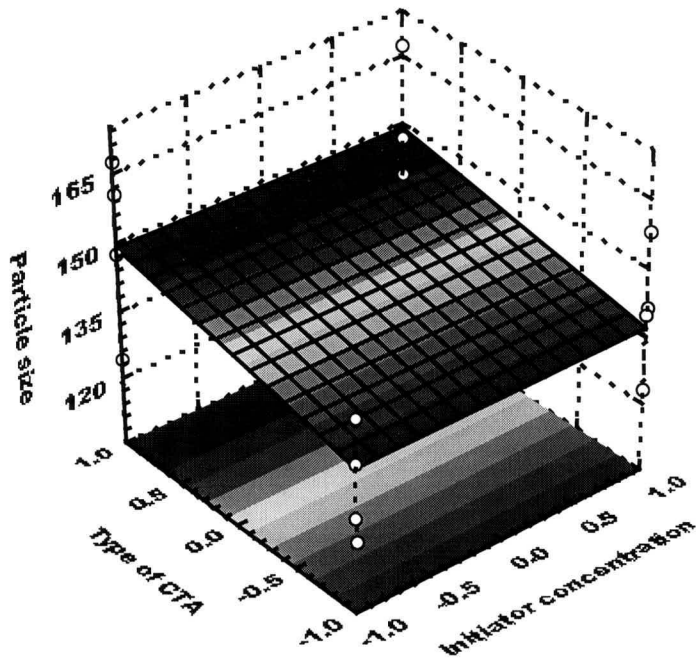


Figure B.20:

Response surface of particle size for the variables initiator concentration and type of CTA.

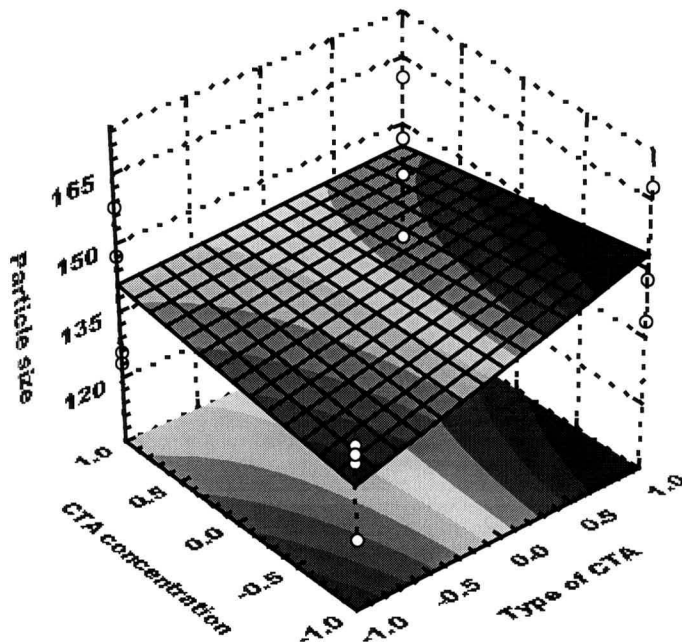


Figure B.21:

Response surface of particle size for the variables initiator concentration and CTA concentration.

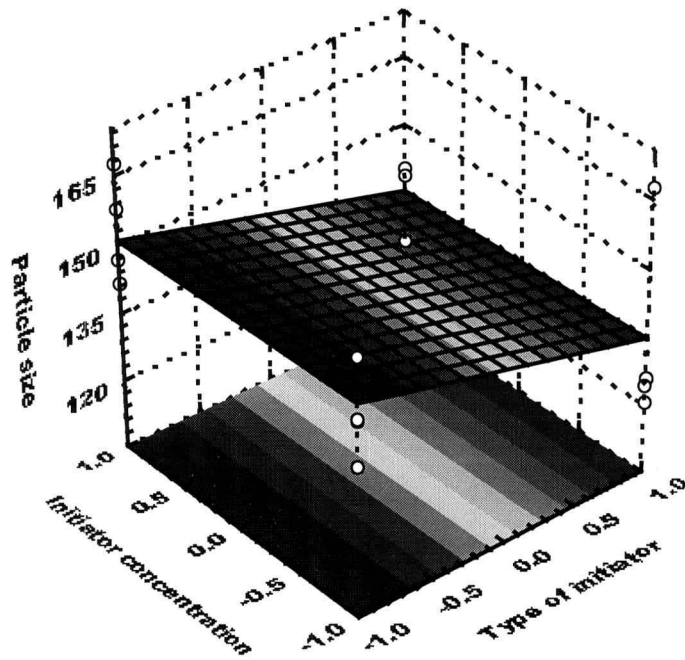


Figure B.22:

Response surface of particle for the variables CTA concentration and type of CTA.

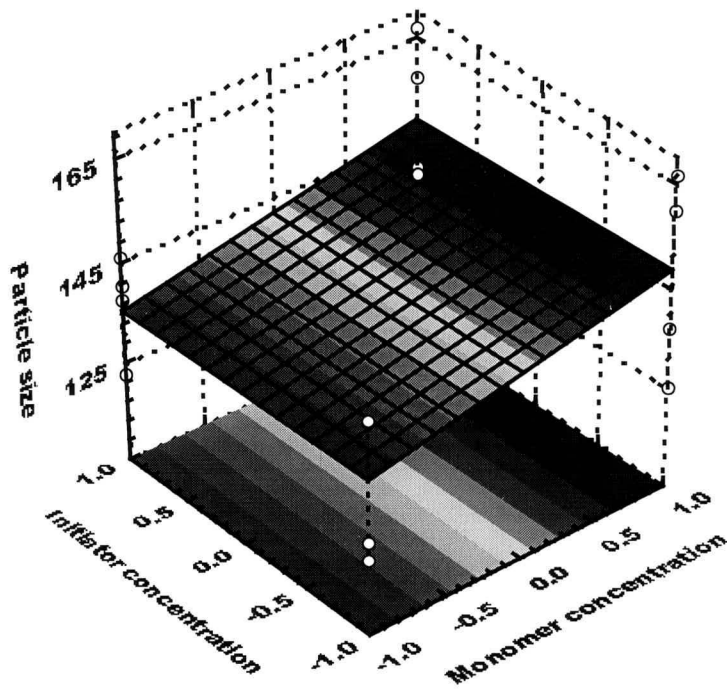


Figure B.23:

Response surface of particle for the variables monomer concentration and initiator concentration.

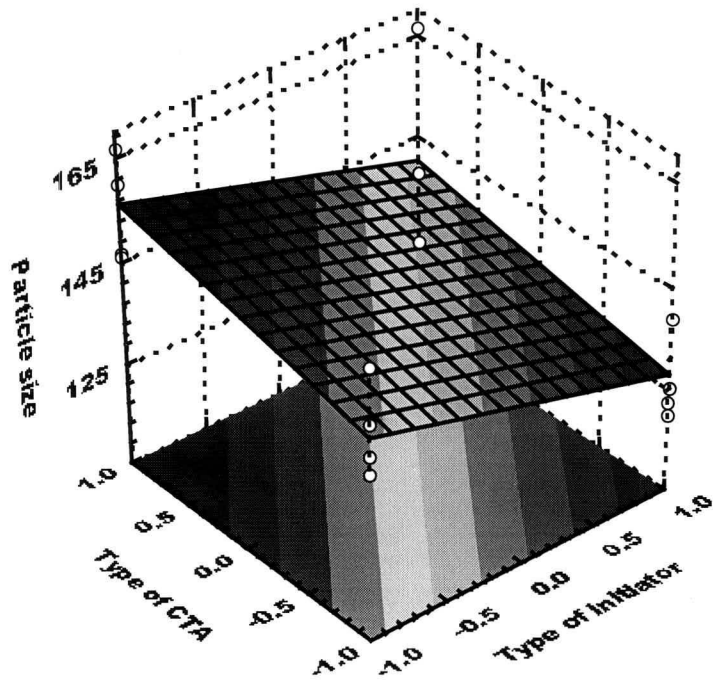


Figure B.24:

Response surface of particle for the variables type of initiator and type of CTA.

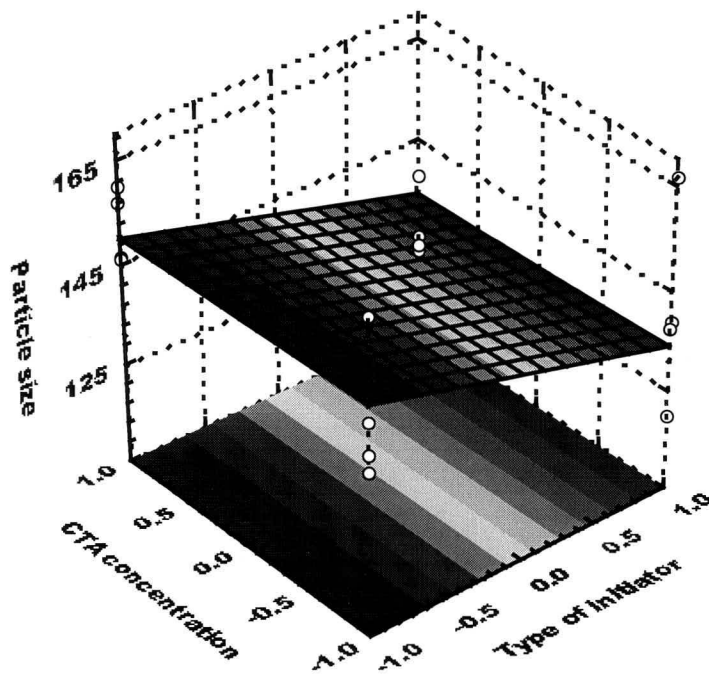


Figure B.25:

Response surface of particle for the variables CTA concentration and type of initiator.

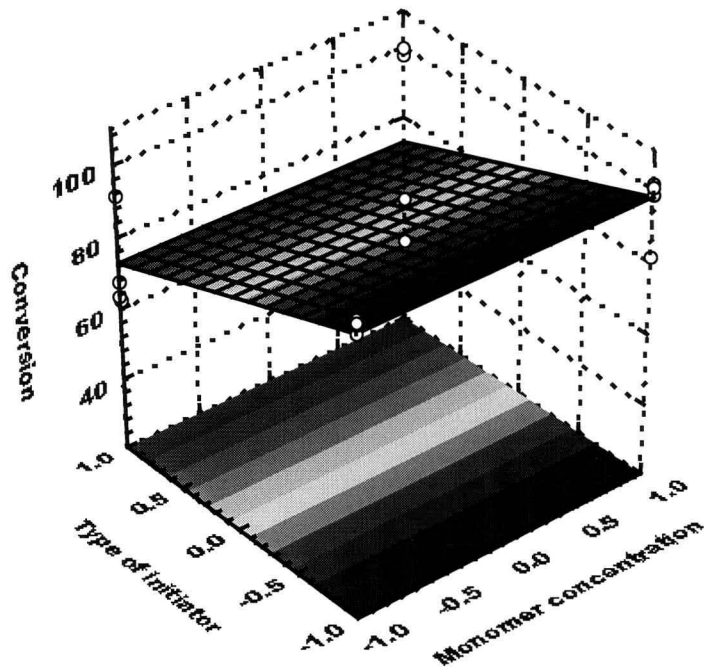


Figure B.27:

Response surface of conversion for the variables monomer concentration and type of initiator.

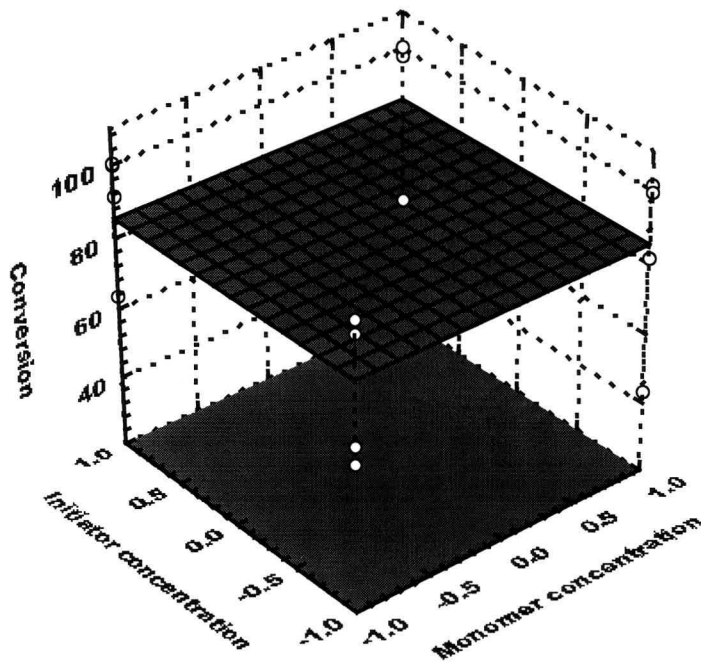


Figure B.28:

Response surface of conversion for the variables monomer concentration and initiator concentration.

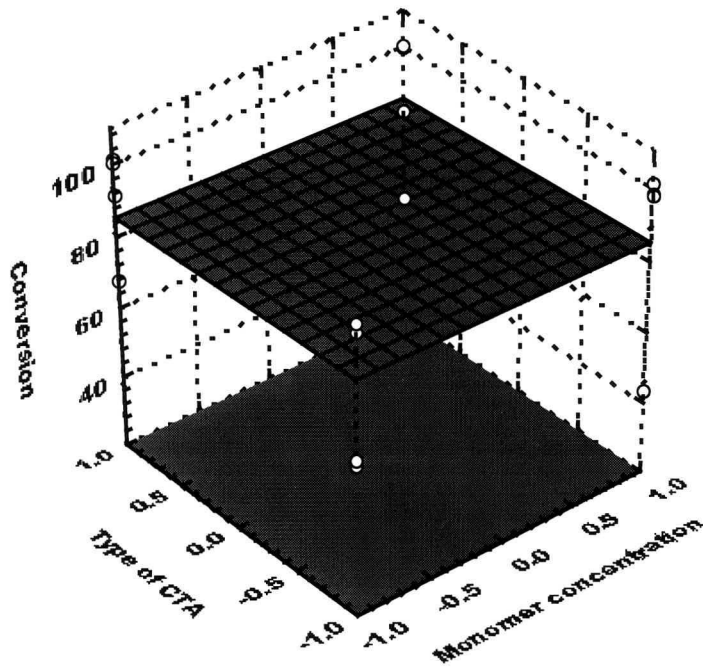


Figure B.29:

Response surface of conversion for the variables monomer concentration and type of CTA.

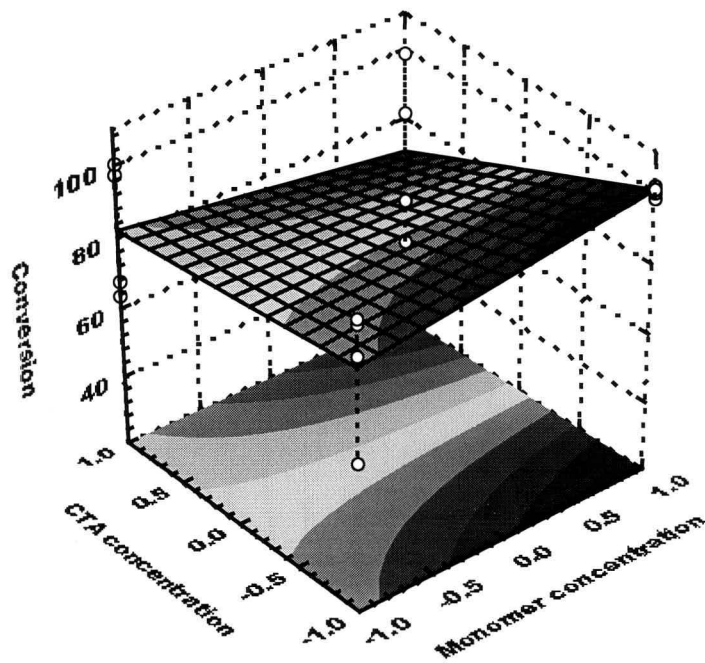


Figure B.30:

Response surface of conversion for the variables monomer concentration and CTA concentration.

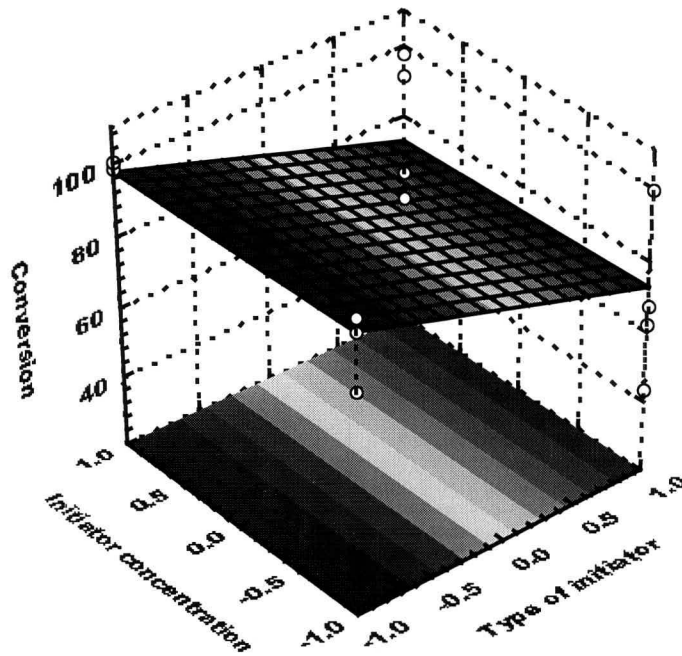


Figure B.31:

Response surface of conversion for the variables initiator concentration and type of initiator.

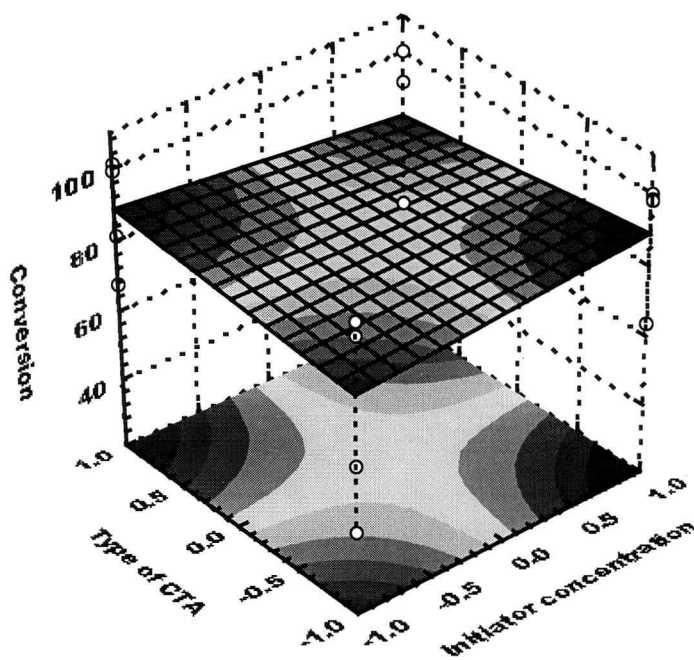


Figure B.32:

Response surface of conversion for the variables initiator concentration and type of CTA.

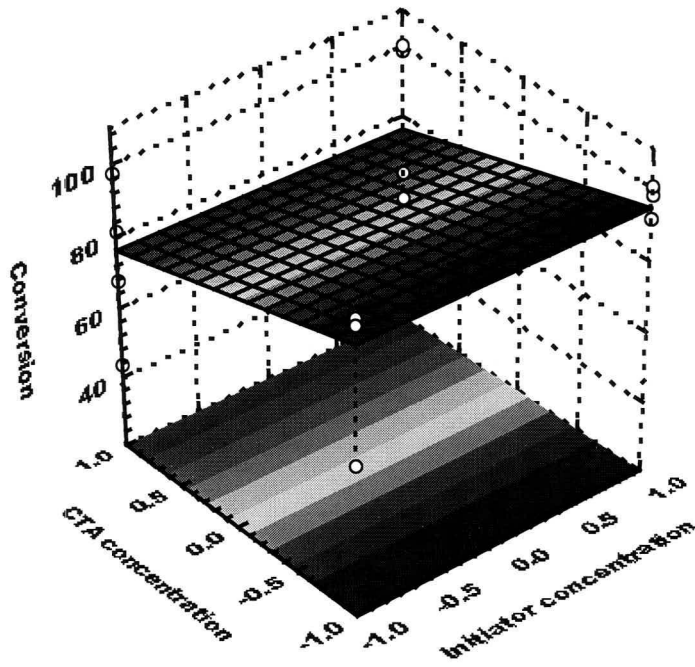


Figure B.33:

Response surface of conversion for the variables type of initiator and CTA concentration.

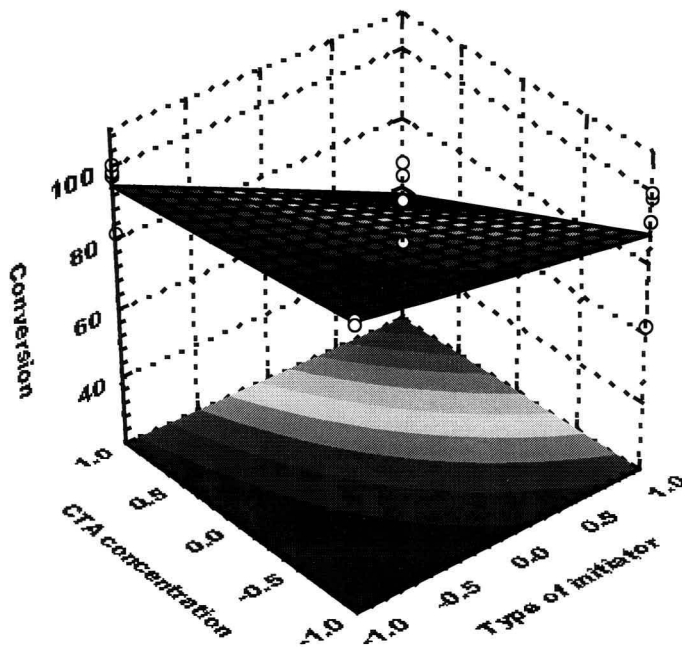


Figure B.34:

Response surface of conversion for the variables initiator concentration and CTA concentration.

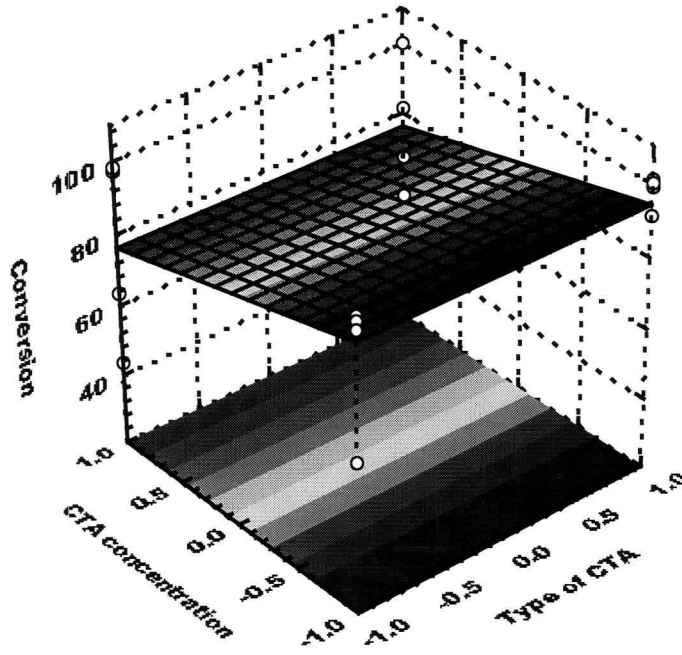


Figure B.35:

Response surface of conversion for the variables type of CTA and CTA concentration.

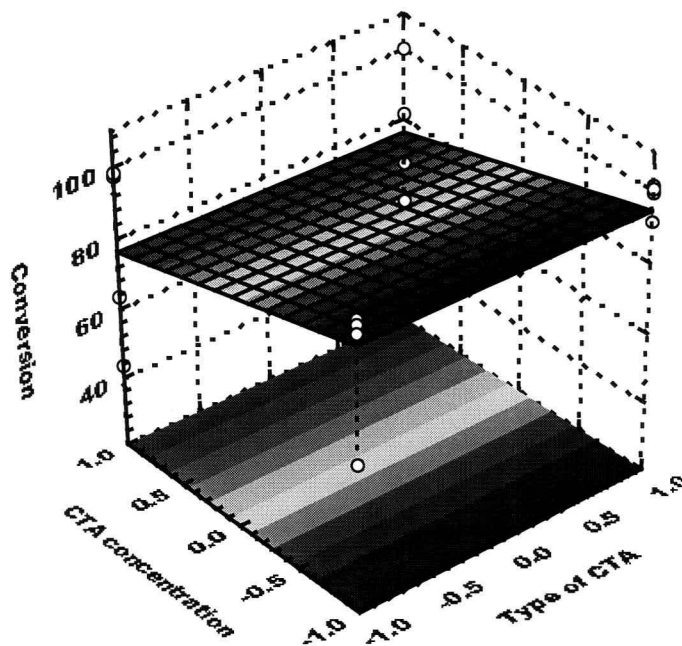


Figure B.36:

Response surface of  $T_g$  for the variables type of CTA and CTA concentration.

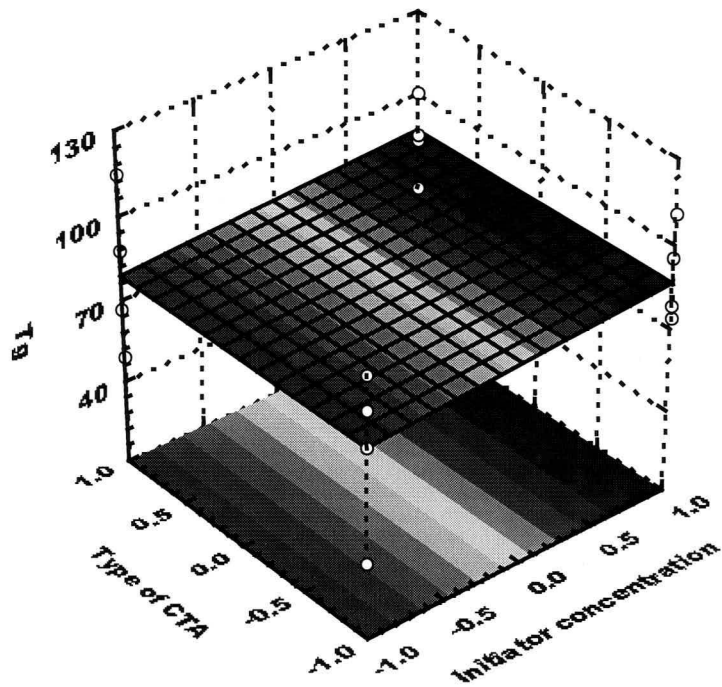


Figure B.37:

Response surface of  $T_g$  for the variables type of CTA and initiator concentration.

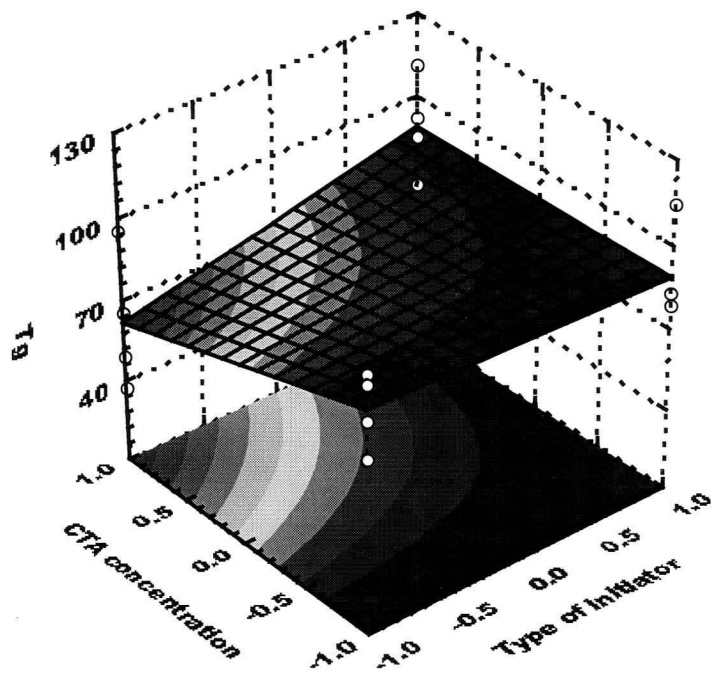


Figure B.38:

Response surface of  $T_g$  for the variables type of initiator and CTA concentration.

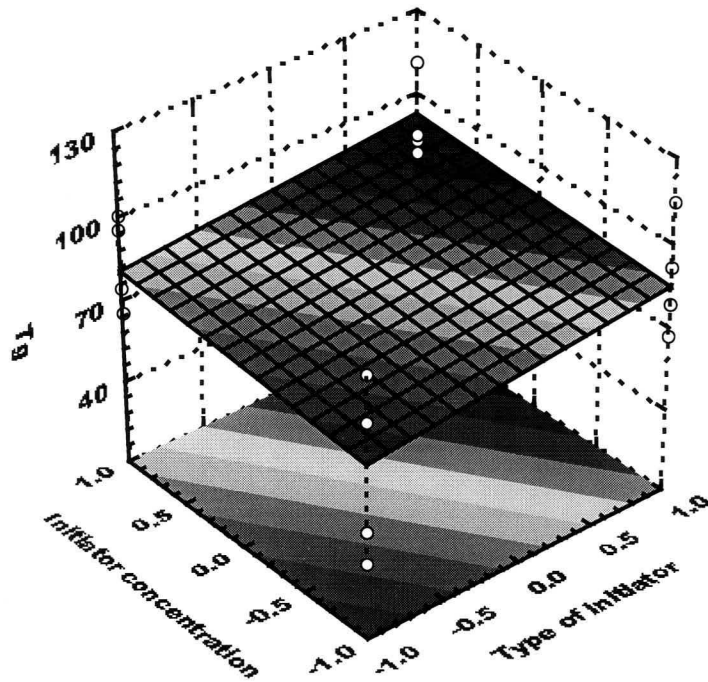


Figure B.39:

Response surface of  $T_g$  for the variables type of initiator and initiator concentration.

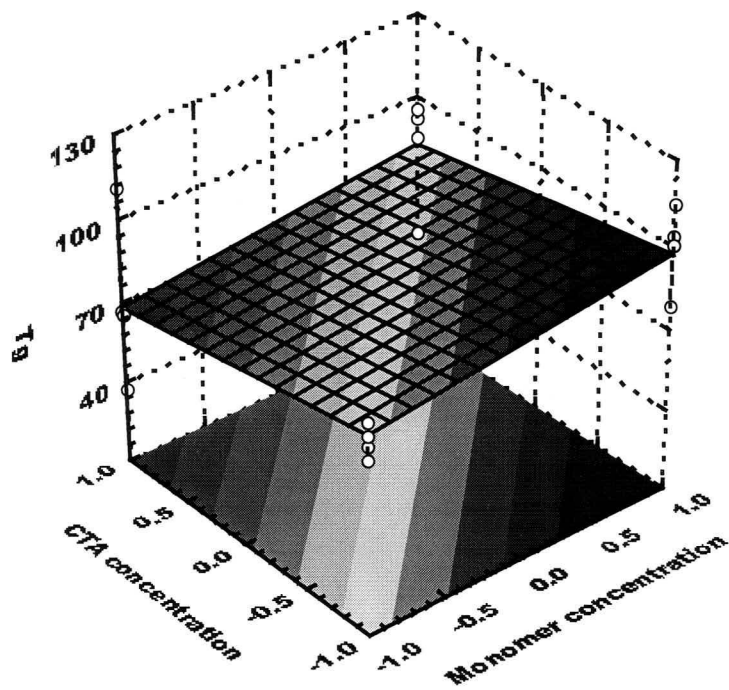


Figure B.40:

Response surface of  $T_g$  for the variables monomer concentration and CTA concentration.

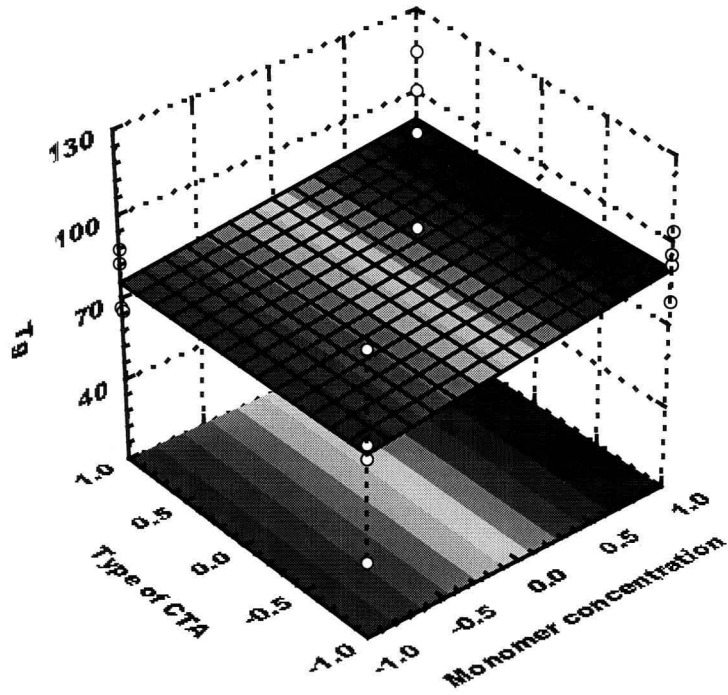


Figure B.41:  
Response surface of  $T_g$  for the variables monomer concentration and type of CTA.

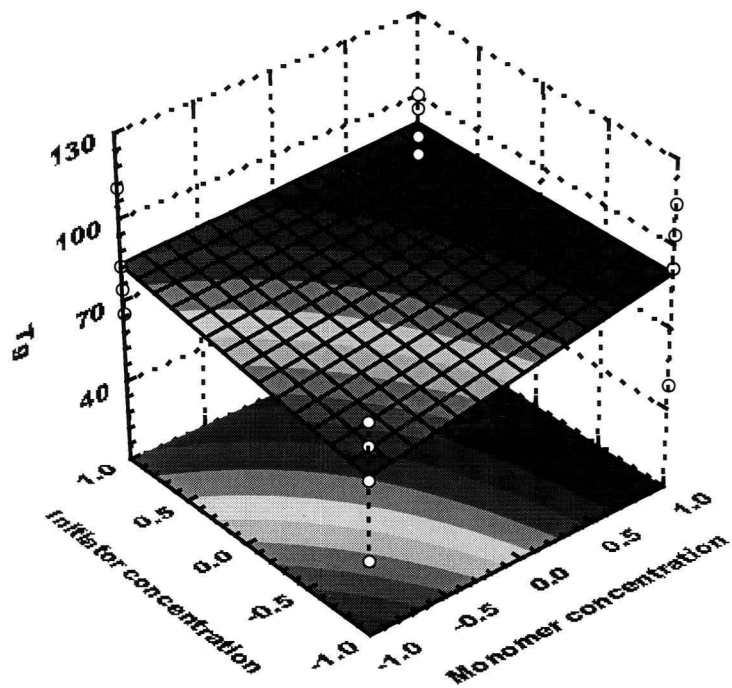


Figure B.42:  
Response surface of  $T_g$  for the variables monomer concentration and initiator concentration.

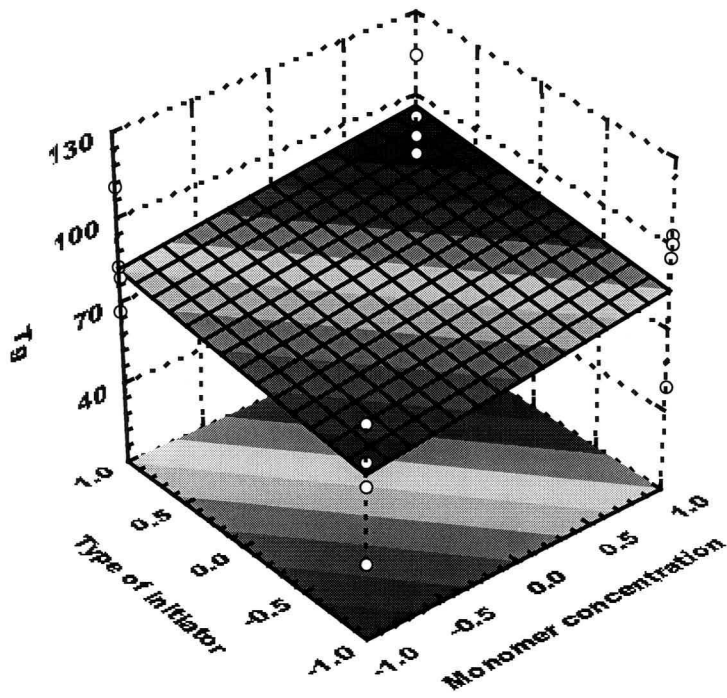


Figure B.43:

Response surface of  $T_g$  for the variables monomer concentration and type of initiator.

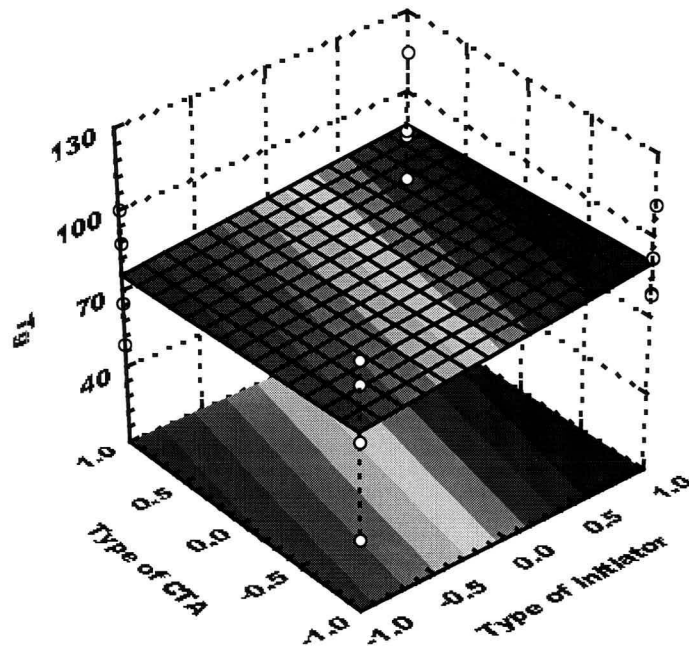


Figure B.44:

Response surface of  $T_g$  for the variables type of initiator and CTA

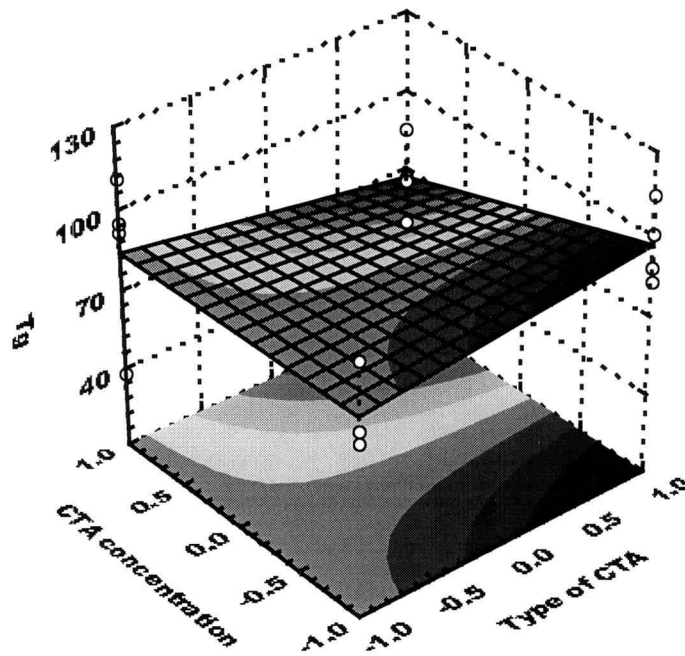


Figure B.45:

Response surface of  $T_g$  for the variables CTA concentration and type of CTA

## Appendix C

### NORMAL PROBABILITY PLOTS OF THE EFFECTS OF THE $2^{5-1}$ -FRACTIONAL FACTORIAL DESIGN

The normal probability plots of the effects of the  $2^{5-1}$  factorial design for  $\ln(M_n)$ , MMD, particle size and conversion are given here.

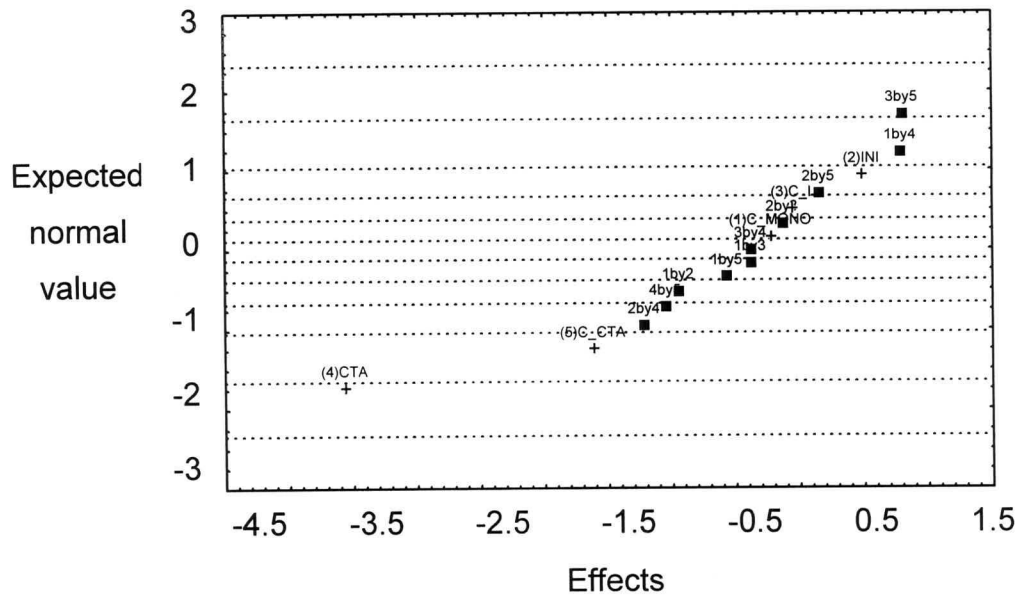


Figure C.1:

Normal probability plot of the effects of  $\ln(M_n)$ .

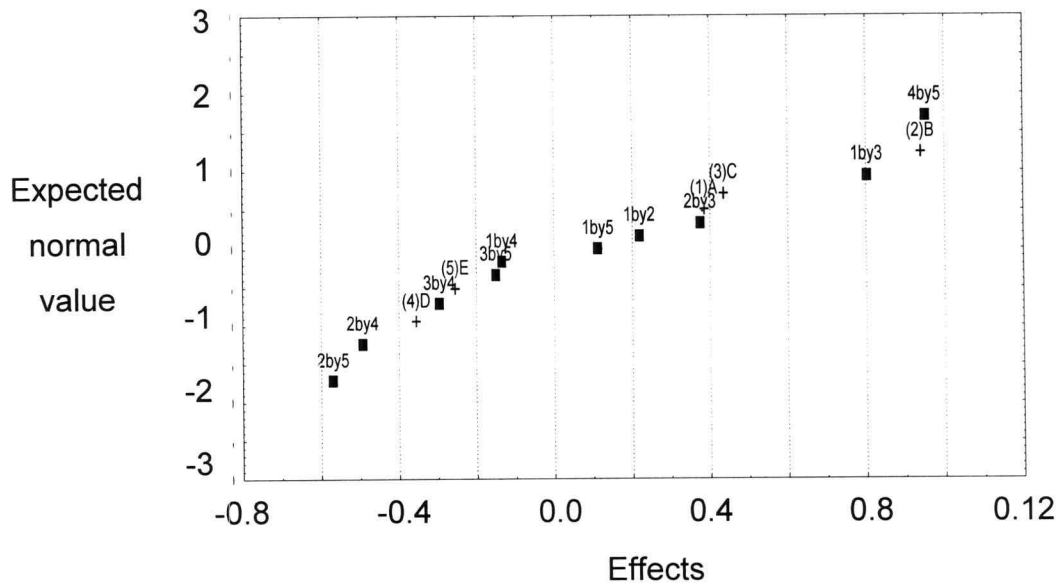
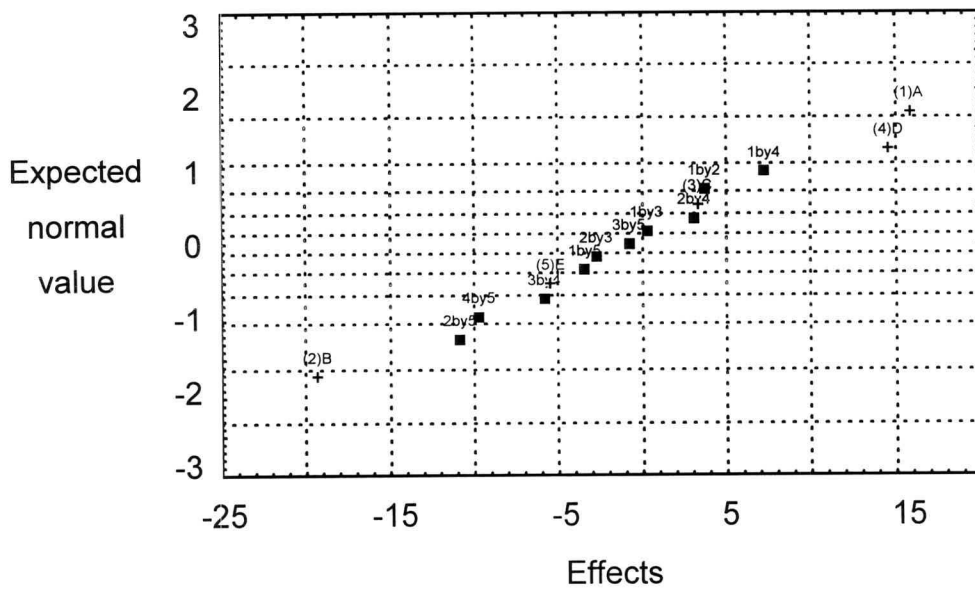
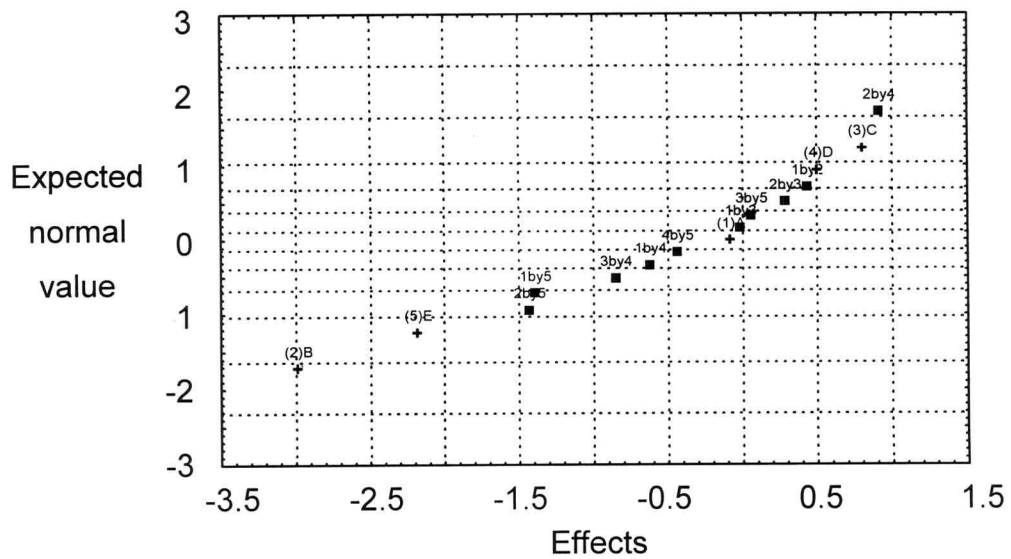


Figure C.2:

Normal probability plot of the effects of  $M_w/M_n$ .



**Figure C.3:**  
Normal probability plot of the effects of particle size.



**Figure C.4:**  
Normal probability plot of the effects of conversion.

## Appendix D

### PARETTO CHARTS OF THE EFFECTS OF THE $2^{5-1}$ FRACTIONAL FACTORIAL DESIGN

The Pareto charts of the effects of the  $2^{5-1}$  factorial design for  $\ln(M_n)$ , MMD, particle size and conversion are given to show which factors has a major influence on the respective responses.

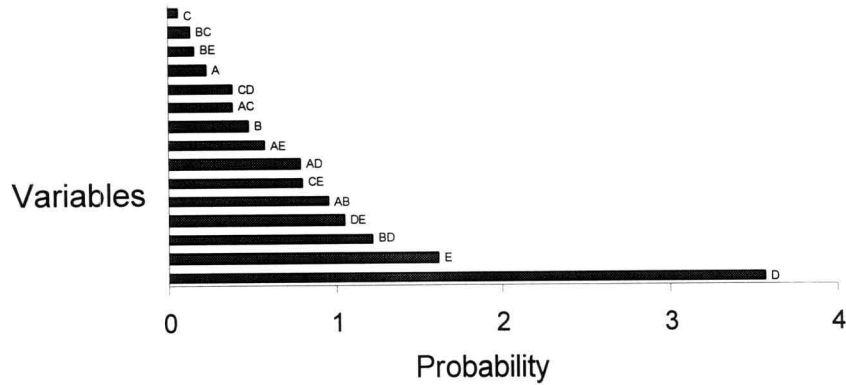


Figure D.1:  
Pareto chart of the effects of  $\ln(M_n)$ .

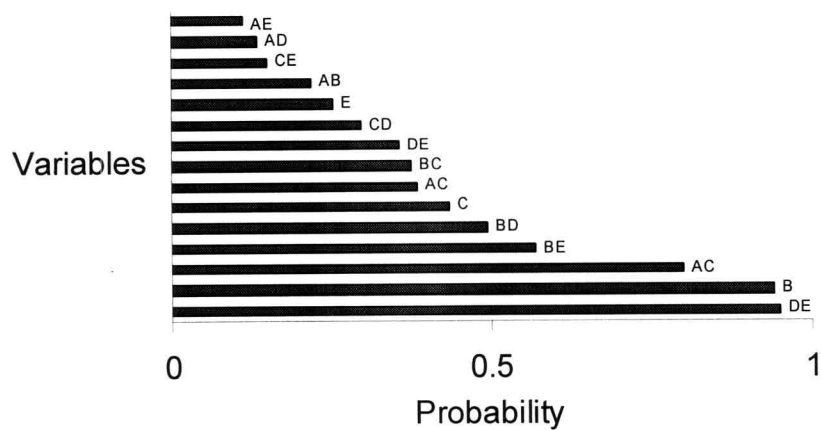
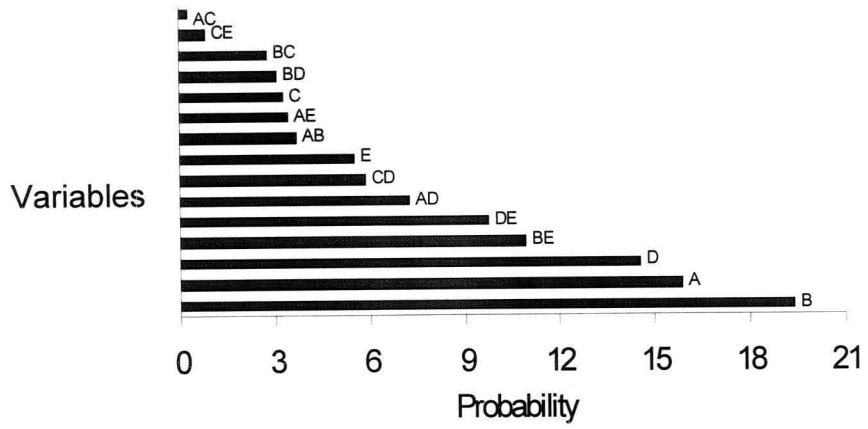
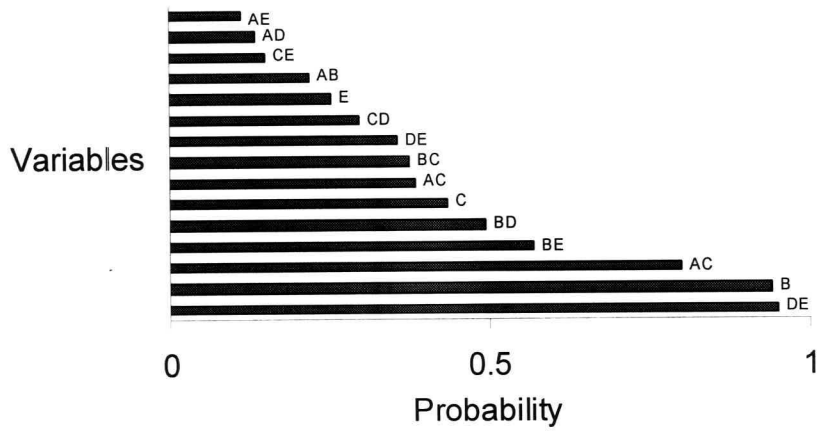


Figure D.2:  
Pareto chart of the effects of  $M_w/M_n$ .



**Figure D.3:**  
Pareto chart of the effects of  $M_w/M_n$ .



**Figure D.4:**  
Pareto chart of the effects of conversion.

**Appendix E****STEPWISE REGRESSION OF THE  $2^{5-1}$ -FACTORIAL DESIGN**

The following tables give a summary of the stepwise linear regression that was done for each of the responses in the  $2^{5-1}$ -fractional factorial design to determine which variables had a significant effect on the individual responses.

**Table E.1:**

**Summary of the stepwise regression of the response  $\ln(M_n)$ .**

Variable	Step	Multiple R <sup>2</sup>	F -value	p-level	Variables included
D	1	0.60	21.39	0.14	1
E	2	0.73	5.94	0.25	2
BD	3	0.80	4.23	0.29	3
DE	4	0.85	3.90	0.30	4
AB	5	0.90	4.11	0.29	5
CE	6	0.93	3.71	0.30	6
AD	7	0.95	5.22	0.26	7
AE	8	0.97	3.68	0.31	8
B	9	0.98	3.58	0.31	9
AC	10	0.99	3.08	0.33	10
CD	11	1.00	6.11	0.24	11
A	12	1.00	3.43	0.32	12
BE	13	1.00	2.19	0.38	13
BC	14	1.00	5.09	0.27	14

**Table E.2:**  
**Summary of the stepwise regression of the response MWD.**

Variable	Step	Multiple R <sup>2</sup>	F –value	p-level	Variables included
DE	1	0.23	4.29	0.29	1
B	2	0.46	5.55	0.26	2
AC	3	0.63	5.40	0.26	3
BE	4	0.71	3.24	0.32	4
BD	5	0.78	2.84	0.34	5
C	6	0.83	2.55	0.36	6
A	7	0.87	2.29	0.37	7
BC	8	0.90	2.59	0.35	8
D	9	0.93	2.99	0.33	9
CD	10	0.96	2.64	0.35	10
E	11	0.97	2.57	0.36	11
AB	12	0.99	2.69	0.35	12
CE	13	0.99	1.47	0.44	13
AD	14	1.00	1.46	0.44	14

**Table E.3:**  
**Summary of the stepwise regression of the response particle size.**

Variable	Step	Multiple R <sup>2</sup>	F –value	p-level	Variables included
B	1	0.31	6.20	0.24	1
A	2	0.51	5.48	0.26	2
D	3	0.69	6.61	0.24	3
BE	4	0.78	4.92	0.27	4
DE	5	0.86	5.57	0.26	5
AD	6	0.90	3.96	0.30	6
CD	7	0.93	3.27	0.32	7
E	8	0.96	3.97	0.30	8
AB	9	0.97	2.00	0.39	9
AE	10	0.98	2.08	0.39	10
C	11	0.99	2.40	0.36	11
BD	12	0.99	3.37	0.32	12
BC	13	1.00	21.30	0.14	13
CE	14	1.00	11.70	0.18	14

**Table E.4:**  
**Summary of the stepwise regression of the response conversion.**

Variable	Step	Multiple R <sup>2</sup>	F –value	p-level	Variables included
B	1	0.43	10.36	0.19	1
E	2	0.65	8.48	0.21	2
BE	3	0.75	4.70	0.28	3
AE	4	0.84	6.50	0.24	4
BD	5	0.88	3.35	0.32	5
CD	6	0.92	3.76	0.30	6
C	7	0.95	4.58	0.28	7
AD	8	0.97	3.75	0.30	8
D	9	0.98	3.17	0.33	9
DE	10	0.99	3.52	0.31	10
AB	11	1.00	8.22	0.21	11
BC	12	1.00	22.84	0.13	12
A	13	1.00	4.17	0.29	13
CE	14	1.00	13.49	0.17	14

**Table E.5:**  
**Summary of the stepwise regression of the response  $T_g$ .**

Variable	Step	Multiple R <sup>2</sup>	F -value	p-level	Variables included
CE	1	0.24	4.44	0.28	1
DE	2	0.38	2.80	0.34	2
BE	3	0.51	3.24	0.32	3
E	4	0.64	4.04	0.29	4
A	5	0.76	5.09	0.27	5
B	6	0.85	5.16	0.26	6
AC	7	0.89	2.57	0.36	7
C	8	0.92	3.30	0.32	8
AB	9	0.95	3.11	0.33	9
BC	10	0.97	4.49	0.28	10
AE	11	0.98	2.43	0.36	11
CD	12	0.99	3.81	0.30	12
AD	13	1.00	2.34	0.37	13
D	14	1.00	50.19	0.09	14

## Appendix F

# PLOT OF THE AVERAGE NUMBER OF RADICALS PER LATEX PARTICLE

**Table F.1**

**Equations used to fit the data points for the  $\bar{n}$  vs. time plots.**

Run number	Equation	R <sup>2</sup>
1	$X^2 = 0.54 + \frac{0.44}{1 + (t/428.61)^{-2.29}}$	0.94
2	$X^2 = \frac{(4.92 \times 10^{-2} + 3.08 \times 10^{-4} t^2)}{(1 + 3.27 \times 10^{-4} t^2)}$	0.98
3	$X^2 = \frac{(6.71 \times 10^{-14} + 9.99 \times 10^{-8} t^2)}{(1 + 9.86 \times 10^{-8} t^2)}$	0.92
4	$X^2 = \frac{(9. \times 10^{-15} + 3.39 \times 10^{-8} t^2)}{(1 + 3.38 \times 10^{-8} t^2)}$	0.86

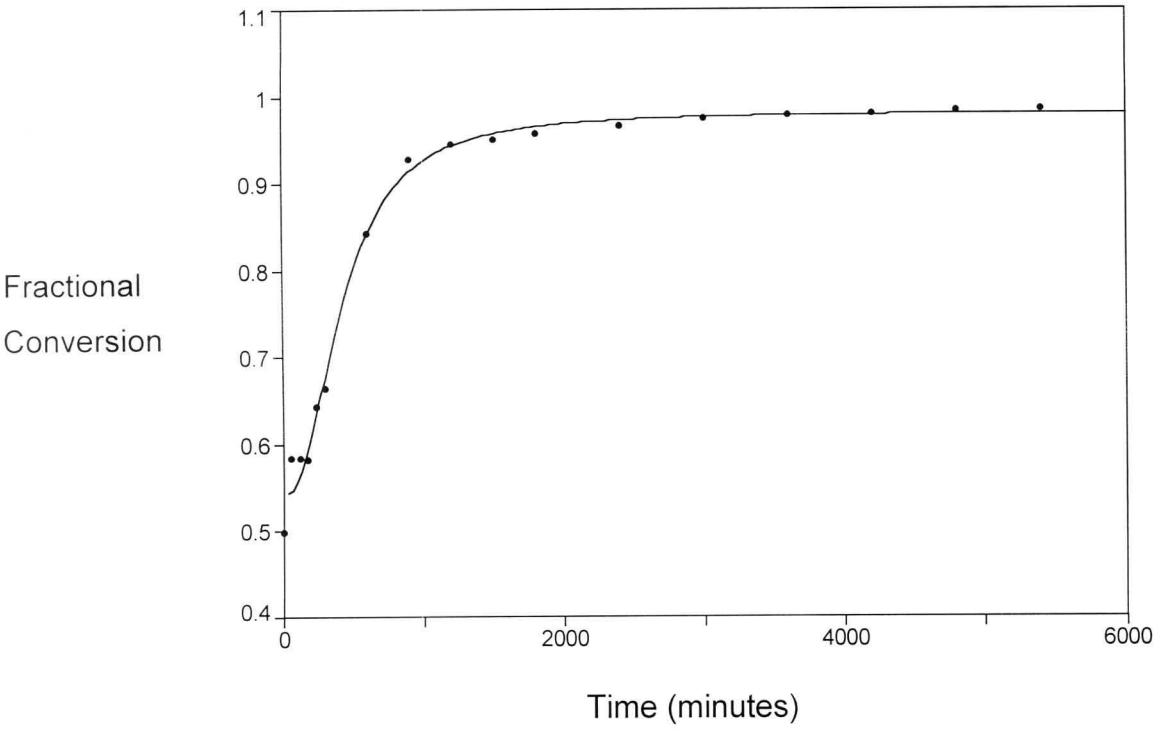


**Figure F.1**

**Graph of the fractional conversion vs. time for Run 1 fitted with a suitable curve.**

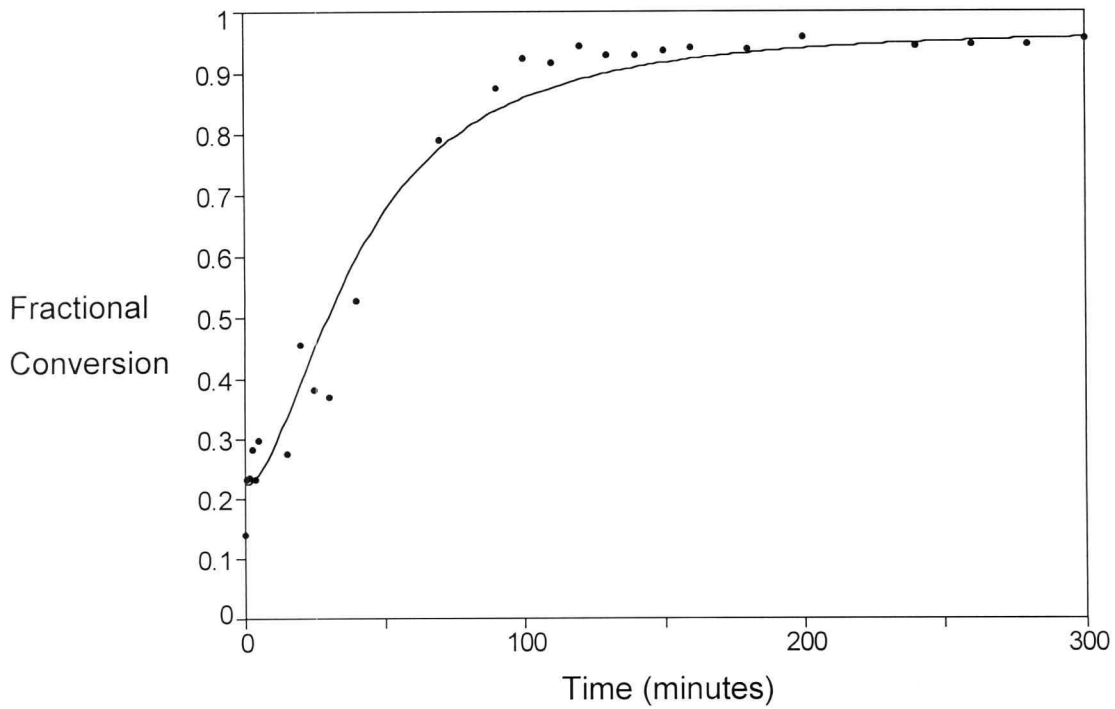


**Figure F.2**

**Graph of the fractional conversion vs. time for Run 2 fitted with a suitable curve.**

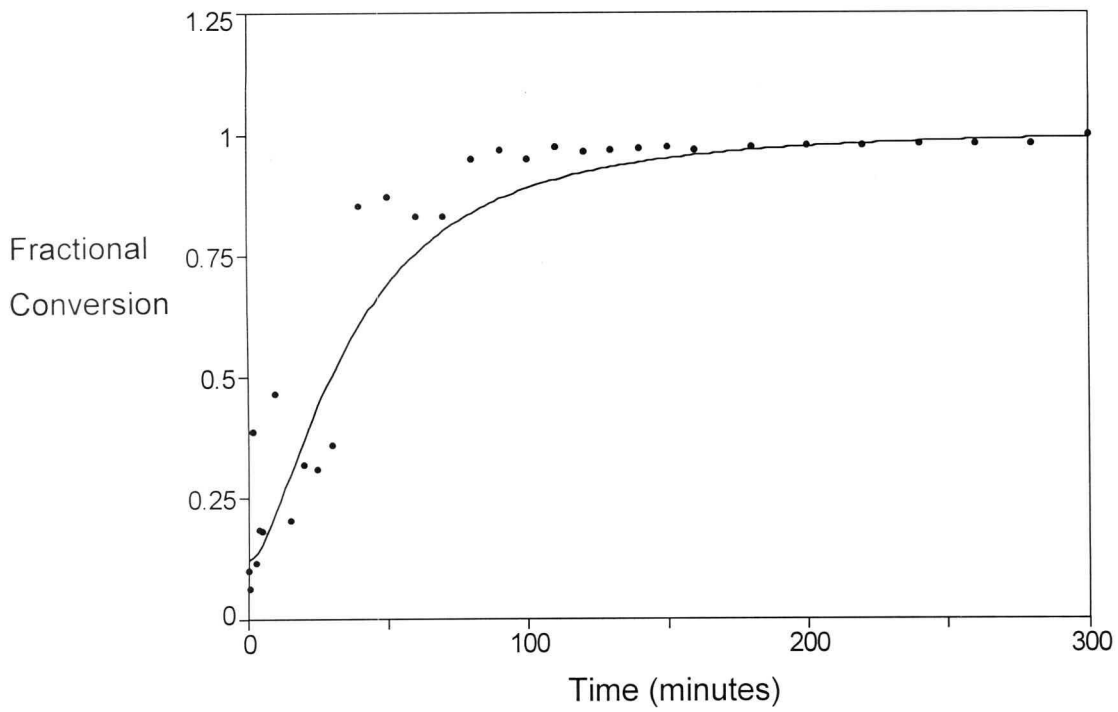


**Figure F.3**  
Graph of the fractional conversion vs. time for Run 3 fitted with a suitable curve.

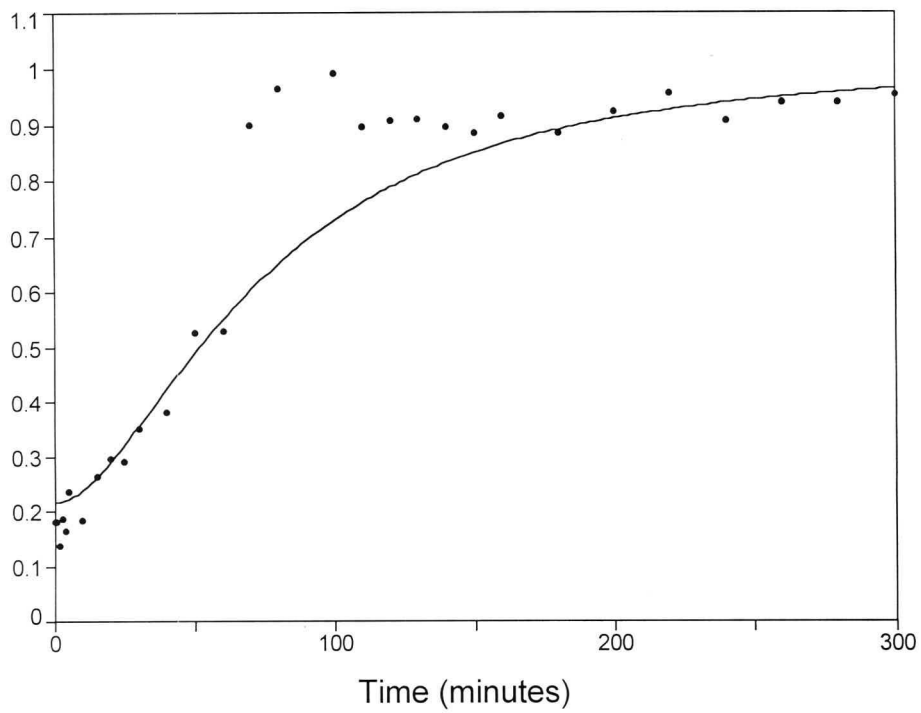


**Figure F.4**  
Graph of the fractional conversion vs. time for Run 4 fitted with a suitable curve.

## Appendix G

### RELATION BETWEEN THE CONVERSION OF MONOMER TO POLYMER AND THE PARTICLE SIZE

It is important to note that there are no correlation between the particle sizes and the fractional conversion for the 16 runs. This can clearly be seen in Figure G.1.

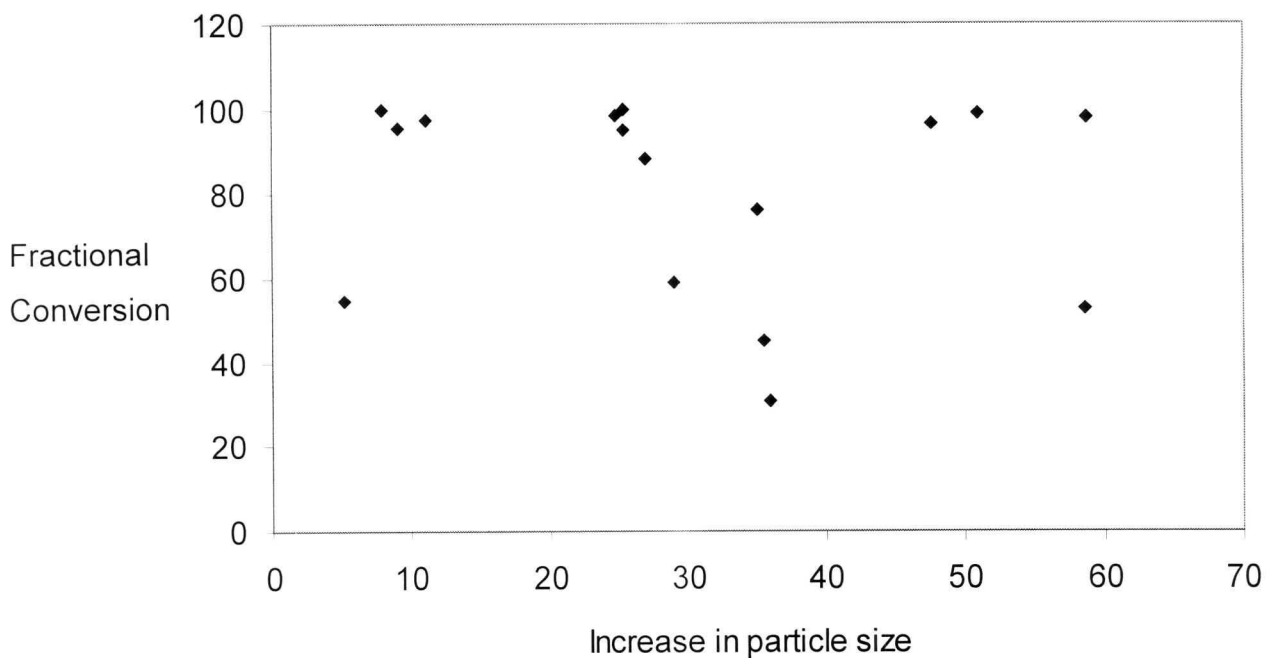


**Figure G.1:**

**The relation between the fractional conversion of monomer to polymer and the fractional increase in the particle size of the latex particles**

This is in contradiction to the theories presented in Chapter 3 that state that if there is no secondary nucleation of latex particles taking place, the particle size should increase as the conversion increases. This leads us to believe that there are unknown factors influencing the kinetics of the seeded emulsion system in the presence of alkyl iodide CTAs.